Silesian University of Technology

Joint Doctoral School

Faculty of Transport and Aviation Engineering

Department of Transport Systems, Traffic Engineering and Logistics

Method of Assessing the Condition of Wheels of Wheelsets of Railcar During Railroad Drive

A dissertation submitted to the Joint Doctoral School of Silesian University of Technology in the fulfilment of the Doctor of Philosophy in Civil Engineering, Geodesy and Transport

Author:

Yohanis Dabesa Jelila (MSc and Doctoral Candidate)

Supervisor: Wiesław Pamuła (PhD, DSc)

Co-supervisor: Adam Mańka (PhD)

May 10, 2024

Declaration

I, Yohanis Dabesa Jelila, declare that the work presented in this dissertation entitled as "Method of Assessing the Condition of Wheels of Wheelsets of Railcar During Railroad Drive," is original and has been carried out by me under the supervision of dr hab. inż. Wiesław Pamuła Professor of Silesian University of Technology and co-supervisor dr inż. Adam Mańka. This work has not been submitted for any degree or examination in any other university or institution.

I carefully referenced all the sources used in my work and provided complete details of the references in the bibliography section of the dissertation. I understand that plagiarism is a serious academic offence and declare that the work presented in this dissertation is my own and does not contain any material previously published or written by another person without proper acknowledgement or any material that has been submitted for the award of any other degree or examination.

Yohanis Dabesa Jelila

Katowice, May 10, 2024

Acknowledgement

First, I would like to express my deepest gratitude to my advisor, Professor Wiesław Pamuła and co-advisor, Dr. Adam Mańka, for their unwavering support, guidance, and encouragement throughout my PhD journey. Their expertise and invaluable insights have been instrumental in shaping my research and helping me overcome various challenges along the way. I am grateful for their patience, dedication and commitment to my success, and I am proud to have had the privilege of working under their supervision.

Next, I would like to acknowledge the financial support provided by the Silesian University of Technology, which made my PhD studies possible. I am grateful for their investment in my education and research, and I am committed to using my education and skills to make a positive impact in the world. I would also like to thank the Joint Doctoral School administrative staff who have been instrumental in documenting, supporting and facilitating me throughout my studies.

Third, I would like to express my love and gratitude to my wife, Hiwot Tesfaye, who has been my rock and my biggest supporter throughout this journey. She has been there for me through every challenge and every triumph, providing me with unconditional love and support every step of the way. Her love and support have been the driving force behind my success and I am truly blessed to have her in my life. I am forever grateful for her love, encouragement, and sacrifice.

Last but not least, I also would like to extend my sincere thanks to my family, colleagues, and friends for their love, inspiration, motivation, and support. Their encouragement, belief in me, and understanding during the long and often challenging process of completing my PhD have been invaluable. I am thankful for their sacrifices, understanding, and unwavering support, and I could not have done it without them.

Abstract

Effective condition monitoring and maintenance of wheels of wheelset of railcars require ongoing diagnostics of the technical condition of the vehicle components, in particular the wheel systems. The condition of the railcar wheels determines the efficiency and safety of the rail vehicle traffic. In this light, this dissertation presents a method for assessing the wheel condition of a railcar during railroad drive operations. The study aims to diagnosis the condition of tram vehicle wheels using micro-electromechanical systems (MEMS)-based accelerometer sensors that record rail vibrations during the passage of the vehicles. The study analyses sensor signals in the time-frequency domain to assess the condition of wheels during railroad drives.

The developed method for processing the collected sensor data is based on assessing the energy of vibrations at different frequency bands. The wavelet-based maximal overlap discrete wavelet packet transform (MODWPT) is chosen as the basis for processing. As a criterion for assessing the wheel conditions, the relative weighted difference (DW) between the extreme values of the vibration energy of “good" and damaged wheels in a given frequency range is proposed. Optimisation of transform parameters is carried out, the type of base wavelet used, the required level of decomposition and characteristic frequency bands are determined to be an important parameter for the assessment of the condition of the wheels. The optimisation task is carried out using data from initial vibration measurements during tram journeys in the depot.

The study validates the method during field test drives sessions of trams on shunting tracks at the tram depot using a prototype accelerometer sensor based on MEMS technology. The MEMS sensor with 3-axis is mounted underneath of rail track and utilised to record the vibrations of the running wheels. The recorded acceleration is sampled at a frequency of 1 kHz. During drive test sessions, the vehicle was fitted with wheels damaged to varying degrees. The energy of the recorded signals is calculated using the

MODWPT transform coefficients with the Coiflet3 base wavelet at the 8^{th} decomposition level within the frequency band of 420 – 422 Hz.

The results of the validation confirm that the possibility of using sensors in MEMS technology to assess the condition and, above all, to signal passages with damaged wheels. The use of the MODWPT transform effectively describes vibration anomalies, and thus indicates damaged wheels. The established parameters of the MODWPT transform may need to be corrected when the drives are made on tracks in a poor technical condition and when the travel speeds exceed a few km/h. The developed method has been successfully used to detect the wheel fault conditions while driving.

In conclusion, the study demonstrates the potential of MEMS accelerometer sensors and MODWPT transform for assessing the condition of wheels of the wheelsets systems in the railcars. The developed method shows promise in detecting wheel fault conditions during tram operation, which can improve maintenance practices and ensure the safety of rail vehicle operations. Future research may delve into identifying and categorising sources of vibration energy anomalies within specific frequency bands, evaluating the size and type of wheel damage, integrating supplementary measuring tools with MEMS accelerometers, and implementing machine learning-based techniques for comprehensive wheel condition diagnosis and maintenance strategies.

Keywords: wheel fault condition assessment; MEMS-based sensor; MODWPT; wavelet coefficient; weighted difference; decomposition level; vibration energy; frequency band.

Streszczenie

Efektywne utrzymanie w ruchu pojazdów kolejowych wymaga bieżącej diagnostyki stanu technicznego podzespołów pojazdów w szczególności układów jezdnych. Stan kół wózków determinuje sprawność i bezpieczeństwo ruchu pojazdów. Znana metodyka diagnostyki stanu kół opiera się na analizie sygnałów z czujników umieszczonych na piastach kół, na szynach lub w pobliżu torów. Analizowane są drgania kół lub szyn, dźwięki generowane przez koła lub mierzone są przemieszczenia względne elementów wózka kolejowego. Opracowane rozwiązania pomiarowe zawierają czujniki przespieszeń, mikrofony lub tensometry wymagające starannej obsługi. Analiza sygnałów dokonywana jest w dziedzinie czasu, częstotliwości i czasowo-częstotliwościowej.

Podjęto zadanie weryfikacji metodyki z zastosowaniem pomiaru parametrów sygnału drganiowego. Wybrano jako pole badań ocenę stanu kół pojazdów tramwajowych. Utrzymanie w ruchu pojazdów tramwajowych jest ważnym zagadnieniem dla systemu transportowego Aglomeracji Śląskiej. Komunikacja tramwajowa jest znaczącym elementem systemu i wpisuje się w politykę redukcji śladu węglowego realizowaną przez władze Regionu.

Specyfika konstrukcji pojazdów tramwajowych - znacznie mniejsza waga i niewielkie prędkości poruszania się w porównaniu do taboru kolejowego redukują wymagane zakresy pomiarów parametrów sygnałów. Wykonano wstepne badania i uzyskano widma sygnałów drganiowych, istotne dla diagnostyki uszkodzeń kół, w zakresie cętotliwości 50 – 500 Hz. Maksymalne wartości przyspieszeń drgań nie przekraczały 200 [m/s^2]. Taki zakres parametrów drgań możliwy jest do pomiaru z użyciem dostępnych czujników przyspieszeń wykonanych w postaci mikroukładów elektromechanicznych - MEMS.

Sformułowano pytanie badawcze: W jaki sposób można użyć czujników przyspieszeń w technologii MEMS do oceny stanu kół wózków pojazdów podczas przejazdu? Zaproponowano użycie analizy sygnałów z czujników w dziedzinie czasowo-częstotliwościowej

dla uwzględnienia wpływu ruchu pojazdu podczas badań. Postawiono hipotezy badawcze: Analiza obrazu drgań, w przedziale częstotliwości 0-500 Hz, szyn po których porusza się pojazd umożliwia ocenę stanu kół. Energia drgań szyn w charakterystycznych zakresach częstotliwości wskazuje stan kół.

Przyjęto ograniczenia dla realizacji pomiarów wynikające z praktyki dyżurnych ruchu w zajezdni. Obserwowany jest przejazd pojazdu z niewielką prędkością, gdy poziom generowanego hałasu podczas jazdy wzbudza "niepokój" niedopuszcza się do opuszczenia zajezdni przez pojazd. Prędkość ruchu jest ograniczona do kilku km/godz. Czujnik pomiarowy zostaje umieszczony na torze manewrowym w zajezdni i nie wpływa na ruch pojazdu.

Kwerenda literatury pozwala zidentyfikować kilka podejść do zagadnienia oceny stanu kół. Można wyróżnić metody oceny z użyciem czujników pokładowych montowanych na elementach wózków lub na konstrukcji pojazdów. Rozwiązania pokładowe mogą dostarczyć bieżącej informacji i wskazać konieczność podjęcia serwisowania, wiąże się to jednak z dużymi kosztami montażu czujników jak i utrzymania ich w sprawności. Autorzy opracowań dowodzą dużej przydatności pokładowych czujników dla oceny stanu kół oraz dla realizacji zadań utrzymania w ruchu zgodnie z założeniami strategii CBM (utrzymanie w ruchu oparte na ocenie stanu technicznego).

Zastosowanie czujników poza pojazdem to domena metod opartych na pomiarach oddziaływania kół pojazdu na szyny lub na pomiarach generowanego hałasu w otoczeniu toru. Pomiar stopnia odkształcenia szyny lub rejestracja parametrów drgań wywołnych przez koła pozwala odwzorować przebieg oddziaływania i ujawnia anomalie gdy pojazd posiada uszkodzone koła. Autorzy prezentowanych w literaturze prób analizy sygnałów z czujników dla oceny stanu kół definiują istotne ograniczenia dla uzyskania poprawnych wyników oceny. Wymieniane są przede wszystkich prędkość przejazdu, stan torowiska, rodzaj i stan techniczny wózka kolejowego jako czynniki determinujące zdolność do poprawnego opisu stanu technicznego kół.

Opracowane metody oparte na ocenie hałasu przejazdu pojazdu czułe są na hałas w otoczeniu. Publikowane opracowania zalecają poddanie sygnałów akustycznych z czujników filtracji w dziedzinie częstotliwości dla eliminacji zakłóceń. Autorzy zwracają uwagę na konieczność uważnej oceny źródeł w otoczeniu dla identyfikacji zakresów częstotliwości maskowania dźwięków przejazdu.

Prezentowane w literaturze rozwiązania układów pomiarowych dostarczają strumienie danych, które podlegają analizie w dziedzinie czasu, częstotliowści lub w dziedzinie

czasowo-częstotliwościowej. Autorzy proponują zastosowanie znanych metod analizy opartych na transformacjach przede wszystkim Fouriera i falkowych. Przeprowadzone dyskusje właściwości wybranych metod nie dają jednoznacznego wskazania najlepszej metody analizy. Ważną przesłanką dla wyboru metody analizy, podkreślaną przez autorów prac, jest niestacjonarny charakter danych z czujników. Efektywna analiza wymaga powiązania cech czasowych i cech częstotliwościowych dla uzyskania opisu, który będzie użyteczny do określenia anomalii przebiegów oraz powiązania ich z stanem technicznym kół. Wyróżniono transformacje falkowe ze względu na zdolność do opisu przebiegów w różnych skalach czasowych jak i w różnych rozdzielczościach częstotliwości.

Dokonując przeglądu właściwowści transformacji falkowych zwrócono uwagę na transformację MODWPT opartą na dekompozycji z użyciem pakietów falkowych. Pakietowa analiza oparta na binarnym drzewie dekompozycji dostarcza opisu w większej rozdzielczości zarówno w czasie jak i w dziedzinie częstotliwości stąd uzyskuje się zdolność do bardziej szczegółowego opisu danych pomiarowych. Dobór falki bazowej oraz poziomu dekompozycji jest przedmiotem optymalizacji dla uzyskania efektywnego narzędzia do oceny stanu kół. W literaturze brak prac podejmujących zadanie optymalizacji parametrów MODWPT dla oceny stanu technicznego kół.

Opracowano metodę oceny stanu kół z zastosowaniem danych z czujnika przyspieszeń rejetrującego drgania szyny podczas przejazdu pojazdu. Wybrano jako podstawę przetwarzania transformację MODWPT oraz energię drgań w charakterystycznych przedziałach częstotliwości jako miarę stanu technicznego. Jako kryterium optymalizacji zaproponowano względną różnicę między energią drgań "dobrych" i uszkodzonych kół w danym przedziale częstotliwości. Przeprowadzono optymalizację parametrów transformacji, ustalono rodzaj falki bazowej, wymagany poziom dekompozycji oraz charakterystyczne zakresy częstotliwości istotne dla oceny stanu kół. Zadanie optymalizacji wykonano z użyciem danych ze wstępnych pomiarów drgań podczas przejazdów tramwajów w zajezdni.

Przeprowadzono walidację metody podczas próbnych przejazdów tramwajów na torach manewrowych zajezdni. Użyto prototypu czujnika przyspieszeń opartego na akcelrometrze 3-osiowym wykonanym w technologii MEMS. Rejestrowano przyspieszenia drgań szyn po których przemieszczał się pojazd z częstotliwością 1 kHz. W pojeździe zamontowano uszkodzone w różnym stopniu koła. Obliczono energię zarejestrowanych sygnałów z użyciem współczynników transforamcji MODWPT z falką bazową Coiflet3 na 8 poziomie dekompozycji w przedziale częstotliwości 420-422 Hz. W celu selekcji "dobrych" i uszkodzonych kół wyznaczono próg detekcji.

Wyniki walidacji potwierdzają możliwość zastosowania czujników w technologii MEMS do oceny stanu a przede wszystkim do sygnalizacji przejazdów z uszkodzonymi kołami. Zastosowanie transformacji MODWPT skutecznie pozwala opisać anomalie drganiowe i tym wskazać uszkodzone koła. Ustalone parametry transformacji MODWPT mogą wymagać korekty gdy przejazdy wykonywane będą na torach w złym stanie technicznym i gdy prędkości przejazdów przekroczą kilka km/godz. Opracowana metoda została z powodzeniem wykorzystana do wykrywania usterek kół podczas jazdy.

Słowa kluczowe: ocena stanu kół; MEMS czujnik drgań; MODWPT; energia drgań; przedział częstotliwości.

Extended Summary

Effective maintenance of railway vehicles requires ongoing diagnostics of the technical condition of vehicle components, in particular the wheel systems. The condition of the railcar wheels determines the efficiency and safety of vehicle traffic. A well-known methodology for diagnosing the condition of wheels is based on the analysis of signals from sensors located on wheel hubs, on rails or near tracks. The vibrations of the wheels or rails, the sounds generated by the wheels, or the relative displacements of the wheelset components are measured. The developed measurement solutions include speed sensors, microphones or strain gauges that require careful handling. The analysis of the signal is performed in the time, frequency and time-frequency domains.

The task of verifying the methodology using the measurement of vibration signal parameters were undertaken. The assessment of the condition of tram wheels was chosen as the field of research. Maintenance of tram vehicles is an important issue for the transport system of the Silesian Agglomeration. Tram transport is a significant element of the system and is part of the policy of reducing the carbon footprint implemented by the authorities of the Region.

The specifics of tram vehicles are: much lower weight and low speeds of movement in comparison to rolling stock this leads to the reduction of required ranges of signal parameter measurements. Preliminary tests were carried out and spectra of vibration signals, important for the diagnosis of wheel condition, in the frequency range of 50 – 500 Hz were obtained. The maximum values of vibration accelerations did not exceed 200 [m/s^2]. Such a range of vibration parameters can be measured with the use of available acceleration sensors made in the form of electromechanical microcircuits - MEMS.

The research question is formulated: How can MEMS acceleration sensors be used to assess the condition of wheels of wheelsets of railcars during a railroad drive? The analysis of sensor signals in the time-frequency domain is proposed to take into account

the influence of vehicle movement during tests. The following research hypotheses are formulated: The analysis of the vibration image in the frequency range of 0 – 500 Hz of the rails on which the vehicle moves enables the assessment of the condition of the wheels. The vibration energy of the rails in characteristic frequency bands indicates the condition of the wheels.

Limitations for the implementation of measurements resulting from the practice of traffic dispatchers in the depot are adopted. I practice a vehicle is observed passing at a low speed and when the level of noise generated while driving causes "anxiety" for the dispatcher he prevents the vehicle from leaving the depot. Movement speed is limited to a few km/h. The measuring sensor is placed on the manoeuvring track in the depot and does not affect the movement of the vehicle.

A literature query allows us to identify several approaches to the issue of wheel condition assessment. A distinction can be made between evaluation methods using onboard sensors mounted on bogie components or vehicle structures. Onboard solutions can provide real-time information and indicate the need for maintenance, but this is associated with the high costs of installing sensors and maintaining them in working order. The authors of the studies prove the high usefulness of onboard sensors for the assessment of the condition of the wheels and for the implementation of maintenance tasks in accordance with the assumptions of the CBM strategy (maintenance based on the assessment of technical condition).

The use of sensors outside the vehicle is the domain of methods based on measurements of the impact of the vehicle's wheels on the rails or on measurements of the generated noise in the track environment. Measuring the degree of rail deformation or recording the parameters of vibrations caused by the wheels allows for mapping the course of the impact and reveals anomalies when the vehicle has damaged wheels. The authors of the attempts presented in the literature to analyze signals from sensors for the assessment of the condition of wheels define significant limitations for obtaining correct evaluation results. First of all, the speed of travel, the condition of the track, the type and technical condition of the bogie are mentioned as factors determining the ability to correctly describe the technical condition of the wheels.

The developed methods based on the assessment of vehicle passing noise are sensitive to ambient noise. Published studies recommend subjecting the acoustic signals from the sensors to filtration in the frequency domain to eliminate interference. The authors draw attention to the necessity of careful assessment of sources in the environment in order to

identify the frequency ranges of masking the passage sounds.

The solutions of measurement systems presented in the literature provide data streams that are subject to analysis in the time, frequency or time-frequency domain. The authors propose the use of well-known methods of analysis based primarily on Fourier and wavelet transformations. Discussions of the properties of the selected methods do not give a clear indication of the best method of analysis. An important premise for the choice of the analysis method, emphasized by the authors of the papers, is the non-stationary nature of the sensor data. Effective analysis requires the linking of time and frequency characteristics to obtain a description that will be useful for determining waveform anomalies and linking them to the technical condition of the wheels. Wavelet transformations are distinguished due to their ability to describe waveforms at different time scales and at different frequency resolutions.

When reviewing the properties of wavelet transformations, attention was paid to the MODWPT transform based on decomposition with the use of wavelet packets. Packet analysis based on a binary decomposition tree provides a description in higher resolution both in time and in the frequency domain, hence the ability to describe the measurement data in more detail is obtained. The selection of the base wave and the level of decomposition is the subject of optimisation in order to obtain an effective tool for assessing the condition of the wheels. There are no papers in the literature undertaking the task of optimising MODWPT parameters for the assessment of the technical condition of wheels.

A method was developed to assess the condition of the wheels using data from an acceleration sensor that records rail vibrations during the passage of the vehicle. The MODWPT transform and vibration energy in characteristic frequency intervals were chosen as the basis for the processing. As a criterion for optimisation, the relative difference between the vibration energy of "good" and damaged wheels in a given frequency range was proposed. Optimisation of transform parameters was carried out, the type of base wavelet, the required level of decomposition and characteristic frequency ranges that are important for the assessment of the condition of the wheels were determined. The optimisation task was carried out using data from initial measurements of vibrations during tram journeys in the depot.

The method was validated during test runs of trams on the depot's shunting tracks. A prototype of an acceleration sensor based on a 3-axis accelerometer made in MEMS technology was used. Accelerations of vibrations of rails on which the vehicle was moving

at a frequency of 1 kHz were recorded. The vehicle was fitted with wheels damaged to varying degrees. The energy of the recorded signals was calculated using the MODWPT transform coefficients with the Coiflet3 base wave at the 8^{th} decomposition level in the frequency range of 420 – 422 Hz.

The results of the validation confirm that the possibility of using sensors in MEMS technology to assess the condition and, above all, to signal passages with damaged wheels. The use of the MODWPT transform effectively allows the description of vibration anomalies and thus indicates wheel conditions. The established parameters of the MODWPT transform may need to be corrected when the drives are made on tracks in poor technical condition and when the travel speeds exceed a few km/h. The developed method has been successfully used to detect wheel fault conditions while driving.

Keywords: wheel fault condition assessment; MEMS-based sensor; MODWPT; wavelet coefficient; weighted difference; decomposition level; vibration energy; frequency band.

List of Publications

Journal articles

1. **Y. D. Jelila** and W. Pamuła, "Application of MEMS Sensors for the Condition Monitoring of Urban Tramways Based on MODWPT," IEEE Sens. J., vol. 23, no. 20, pp. 24300–24307, Oct. 2023, doi: https://doi.org/10.1109/JSEN.2023.3309648, [Ministry of Science and Higher Education (MEiN) score: **100 points**].

2. **Y. D. Jelila** and W. Pamuła, "Detection of Tram Wheel Faults Using MEMS-Based Sensors," Sensors, vol. 22, no. 17, p. 6373, Aug. 2022, doi: https://doi.org/10.3390/s22176373, [MEiN score: **100 points**].

3. M. A. Tolcha, G. A. Ademe, **Y. D. Jelila**, M. G. Jiru, and H. G. Lemu, "Analyzing the effect of vibration on crack growth on shaft using fuzzy logic," Meccanica, vol. 57, no. 12, pp. 2929–2946, Dec. 2022, doi: https://doi.org/10.1007/s11012-022-01609-2, [MEiN score: **100 points**].

Conference articles

1. **Y. D. Jelila** and W. Pamuła, "Monitoring of Urban Tramway Conditions: An Employment of MODWPT and MEMS-Based Sensors," TransComp 2023 XXVI International Conference, 2023, Zakopane, Poland. The manuscript is accepted, presented and under publication process in the Journal of Civil Engineering and Transport (ISSN: 2658-2058), [MEiN score: **40 points**].

2. **Y. D. Jelila**, H. G. Lemu, W. Pamuła, and G. G. Sirata, "Fatigue life analysis of wheel-rail contacts at railway turnouts using finite element modelling approach.,"

IOP Conf. Ser. Mater. Sci. Eng., vol. 1201, no. 1, p. 012047, Nov. 2021, doi: https://doi.org/10.1088/1757-899X/1201/1/012047, [MEiN score: **20 points**].

3. **Y. D. Jelila** and H. G. Lemu, "Study of Wheel-Rail Contacts at Railway Turnout Using Multibody Dynamics Simulation Approach," in International Workshop of Advanced Manufacturing and Automation, vol. 2, Springer, 2021, pp. 371–379, doi: https://doi.org/10.1007/978-981-33-6318-2_46, [MEiN score: **20 points**].

4. G. G. Sirata, H. G. Lemu, K. Waclawiak, and **Y. D. Jelila**, "Study of rail-wheel contact problem by analytical and numerical approaches," IOP Conf. Ser. Mater. Sci. Eng., vol. 1201, no. 1, p. 012035, Nov. 2021, doi: https://doi.org/10.1088/1757-899X/1201/1/012035, [MEiN score: **20 points**].

5. A. D. Tura, H. B. Mamo, **Y. D. Jelila**, and H. G. Lemu, "Experimental investigation and ANN prediction for part quality improvement of fused deposition modeling parts," IOP Conf. Ser. Mater. Sci. Eng., vol. 1201, no. 1, p. 012031, Nov. 2021, doi: https://doi.org/10.1088/1757-899X/1201/1/012031, [MEiN score: **20 points**].

Contents

List of Figures

List of Tables

Listings

List of Symbols and Abbreviations

A_j	Vector
a	Scaling parameter
b	Translation parameter
t	Time
f_s	Frequency sample
τ	Time variable
$w(\tau)$	Window function
$x(t)$	Continuous-time signal
$x[n]$	Discrete-time signal
N	Number or length of sample points
ψ	Wavelet function
ψ^*	Complex conjugate function
ω	Angular frequency
j	Square root of -1
H	High-frequency filter
L	Low-frequency filter
A	Approximate coefficient
D	Detail coefficient
r_j	Residue signal
$a(t)$	Instantaneous amplitude
$\varphi(t)$	Instantaneous phase
S	Samples of a signal
g_l, h_l	Low and high-pass filter
$\|\|S\|\|^2$	Signal energy
b_n^j	Frequency bandwidth
$minE_n$	Minimum energy of normal wheels
$maxE_f$	Maximum energy of fault wheels
DW	Weighted Difference
k	Number of combined frequency
ax	Acceleration along x-axis
ay	Acceleration along y-axis
az	Acceleration along z-axis
db	Daubechies base wavelet
$coif$	Coiflet base wavelet
Sym	Symlet base wavelet

AC	Alternative current
ADC	Analogue digital converter
ADSAT	Angle domain synchronous average technique
AE	Acoustic Emission
APD	Amplitude Probability Density
AR	Autoregressive
ARMA	Autoregressive Moving Average
ARMP	Adaptive Redundant Multi-wavelet Packet
BSS	Blind Source Separation
CBM	Condition-Based Maintenance
CFT	Continuous Fourier Transform
CWT	Continuous Wavelet Transform
DFT	Discrete Fourier Transform
dl	Decomposition level
DWT	Discrete Wavelet Transform
EMD	Empirical Mode Decomposition
EWT	Empirical Wavelet Transform
FA	Fourier Analysis
FDD	Fault Detection and Diagnosis
FDI	Fault Detection and Isolation
FE	Finite Element
FFT	Fast Fourier Transform
FM	Frequency Modulation
FT	Fast Transform
HHT	Hiltert Haung Transform
HST	High-Speed Trains
HT	Hilbert Transform
IOT	Internet Of Things
ISK	Improved Spectral Kurtosis
IWT	Integral Wavelet transform
MBS	Multibody Dynamics
MEMS	Micro-Electromechanical System
MODWPT	Maximal Overlap Discrete Wavelet Packet Transform
MRA	Multi-resolution Analysis
NDT	Non-Destructive Testing
PSD	Power Spectra Density
RF/ID	Radio Frequency/ Identification
RMS	Root Mean Square
RTOF	Round trip time of flight
SD	Standard Deviation
SE	Spectral Entropy
SNR	Signal to Noise Ratio
STFT	Short-Time Fourier Transform
T-F	Time-Frequency
TFDs	Time-Frequency Distributions
TH	Threshold
TSA	Time-Synchronous Average

1

Introduction

1.1 Background of the study

Railroads are a crucial part of the infrastructure of every nation because they can move large volumes of goods and thousands of passengers in a short period of time Gapiński et al. [2020]. Potential factors determining the success of rail transport are its durability, reliability, safety, and operational strategy Jin et al. [2022], Kuminek et al. [2015]. One of the strategies for promoting and encouraging rail transportation is that it runs on clean energy, which emits no pollutants. For this purpose, the use and development of rail transport is primarily dedicated to urban and rural areas of the world, with a huge investment cost.

For a railway network to operate safely and efficiently, the healthy contact condition of wheels and rails must always be maintained. This can be done through fault diagnosis, onboard condition monitoring, and maintaining the safe operation of a train's wheelsets.

Figure 1.1: Typical wheel defects captured from a tram depot

The wheelset of a railway vehicle is a critical component that contributes significantly to the stability of the vehicle while it is in motion by ensuring ride quality, transmitting traction, and braking force to a railroad. The tasks of supporting, guiding, and braking are centralized by wheelset components (wheel, axle, and axle box), and therefore, the safety of traffic depends primarily on the health condition of wheelsets, which support the weight of the vehicles on the track.

Among wheelset components, wheels are critical and one of the most heavily loaded components of rolling stock, and their faults are the leading cause of train accidents. Wheels are subjected to cyclic impact forces and are exposed to different track conditions, such as complex external track irregularities. As a result, the wheel suffers from numerous defects, which influence the smoothness of its rotation. Among the various defects of the wheels, wheel flat, wheel wear, eccentricity, discrete defects, periodic non-roundness, non-periodic, corrugation, roughness, spalling, and shelling fall within the main category. Figure 1.1 presents an examples of such a typical wheel defects. Such defects trigger high-strength collisions of the wheel-rail, promote wheel-rail damage, and cause component failure Alemi et al. [2017].

The wheel-flat fault is the most common localised defect that gives rise to another

family of wheel damages. It is a defect originating from wheel-rail sliding and occurs when hard braking is applied to the wheel element. Hard braking forces the locked wheel to revolve around the centre of the axle, which causes excessive deformation and scratches to the surface of the wheels and rails. When the wheel rotates with a deformed irregular surface, it interacts adversely with the environment (rain, ice, and sand) and causes the wheel-rail adhesion wear, which deteriorates the contacting surface. Additionally, a significant amount of damage and fault is caused by the high contact forces that exist at wheel-rails; this is largely due to the large weights involved in rail traffic and the hardness of the wheel-rail materials Belotti et al. [2006].

The repetitive impacts on a wheel-rail system, along with the significant forces involved, inevitably lead to the rapid deterioration of both the rolling and fixed railway assets. The resulting fault from impulsive force will cause materials to degrade if not given proper attention, ultimately leading to complete and irreversible failure. Wheel-flat faults play a significant role in causing and spreading other types of damage to wheels. In this work, the terms wheel-flat, wheel fault and wheel conditions are used interchangeably.

When locomotives travel with a faulty wheel, each wheelset turns, causing track disturbances and wheel-rail surface damage. The ups and downs and guiding forces from contact with the tracks render the upper half of the track and the vehicle itself. This condition helps for monitoring and diagnosing the wheel condition based on the characteristics of the motion of a vehicle. For instance, a train running on a track with a flat wheel subjected to cyclic impulsive loads, and such a wheel jumps off the track surface.

A train vehicle driving on the straight, sharply curved rail track and turnout cross-sections subjected to an impact force experiences two contact patches. These contact patches are wheel tread and rail-head contact, wheel flange and rail-gauge corner contact, but the contact condition is more severe in the latter, according to Xu et al. [2016]. Such a contact condition results in unnecessary vibration and wheel flange surface material loss from the contacting parts and contributes to the wear of the wheel tread, flange, and deformation of the rail gauge corner. Therefore, early fault diagnosis and maintenance of wheelset components, precisely the wheel element, as early as possible is a vital concept for condition monitoring of wheelset components of a railcar.

Wheel-rail maintenance workers and managers are striving to identify problems with wheels to avoid costly system-wide repairs. The wheel's assembly state should be monitored and maintained effectively before huge damage happens. Early wheel fault detection is required to ensure train safety and stability. Therefore, condition-based maintenance (CBM) has proven to be a profitable strategy for railway assets. By detecting component issues at the earliest possible stage, the CBM can aid in guaranteeing improved safety and functionality. CBM can extend component lifetimes by minimising downtime and enabling maintenance workers and operators to optimise any replaceable component in a particular operational condition by altering the dependency on scheduled maintenance and ensuring a unique component repair schedule Bernal et al. [2018].

Train wheel condition monitoring and fault diagnostic techniques are widely practised in the railway industry, with applications of predictive and condition-based maintenance Dalpiaz and Rivola [1997]. To simplify, there are two broad methods of diagnosing and monitoring the state of the wheel defect on a railcar. These assessment methods include both conventional and innovative detection methods. Conventional detection methods include visual inspection, magnetic particles, and ultrasound testing methods to assess the state of the wheel. However, these techniques could not provide CBM and thus are not considered in this study. Innovative detection methods are types of preventive maintenance techniques, and they are efficiently employed for CBM purposes. There are two main categories of innovative detection methods: (1) onboard and (2) track or wayside detection methods.

Onboard detection approaches are methods employed on the train to detect the nature of the fixed assets, such as switches and rail conditions, whereas track or wayside-mounted detection approaches are applied to study the health condition of the moving components on the train, such as wheels, axles, and bearing elements. Wayside detection methods assess the condition of a moving vehicle by utilizing a strain gauge, temperature sensor, mechanical sensors, vibration, and noise-based sensor systems by mounting them at a single point where all trains pass by. This method is inexpensive; however, the disadvantage is that they cannot detect the running state of the vehicle throughout the entire process in a real-time scenario.

On the other hand, onboard detection methods can perform a diagnosis of the vehicle's state in real-time by installing sensors on the axle box. The drawbacks of this

approach are the large volume of work required for data preparation, the tedious calibration method, the measurement results being affected by different signals which lead to misjudgment and the specific design of instrumented wheels are required for different vehicles Li et al. [2017]. The deployment of either a wayside or onboard detection method depends on the type of resource that are going to be monitored and diagnosed. For this study, wayside detection methods is considered for monitoring and diagnosing the wheel condition of a railcar during drive operation.

Nowadays, the need for reliable and efficient train wheel fault diagnosis methods has been recognized as an essential aspect of railway maintenance and safety. The development of accurate and effective methods for train wheel fault diagnosis is crucial to guarantee the secure and effective functioning of railway systems. Several techniques have been proposed and developed for train wheel fault diagnosis over the past 30 years. This includes acoustic emission (AE) analysis, vibration analysis, and non-destructive testing (NDT) methods. The vibration analysis technique has the potential to map the condition of wheelsets and rail infrastructure. This technique uses sensors for collecting measurement data and uses different time-frequency analysing tools to extract valuable features of the signals captured.

In recent years, time-frequency analysis techniques have emerged as a promising approach for train wheel fault diagnosis. These techniques provide a more comprehensive and effective way to analyse and interpret the signals collected from the train wheels. The method can be effectively used to diagnose various types of faults and anomalies within the wheelset components.

1.2 Motivations of the study

Rail transport can be light rail transit, high-speed trains (HST), freight vehicles, and other types. In many cities, trams are an important part of the mass transit. Fluent urban transportation improves the lives of citizens, attracts entrepreneurs, and reduces traffic in cities, which benefits citizens and the environment at large. Due to enormous benefits of the rail transport, this transport system has seen rapidly growing in many urban areas of the worldwide in recent years. Tram networks are being modernized are in an increasingly complex manner, and costly ways, and new tram lines are being built.

Modern tram communication relies on the safety and reliability of the track infrastructure. However, the old tracks are still in use, and they affect the life of the contacting surface, tram speed, and passenger comfort, generating irritating noise and vibration emissions in the nearby environment. This will cause deterioration of track infrastructure, including rail track turnouts, affect tram wheelsets, cause traffic congestion, derailment accidents, and hurt the general safe operations of the railcar.

Unlike long-distance trains that travel over flat terrain, city trams encounter much sharper curves and traffic intersections, resulting in more frequent wheel faults and failure. The consequences of a tram wheel failure are enormous, and in some cases, the failure of a tram wheel system can be catastrophic if it occurs in a densely populated area like cities. A significant amount of money is budgeted each year for wheel-rail track infrastructure construction and its maintenance in Poland to reduce tram wheels system failure during railroad drive operation. To achieve the reliability of railway tracks and the safety of the tram wheelset system must be diagnosed, maintained, and fixed at the early faulty indication stage.

The cost of maintaining the tram wheelset system is substantial. Tram vehicles are operated on heavily used tracks, sometimes in poor condition. Horizontal curve radii are much smaller than railway radii. This will affect the conditions of the wheel-rail contact in a different way and will force the contacting body to wear and tear repeatedly. The running gear, especially the wheel profile, was subjected to intense wear and out-of-roundness. The wear of the rolling surface affects the value and direction of forces between the wheels and the rail, affecting the vehicle's safety on the track.

In addition, the quality of the wheel profile and the wear of the wheelset affect the ride comfort, the wheel-rail interaction, and produce unnecessary noise and vibration. The noise and vibration generated affect the buildings close to the track and tram infrastructure, in general, Staskiewicz and Firlik [2017]. Nowadays, both high- and low-floor trams are in service due to the availability of old tracks, and the replacement of modern tracks is underway. Using hybrid rail tracks results in the tread of the wheel being subjected to high and variable loading conditions Staskiewicz and Firlik [2017]. As a result, old or bad track causes wheel failure and forces the wheel to operate under complex loading conditions.

Furthermore, train wheel fault diagnosis methods that are commonly practised by maintenance operators, such as visual inspections, non-destructive methods, and acoustic emission monitoring, are limited in their effectiveness and efficiency. Visual inspections are prone to human error and human experience and can only detect visible faults, while acoustic emission monitoring requires specialised equipment and trained personnel, making it costly and time-consuming.

Therefore, the need for efficient methods for train wheel fault detection is paramount for ensuring the safety of tram operations. Critical components such as wheelset components and rail tracks should be ensured and checked when they provide a service. Any damages or faults within these components of tramway infrastructure can cause a tram derailment, loss of passenger life, damage to costly infrastructure, and also result in a long schedule for corrective maintenance. In light of the increasing demand for rail transportation, it is important to implement a reliable and efficient method for the diagnosis of tram wheel faults.

The growing demand for the development of efficient methods for train or tram wheel fault diagnosis is on the rise. Advanced signal processing techniques, such as time-frequency analysis, have shown great potential to detect and diagnose train wheel faults. The use of these techniques can provide a more comprehensive and accurate assessment of wheel faults, improving the reliability and efficiency of train wheel fault diagnosis.

The motivation for conducting a research study and preparing a dissertation on the method of assessing and diagnosing of the fault condition of railcar wheels arises from the current demand for fault diagnosis at the tram depot maintenance centre for innovative monitoring the condition of wheels and wheelset system. Despite the numerous techniques developed for assessing and detecting the fault condition of tram wheels in recent decades, current capabilities need further improvement to provide a safe, durable, and reliable transport service.

Based on these current demand, the utilisation of MEMS-based sensors and time-frequency analysis techniques lies in the need to address the limitations of current fault diagnosis methods and contribute to the advancement of railway safety and efficiency. The development of an efficient and reliable method for the diagnosis of train wheel faults using time-frequency analysis can provide valuable information on the behaviour

of railcar wheels and help improve the maintenance and repair of tram wheelsets system.

1.3 Problem statement

Urban trams and light rail transit ride on a very dynamic geographical elevation with a short curve, turnout, high traffic intersections, allowing them to efficiently utilise the space available in the city. The regular and continuous movement of tram vehicles on a dynamic rail track causes deterioration such as wear, tear, and flattening of the wheel and rail component, a leading problem in the modern urban transportation system. This deterioration causes uneven or irregular surface formation and results in impact loading of the wheel-rail surface.

When the wheels impact the rail surface, the fault surface causes abnormal vertical vibration. When the wheels hit the rail surfaces, they load heavily on the contact surface and generate impact noise to the environment, which may cause the failure of the wheelset system in the long run. Nearly half of the railcars accidents were caused by wheel-rail system failures, and these failures can be costly to repair. The most dangerous infrastructure elements for rolling stock that cause complex loading (impact and dynamic loading) events are overpasses, crossings, and switch crossovers.

In addition, the tram crosses the highway at several intersections, frequently forcing emergency braking of trams. Frequent hard braking causes wheel locking forces excessive deformation, heat dissipation, and the wearing of the contacting surface, which causes various faults on the surface of the wheel-railway infrastructure. Due to track design, variable elevation, and dynamical loading of the rolling stock, failure of the wheelsets' in-service operation will occasionally result in a catastrophic failure that endangers passengers' lives and costs much for breakdown maintenance.

For instance, the Municipality of Katowice dispatches 130 trams per day for passengers' transportation. Maintenance and checkups of tram wheelset systems are usually done for these fleets of trams before and after dispatches every day. Monitoring and maintaining the condition of each tram wheelset is a heavy task compared to the number of employees working in the rolling stock workshop. To maintain and diagnose the healthy functioning of a tram wheelset, experts in the rolling stock maintenance division

perform various maintenance approaches in the workshops.

Currently, the experts of the workshop use visual, gauge and noise-based diagnosis approaches, which are simple inspection methods. The drawbacks of these diagnosis techniques are that they require very experienced operators, are limited to individuals' capabilities, are time-consuming, and are affected by environment.

Furthermore, using these traditional inspection approach, the experts do not know when to perform maintenance before failure, early failure detection, and condition monitoring in real-time, which is very challenging. Therefore, the need for an efficient method for wheel fault condition assessment and diagnosis is high, and the workshop maintenance divisions are looking and requesting for further fault diagnosing methods that are adaptive, simple, efficient, and low-cost approaches to enhance the wheel fault diagnosis for real-time condition monitoring of tram wheelsets system during operations.

For this purpose, vibration analysis of a signal acquired from railcars during railroad drive operation using a MEMS-based sensor is proposed. Preliminary studies show that the frequency bandwidth of vibrations is significant for evaluating the condition of wheels falling within a few hundred Hz, which is possible to measure with the MEMS-based acceleration sensors. The use of low-cost, low-power MEMS sensors ensures economic viability.

The research question of the study is specified as:

In what way MEMS-based acceleration sensors can be applied to assess the condition of wheels of wheelsets of railcars during railroad drive?

The use of MEMS-based acceleration sensors limits the scope of available measurement data for processing. These devices can deliver acceleration measurements in a number of axes in space. Basically, these are the three perpendicular planes – x, y, and z. The range of acceleration values can surpass 200 [m/s^2] and the resolution of measurements can achieve 0,01 [m/s^2]. The frequency response can reach 4 kHz. This limited scope of measurement data requires a careful approach for extracting diagnostic information.

The time-frequency-based analysis is proposed for determining the properties of the collected data. The study assumes that wheel irregularities produce disruptions in the

frequency spectrum of recorded accelerations and that these vibrations can be used to derive information on the condition of the wheels. The rail vibration energy in the characteristic frequency spectrum indicates the wheel fault condition.

The provisional research hypotheses answers are put forward as the following.

1. The analysis of the vibration signals or image with a 0-500Hz limited frequency spectrum, of the railways during a railroad drive, enables the assessment of the fault condition of wheels.
2. The energy of vibration signals in characteristic frequency bands during a railroad drive indicates the condition of wheels.

The tasks required for proving these hypotheses encompass a series of steps, which are not limited to the following.

The initial step involves the collection of vibration data from rails, which is generated by railcars during actual railroad drives. The railroad drives map the conditions of dispatching trams for transport services. During this stage, it is crucial to ensure that the acquired data is not corrupted by vibrations caused by bad rail conditions.

Subsequently, signal processing and analysis are imperative. The choice of an effective method for extracting "fault wheel condition" is crucial for performing the analysis. For a such signal processing, the candidates are time-frequency analysis techniques. A promising method within the realm of time-frequency analysis techniques enables the mapping of frequency anomalies, which specifically targets relevant features for wheel fault condition assessment. Determining the parameters of the analysis technique is the goal of this step.

Thirdly, it is necessary to develop a fault wheel assessment test on the field. This involves creating a field test that establishes the relations between vibration patterns and wheel conditions, taking into account the description parameters of the vibration data. Energy, in characteristic frequency bands, is recognised as the most informative for determining wheel fault conditions.

Lastly, validation of the proposed method is carried out. This involves conducting drives tests sessions and tuning of parameters of the method in real-world scenarios.

1.4 Objectives

The objective of the study is to develop and validate a method for assessing the condition of wheels of railcars using vibration analysis during railroad drives operation. The study aims to establish relations between vibration patterns and wheel fault conditions, enabling efficient and reliable assessment of the condition of railcar wheels.

Specific objectives:

- Propose a way of identification of irregularities of the vibration frequency spectrum.
- Determine the characteristic frequency bands of vibrations significant for describing the condition of wheels.
- Propose measures for collecting vibration data during railroad drives with the minimum resources possible.
- Develop an implementation of the vibration data analysis that will facilitate wheel-rail maintenance workshop operations.

The wheelset of railcar wheel faults and surface defect assessment during in-service operation are key topics in the field of railway research, as they have a large impact on the economic and safety aspects of train set design, operation, and rolling stock maintenance. One of the main causes of the increased dynamic impacts dependent on the vehicle at the wheel-rail point of contact is defects or irregularities on the running surface of the wheels, and solving these problems is very impressive. Today, the advancement of railway engineering requires scientific research to improve current problems related to safety issues, time, resources, and the structural integrity of wheel-rail systems.

1.5 Dissertation layout

Chapter 1, presents the background of wheel fault analysis in railway infrastructure, identifies the research problem and defines measures for resolving it. In particular, the solution scope is marked, research hypotheses are put forward, objectives and study goals are detailed.

In chapter 2, the literature review in the field of fault diagnosis, related to the stated research problem, is presented and discussed. The properties of time-domain analysis, frequency-domain analysis, and joint time-frequency-domain analysis methods are evaluated for extracting frequency features for diagnosing faults in wheel and railway systems.

Chapter 3, presents the method for assessing the condition of wheels of wheelsets of railcars during railroad drives. The variants of the method are discussed. Vibration data collected using MEMS-based acceleration sensors constitutes the input of the devised method and MODWPT is used to obtain the description of the data.

The validation of the method is presented in Chapter 4. Vibration data collected at the tram depot of Silesian Trams is analysed using the proposed method. The parameters of the method are tuned and optimised to achieve the best-diagnosing properties.

In Chapter 5, the IoT solutions of the sensor node for wheel condition monitoring for a practical application that optimises energy consumption, efficient wireless communication and low-cost maintenance is elaborated.

Finally, chapter 6 summarises the overall findings gained and puts forward a future perspective as a recommendation for a scholar in the same field.

2

Methods for Assessing Wheel Condition; Literature Review

The goal of the design of methods for assessing wheel conditions, in the area of fault diagnosis and condition monitoring, is to define measures to identify fault conditions in the wheelset components and railway infrastructure. The measures should be robust enough for application in maintenance operations at workshops or on railway in-service operations. In this regard vibration analysis techniques are prominent. time-domain analysis, frequency analysis, and time-frequency-domain analysis dominate.

In this chapter, a survey of the existing literature on monitoring conditions of railway wheel faults is presented. This review aims to provide an in-depth understanding of the current state of knowledge and identify research gaps in the field. The vibration signal analysis framework, particularly focusing on digital signal processing techniques such as time-frequency methods, is identified as one of the most valuable approaches and

employed to address the research question at hand.

2.1 Condition monitoring of wheels of railcars

The condition monitoring of the railway wheels is a process of continuously observing and checking the progress of the functionality of the wheelset component to ensure the optimal performance and safety of rail transport. This condition monitoring uses various techniques and tools to detect defects, abnormalities, or faults in the wheels. By collecting real-time information and monitoring the dynamic behaviour of a train, railway wheel monitoring aims to identify faulty conditions that can impact the overall performance and safety of the rolling stock. Some of the common fault condition problems that can occur within a railway wheels include flat wheels, wear, discrete defects, polygonal wear, out-of-roundness, and spalling, which are local surface defects that can cause increased contact forces between the wheel and the rail, causing excessive vibrations and potential vehicle derailment.

In the past 30 years, extensive research has been conducted on wheel fault diagnostics, resulting in the development of numerous techniques. A recent study done by Kostrzewski and Melnik [2021] presents a comprehensive literature review and bibliometric analysis to examine the monitoring of conditions of rail transport systems. The authors outlined the current trends in condition monitoring approaches and their significance in the maintenance of rail transport systems throughout the previous decades. The article also discusses the evolution and trends in condition monitoring for rail transport systems, highlighting the shift from manual maintenance to sensor-based technologies. In this regard, the studies identified key trends such as increasing sensor use, automation of diagnostic procedures, and the need for sophisticated data interpretation methods. Furthermore, future predictions such as further automation, the application of artificial intelligence, and the Internet of Things to enhance condition monitoring are presented. The paper also suggests a research agenda focused on optimising sensor usage and exploring alternative monitoring methods.

The manual maintenance techniques applied to monitor the condition of railway wheels include visual routine inspections conducted by skilled field technicians. These manual inspections involve measurements of important wheelset parameters such as the

wheel back-to-back distance and wheel tread profile Osman and Yacout [2023], Emoto et al. [2022]. However, manual measurements are time-consuming and require significant effort from engineers and technicians Mal et al. [2022]. In addition, these methods are inherently inaccurate due to the potential of human error and are inefficient. To overcome these limitations, there is a need to develop automated inspection systems using sensors and image data. These systems can provide accurate measurements, reduce maintenance costs, and improve the efficiency of inspections.

Alemi et al. [2017] present condition monitoring approaches for detecting railway wheel defects, emphasizing the importance of data acquisition for maintenance planning. The authors classify the collection of in-service data into onboard and wayside measurements, exploring advanced techniques and identifying areas for further research. The paper also compares physical, statistical and condition monitoring methods for assessing the conditions of railway wheels. The conclusion of the paper suggests the use of multiple sensors and stations to improve data acquisition, leading to better diagnostic approaches and increased detection efficiency. The limitations of this study may be the focus on existing data acquisition techniques without proposing new solutions, and it does not address the implementation challenges of these techniques in real-world scenarios.

Fu et al. [2023] review recent wayside railway wheel flat detection techniques, emphasizing the shift towards simplified devices, multi-sensor fusion, and intelligent algorithms. The authors discuss stress-based methods using sensors like strain gauges and fibre bragg gratings for dynamic stress measurement. However, the challenge of detecting wheel flats with limited information from single-pass wayside methods, forces for looking towards advanced signal processing algorithms. Based on this review article, further simulation studies are needed to evaluate the impact of train speed, train weight, and severity reflected in wayside measurement data on the wheel flat detection.

Furthermore, a diagnostic and detection algorithm for onboard wheel flats was suggested by Bosso et al. [2018]. This algorithm relies on computing a wheel-flat index number to detect and quantify the severity of flat wheels at an early stage. To calculate the flat severity index of the wheel, the authors used properties of acceleration measurements, wheel rotation angle, vehicle velocity, and flat surface depth. These properties are combined in a time-domain analysis to detect the presence and severity of wheel

flats. The study measures vertical axle-box acceleration and wheel angular position for wheel flat phenomenon detection. The method relies on the fact that a flat section of the wheel generates a significant vertical acceleration with each rotation when it encounters the rail. However, during data acquisition and testing, a lower sampling frequency (1000 Hz) was used, which has the effect of altering the detection and diagnosis of wheel flats that produce high-frequency components.

Sun et al. [2021] proposed a framework for railway wheel condition monitoring using vertical axle-box vibration acceleration sensors. They applied the angle domain synchronous averaging technique (ADSAT) to extract the wheel defect features from the sensor data. The study compares the proposed ADSAT and traditional methods by demonstrating that the ADSAT-based method achieved higher-order detection and also mitigates the influence of background noise than traditional methods. The authors validated the effectiveness of the proposed method through simulation and real field investigations. However, the noise reduction capability is not easy to quantify in field data due to the difficulty in evaluating the power of the desired signal component and also due to vibration data properties; the proposed method has limitation to detect the direct component of wheel irregularity, which is evident in the manual measurement results.

Detection of railway wheel polygonization through numerical time-frequency analysis of axle-box acceleration is proposed by Song et al. [2020]. The authors evaluate the evolution and severity of wheel polygonization by analyzing the acceleration data from the axle box. Nevertheless, this study only presents findings based on computational simulations. In addition, axle-box vibration data is less sensitive to studying the polygon wear of railway wheels, and the proposed method is insensitive to low-speed fluctuations.

On the other hand, Wang et al. [2020] present a three-dimensional vehicle-track coupled dynamics model that includes axle-box bearings and considers non-linear factors like bearing stiffness, clearance, wheel-polygonal wear, and wheel-rail contact forces. The authors highlight that axle-box bearing forces increase with vehicle speed and polygonal wear amplitude, especially at higher speeds, which can lead to bearing and wheel degradation. The proposed method was validated by involving numerical simulations and field tests, with a limitation being the focus on specific wear patterns and their impact. This may not include all potential variables affecting axle-box bearings.

Zhao et al. [2020] studied the different effects of drive and trailer wheelsets on polygonal wheel wear. The study was conducted using a frictional self-excited vibration analysis method. The results show that the unstable vibration frequency of the driving wheelset leads to polygonal wheel wear in the order $19-20^{th}$, and the trailer wheelset leads to polygonal wheel wear in the order $20-21^{st}$.

A wear monitoring parameter for wheel-rail contact based on emitted noise has been proposed by Bergseth et al. [2019]. This study found that contact noise and vibration-induced increases as a transition in the wear fault regime (low to moderate, severe to disastrous wear) happens. Even though the degree of roughness in the track and the vehicle speed are some of the many factors influencing rolling noise, the suggested approach only measures extreme wear change at the maximum levels of wear values and does not specify when severe wear situations arise from noisy emissions. Also, only higher-frequency components >5 kHz are considered in the evaluation and analysis of the noise signals.

Thakkar et al. [2010] designed an onboard measuring device for wheel flange faults in railway vehicles using an inductive displacement sensor. The device is capable of functioning during both stationary and moving states of the vehicle, capturing data on the thickness of the wheel flanges to identify potential faults. However, this study does not analyse the time-frequency response of individual wheels, making it challenging to distinguish specific fault conditions within each wheel component.

Chen et al. [2021a] introduce hybrid microphone array signal processing to identify faulty wheels and estimate ground impedance. Mosleh et al. [2021] uses an envelope spectrum analysis approach for flat-wheel detection in railway train wheels. Lanza di Scalea and McNamara [2004] applied longitudinal and lateral transient vibration characterisation of railroad tracks using wavelet transforms. Brizuela et al. [2011] report work introduce an ultra-sound technique based on measuring the changes in the round-trip time of flight (RTOF) of the ultrasound pulse to the rail–wheel contact point for detecting and quantifying wheel flats.

Madejski and Gola [2006] discusses an autonomous tram wheel condition monitoring system developed, which has led to significant savings in wheel re-profiling and reduced noise levels. The system processes measurement data at the trackside and wirelessly

transfers it to a control room database for diagnostic analysis and action recommendations. It utilizes radio frequency/identification (RF/ID) tags for tram identification and sensors built into the track for detecting wheel flats and material build-up.

Barman and Hazarika [2020] investigated an accelerometer-based system that detects and identifies the faults of a train using linear and quadratic time-frequency analysis. The linear analysis includes a short-time Fourier transform and wavelet transform, whereas the quadratic time-frequency analysis mainly uses the Wigner-Ville transform. This transform offers high resolution in both time and frequency. The authors used the Wigner–Vile transform analysis of the vibration signal during the movement of a train over the track and faults was detected. However, studies employing frequency methods do not incorporate time data, and the specific timing of impulsive loading during fault conditions remains unknown.

Gao et al. [2020], proposed a flat-wheel detection and quantification method based on measuring the wheel-rail impact force of the entire wheel circumference. The method utilises two reflective optical position sensors positioned along the rail to detect displacement. Analysis of impact-response curves is used to assess the condition of the wheel and determine parameters related to its flatness.

Komorski et al. [2017] presented wheel-flat detection using advanced acoustic signal analysis techniques. The researchers captured the sound characteristics of tram wheel faults by deploying three sets of microphones positioned along the tram tracks. They utilised the Hilbert transform and spectrum envelope analysis to identify any potential faults. The findings from the experiments demonstrate that acoustic signals obtained near a passing rail vehicle effectively convey valuable diagnostic information for identifying flat wheels. However, it is noted that these acoustic signals can be significantly influenced by other ambient sounds, necessitating additional filtration processes for accurate detection

Jianhai et al. [2002] used continuous wavelet transform to detect irregular meshing in wheels with tread defects. The vibration signals collected by the sensor from a railway wheel are used and processed for detecting wheel flats. For this analysis, a sampling frequency of 10 kHz is chosen for a vehicle speed of 60 km/h. The applied method is more effective at detecting flat spots on wheels than it is for identifying wear on treads,

with the signal response of a flat wheel exhibiting the greatest amplitude.

Ghosh et al. [2021] report the use of fast Fourier and wavelet transforms to detect the condition of rail tracks in real-time. The results show that corrugation faults are more likely to be detected by the fast Fourier transform than by the wavelet transform, while crack damage is more likely to be detected by the wavelet transform than the fast Fourier transform. In this study, vibrations are measured using accelerometer sensors mounted on the axle boxes of service trains, which are susceptible to interference from other vibration sources. The proposed detection approach is better suited for identifying rail corrugation but less effective in detecting wheel defects.

Zhang et al. [2017] established an adaptive parameter blind source separation approach for the diagnosis and monitoring of wheel defects. This method processes signals from acceleration sensors mounted on the wheels, and it can separate weak fault sources from a mixture of vibration signals related to train movement. Additionally, Liu et al. [2019] presents a similar approach for the detection of wheel thread defects. The study utilises wayside-mounted fibre bragg gratings to measure rail deflections and defect-sensitive features are obtained using Bayesian blind source separation techniques. However, numerous variables, such as train speed variation, sharp rail geometric variation, and the location of the fibre bragg gratings sensor with respect to sleepers influence defect detection results.

Li et al. [2017] proposed an adaptive multi-scale morphological filter for the fault detection of railway wheel flats. The input signal of the filter is the vibration signal of the railway vehicle's axle box caused by the wheel flat. An adaptive multi-scale morphology filtering analysis algorithm extracts the wheel-track impact features from strong background noises. For validation purposes, simulation results of simple vibration models consisting of one impulsive function and two sine-cosine harmonic waves with Gaussian white noise are used. However, no field-investigative data are provided.

In their study, a method for identifying flat wheel lengths based on data analysis was proposed by Ye et al. [2019]. The researchers utilised a multibody dynamics (MBS) model to generate artificial axle-box acceleration data for a 20 mm flat wheel under varying vehicle speeds. To estimate the length of the wheel flat, they employed a Kriging surrogate model to represent axle-box acceleration and utilised particle-swarm optimisa-

tion. However, it is important to note that the precision of this approach relies on factors such as the MBS model, wheel-flat mode, and feature-selection technique. Additionally, more features reflecting real-time conditions of wheel flats are necessary for accurate detection in practical scenarios.

Most of the established techniques in the literature above rely on well-saturated measurement approaches, which assume there is no signal interference in a real-time operation, for recording accelerations, analysis and identifying wheel defects. Therefore, it is essential to detect wheel faults amidst changing operation conditions and the intense interference that can distort the fault signal feature measurements using different sensors. The gathered data undergo analysis using different frequency-based methods. While these strategies effectively identify faults, their practical application in the field of wheel maintenance may be challenging or expensive.

The constantly changing operating conditions that damage the conical shape of the wheel are responsible for a significant portion of the wheel-rail wear, flat spots, polygonal wear, and tread spalling complexity Thompson [2008], Gan et al. [2015]. As far as wheel abnormalities reduce safety operations, the condition monitoring system is the most promising and effective technique for providing safety and economic improvement for industrial railway companies. An efficient condition-based maintenance system that can provide timely information on the condition of the wheels and other key components to railway operators is required to ensure operational safety and reduce maintenance costs.

The monitoring and diagnosis of train wheel condition is one of the essential aspects that most researchers are working on nowadays to provide good service and save resources in the rail transportation sector. Several studies have been done and various diagnostic techniques have been established Abid et al. [2021]. Most of the established condition monitoring, fault diagnosis and detection techniques (FDD) range from traditional model-based approaches to modern pattern recognition approaches. In this dissertation, the attempt made is to narrow down the general fault detection approaches to specific technique categories of data-driven methods, which is followed by signal-based approaches, and finally focused in detail on vibration-based techniques.

Data-driven methods are model-independent methods that are used to extract information from the measured signals to predict the occurrence of a fault or malfunction.

The raw information from the measured variables is first transformed into useful fault-characterizing features by signal processing tools.

Signal analysis-based approaches use both statistical and non-statistical approaches to extract the features of a signal. Statistical approaches are very practical for quick fault detection but are generally not suited for classification and diagnosis purposes. On the other hand, non-statistical interpretation of the observed signal is also carried out through machine learning fault detection techniques.

With the development of technology and the advancement of computing methods, machine learning has become a popular feature extraction, selection, and fault diagnosis method. The key principle in the feature selection process is to obtain a feature subset that produces fast detection and accurate classification of faults. The major challenge in designing intelligent FDD methods like machine learning algorithms is developing a knowledge base from raw historical data, and this method is not the subject of this dissertation.

Among data-driven methods, vibration signal-based fault diagnosis methods have high-performance accuracy. Therefore, many researchers have proposed this method to diagnose gear, bearing, alternative current (AC) motor, and rotating machinery faults. Modern vibration techniques employ different monitoring approaches to identify faults in machinery, and the diagnostics technique is a well-established field and employs various methods, mainly time-domain statistics, spectral analysis, wavelet transform, Hilbert transform, and empirical mode decomposition.

Whereas, conventional vibration techniques are incapable of diagnosing transient faults during their early stages of development and exhibit low sensitivity for diagnostic capability. The presence of multiple vibration sources, non-stationary dynamic phenomena, and the influence of transfer functions on the vibration source and transducers put great constraints on classical vibration techniques. As a result, techniques for processing vibration signals for fault diagnosis and monitoring requires additional research to determine the most effective methods.

For the railcars to run smoothly and safely, the health of the railway wheel is essential. In this dissertation work, the focus is to use vibration signals induced by vehicles during railroad drives to diagnose and monitor the train wheel fault. The vibration

signal produced by a rotating wheel is used for fault diagnosis and condition monitoring purposes Abid et al. [2021]. Nowadays, the diagnosis of bearing faults is of interest to many researchers, and much research has been done to solve the problem of bearing elements using signal vibration analysis. However, the diagnosis of wheel faults, which are probably one of the leading causes of bearing faults in railway infrastructure, has not been studied in different aspects.

From the perspectives of system configuration design, sensor performance, data acquisition systems, and wheel defect identification algorithms based on online monitoring data, more efforts are yet to be made to improve the performance of existing detection methods to make real-time wheel fault detection methods more easily applied. Although there have been numerous real-time wheel defect detection techniques in these decades, the current capabilities require further improvement. Therefore, the details of wheel fault diagnosis categories, analysis of each method, and selection of the best method for the implementation of a particular application are presented in this chapter as the following.

2.2 Vibration-based condition monitoring

Vibration-based condition monitoring of railway wheels plays a vital role in guaranteeing the safety and effectiveness of train operations. When a fault is initiated in a railway wheel system, the vibration characteristics of the wheelsets and their components start to change. This shows that by monitoring the vibrations of the wheels, potential faults can be detected early on with diagnostic tools that support timely maintenance and prevent serious issues from occurring. This can be achieved by installing different sensor devices, such as accelerometers, strain gauges, and eddy current sensors, on the wheelset and rail track, which can detect abnormalities in the vibration pattern. Mounting of the sensors either on rail tracks or wheelset components is determined based on the type of infrastructure intended to be monitored. These mounted sensors collect data on the frequency and amplitude of vibrations, which can then be analysed using advanced signal processing techniques. This monitoring approach allows for the identification of wheel faults

Vibration-based fault condition monitoring and diagnosis is a well-established field

that encompasses a wide range of techniques employing mainly time-domain analysis, frequency-domain analysis, and time-frequency domain analysis to extract features from vibration signals collected by sensors. Among the methods, the time-frequency method is a widely used and effective technique nowadays. The detail descriptions and recent development related to each technique is provided in the following subsections based on different application requirements.

2.3 Time-domain analysis of vibration signals

Time series data is a waveform of signals from the data acquisition device at its raw level. Time-domain data is a collection of time-indexed data points that represent the measurement parameters such as acceleration, velocity, or proximity are determined by the type of transducer utilised to gather the signal, as discussed in Jardine et al. [2006]. A time-domain analysis is performed directly on the time waveform data. When analysing a vibration signal in a time series, time-domain analysis is used to determine the amplitude and phase information contained in the signal.

Traditionally, time-domain analysis uses descriptive statistics techniques such as mean, peak, peak-to-peak interval, standard deviation, crest factor, and higher-order statistics such as root mean square, skewness, and kurtosis to extract valuable features from a time waveform signal.

On the other hand, time-synchronous average (TSA), root mean square, skewness, and kurtosis are among the popular time-domain analysis techniques used for fault diagnosis approaches. In addition, advanced time-domain analysis techniques such as autoregressive (AR) and autoregressive moving average (ARMA) models were highly utilised to fit waveform data to a parametric time series model and extract features of rotating machines such as wheelsets, rolling element bearings, and gear tooth fault diagnosis, as described by Cheng [2014]. These techniques can be used for the diagnosis and detection of mechanical equipment failures. However, when a mechanical component fails, the frequency components of the signals change, making it difficult to distinguish the fault characteristics of the feature because the frequency information is hidden in the time domain.

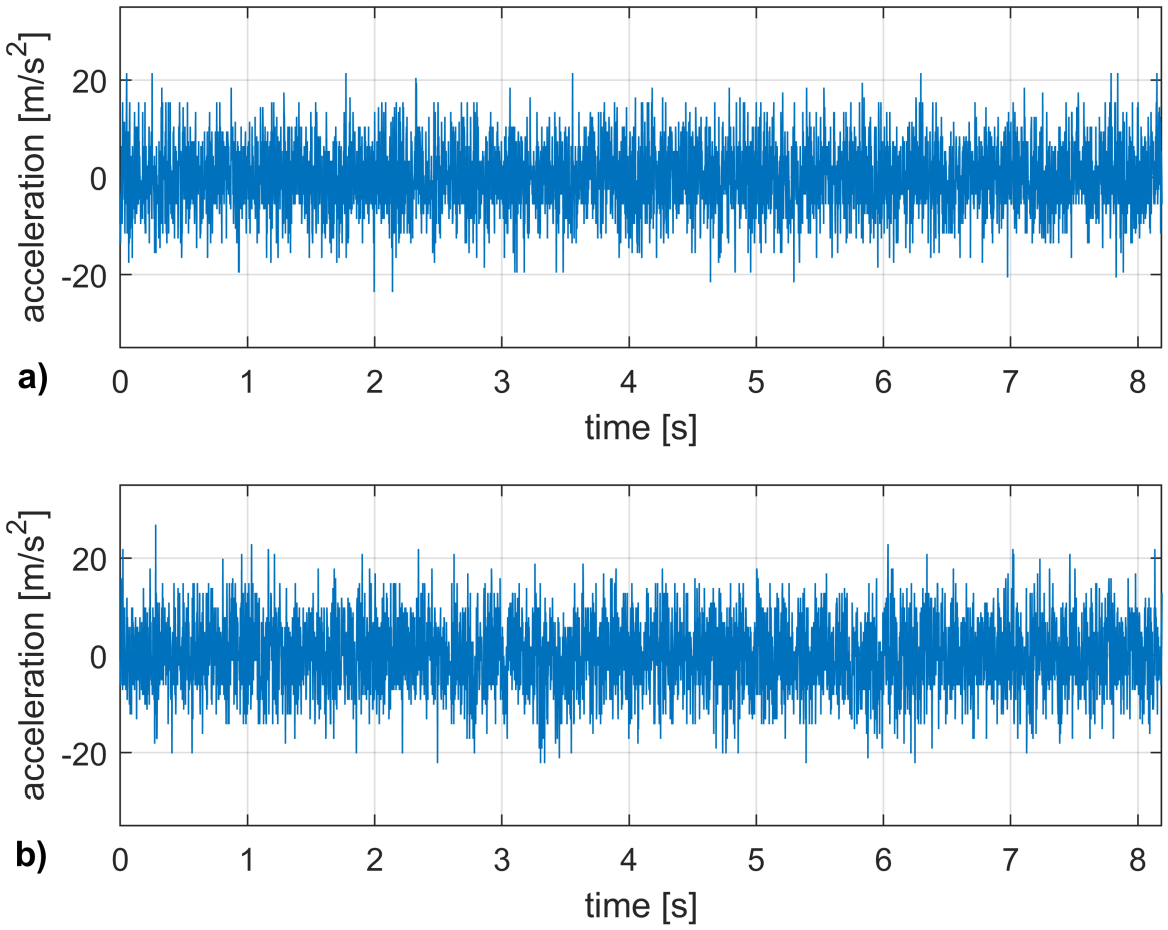

Figure 2.1: The lateral acceleration signals of railcars collected by MEMS sensor; (a) fault free wheel signals and (b) fault wheel signals

The time series signals shown in Figure 2.1 were collected by mounting a MEMS sensor on the rail track of Katowice tramways in Poland for wheel condition monitoring. As shown in the figure, the lateral acceleration of the railcars under a) normal or fault-free and b) with a fault conditions are collected for monitoring the condition of two different wheels. By closely looking at the time series information presented in the Figure 2.1, it is difficult to differentiate between the fault-free and fault wheel conditions of a railcar. The amplitude and time information contained in the graphs do not clearly indicate the difference between the signals. Therefore, another feature-extracting and analysing technique should be implemented to differentiate the content of the acceleration signals.

As shown in Table 2.1, time-domain feature extraction techniques and their capabilities are shown. The mathematical representation of the special parametric models, descriptive statistics properties of each feature extracting elements and reference related to each description in time-domain analysis are presented in the table.

Table 2.1: Time-domain feature extraction categories

Feature extracting type	Fundamental equation	Feature extraction capability description	Reference
Mean	$x_m = \frac{1}{N}\sum_{i=0}^{N} {x_i}^2$	The mean of the signal is constant and does not much sensitive to change in the signal and this cause the fault diagnosis to be limited	Caesarendra et al. [2013]
Root mean square (RMS)	$x_{RMS} = \sqrt{\frac{1}{N}\sum_{i=0}^{N} {x_i}^2}$	The RMS value will gradually increase as the fault develops. Incipient fault stage information is not provided by RMS, while the fault stage information increases.	Jardine et al. [2006]
Covariance (${\sigma_x}^2$)	${\sigma_x}^2 = \frac{\sum_{i=0}^{N}(x_i - x_m)^2}{(N-1)\sigma^2}$	When it comes to signals or datasets, variance is a measure of how far they deviate from a single mean or reference point.	Shen et al. [2012]
Standard deviation (σ_x)	$\sigma_x = \sqrt{\frac{\sum_{i=0}^{N}(x_i - x_m)^2}{(N-1)\sigma^2}}$	When it comes to signals or datasets, variance is a measure of how far they deviate from a single mean or reference point.	Shen et al. [2012]
Skewness(X_{sk})	$X_{sk} = \frac{\sum_{i=0}^{N}(x_i - x_m)^3}{(N-1)\sigma^3}$	Skewness is a measurement of the asymmetry in the probability density function (pdf) of vibration signal	Ahmed and Nandi [2020]
Crest factor($X_{CF} =$)	$X_{CF} = \frac{max\lvert x_i\rvert}{\sqrt{\frac{1}{N}\sum_{i=0}^{N} {x_i}^2}}$	Impact is quantified using the Crest factor (CF). In the case of "spiky" signals, CF is the best choice	Ahmed and Nandi [2020]
Spectral kurtosis (X_{SK})	$X_{SK} = \frac{\sum_{i=0}^{N}(x_i - x_m)^4}{(N-1)\sigma^4}$	Sensitive to impulsive load. Kurtosis quantifies the probability density function's (pdf) degree of flatness near its centre. The kurtosis value of the bearing normal is well-known as 3 during high-speed bearing rotation.	Villa et al. [2011], Antoni [2006]
Time-synchronous average (TSA)	$X_{TSA} = \frac{1}{N}\sum_{n=0}^{N-1} x(t + nT)$	The periodicity of the vibration signal is characterised by the TSA property. from the noisy vibration data, it extracts periodic wave patterns	Braun [2011], Mobley [1999], Xu et al. [2023]
Autoregressive (AR)	$x_t = \mu_t + \sum_{i=1}^{p}(a_i x_{t-i})$	AR compares the current(estimated) signal values of the vibration to previous time series values using linear regression analysis	Braun [2011], Xu et al. [2023]
Moving average (AM)	$x_t = \mu_t + \sum_{i=1}^{q}(b_i \mu_{t-i})$	A linear regression analysis is conducted, modelling the current signal series as a weighted sum of the time series values.	Ahmed and Nandi [2020]
Autoregressive and moving average (ARMA)	$\mu_t + \sum_{i=1}^{p}(a_i x_{t-i}) + \sum_{i=1}^{q}(b_i \mu_{t-i})$	It is a combination of AR (p)and MA (q)to achieve better flexibility in fitting actual time series	Yao et al. [2022]

Several studies were conducted using time-domain approaches to analyse waveform data for rotary machine fault diagnosis and prognosis. Ignjatovska et al. [2023] presents a methodology for the time-domain analysis of vibration signals from defective rotating machinery, under varying load conditions. The authors utilised a vibration dataset, applied time synchronous averaging (TSA), and evaluated the importance of statistical functions for fault identification. Key findings include the importance of the peak value, the root mean square (RMS), and standard deviation as influential parameters. The study focuses on the initial phases of creating classification algorithms for fault identification, with the aim of improving algorithm accuracy. However, future work must extract features from the frequency domain and time domain to create a comprehensive feature set.

Wodecki [2021] propose time-varying spectral kurtosis for the detection of local damages of rotary machines during time-varying operations. The authors employed time-varying spectral kurtosis to estimate segments of the signal, resulting in a coefficient matrix that considers the changing properties of the signal over time. This matrix is then converted into a binary format and utilised as a filter in the process. However, this study does not discuss the computational complexity or real-time implementation feasibility of the proposed method, which could be important considerations for practical applications.

Antoni and Randall [2006] demonstrates the application of spectral kurtosis (SK) in identifying and assessing faults in rotating machinery that generates transient vibration signals. Additionally, the author presents the idea of a kurtogram, which illustrates the SK based on the frequency and spectral resolution, assisting in creating effective band-pass filters for fault detection. However, the research involves theoretical assumptions like the Gaussianity and stationarity of the noise, independence of the impulses, and validity of the shot noise model. In practice, such assumptions are not always valid. Moreover, estimating spectral kurtosis can be affected by factors such as window length and number of averages, leading to potential bias and variance. Additionally, computing spectral kurtosis and the kurtogram demands significant data and processing time, which could limit their real-time feasibility despite their value.

In summary, although time-domain techniques are commonly employed for fault diagnosis and prognosis or rotary machines, it is crucial to acknowledge the limitations

of these methods. The potential challenges associated with computational complexity, real-time implementation feasibility, theoretical assumptions about noise characteristics, and factors affecting the estimation of spectral kurtosis need to be considered. These issues may impact the practical applicability of these techniques in industrial applications where quick decision-making based on fault detection is essential. While the insights obtained from time-domain analyses are valuable for developing classification algorithms and creating effective band-pass filters for fault identification, addressing these drawbacks using a frequency and time-frequency approach would be imperative for ensuring their broader adoption in real-world applications.

2.4 Frequency-domain analysis

Historically, condition monitoring of railway wheels has relied on Fourier analysis (FA) techniques to convert acquired signals into a more meaningful form. Frequency analysis is one of the most widely used vibration analysis techniques for monitoring the condition of machines. In fact, frequency-domain analysis techniques can divulge information based on frequency characteristics that are not easily observed in the time domain. In comparison to time-domain analysis, frequency-domain analysis can easily identify and isolate specific frequency components in a signal. This is an advantage of frequency-domain techniques over time-domain approaches.

The Fourier transform (FT), the most widely used signal transformation technique, facilitates the transformation of the time-domain signal to the frequency-domain. In addition, frequency analysis techniques enable the extraction of various features of the frequency spectrum that can more efficiently represent machine health conditions. Frequency-domain techniques rely on the proper utilisation of the Fast Fourier transform (FFT). The FT reduces the effect of phase shifts in time-domain data, presenting a more compact representation of the signal.

For example, the measured time-domain vibration signals are often generated by several components of a railway wheel such as the wheels, wheelset, bearings, and axle box. Each of these components produces a unique frequency. The measured signal often contains a summation of the produced frequencies rather than the individual produced frequencies. The spectrum of frequency components generated from the time-domain

waveform helps to identify the vibration sources from which components are produced.

Railway wheel components generate various types of vibration signals in the time domain. These can be random signals and periodic signals, for both healthy and faulty conditions Bocciarelli et al. [2004]. The frequency representations of these signals in the frequency domain are often performed using FA, which is generally classified into three types: (i) Fourier series (FS), (ii) continuous Fourier transform (CFT), and (iii) discrete Fourier transform (DFT). The fundamental idea of FA is dependent on periodic functions that can be expressed as a summation of complex exponential functions Sheng et al. [2007].

A Fourier analysis is used to extract features of a frequency spectrum that can more accurately reflect the machine's healthy status during operation. These include: (i) envelope analysis, also called high-frequency resonance analysis, which is a signal processing technique that is considered a powerful and dependable method for detecting faults in rotating elements; and (ii) frequency-domain features, which provide a quick overview of a machine's condition without specific diagnostic capability and which include arithmetic mean, matched filter RMS, the RMS of spectral difference, the sum of squares spectral difference, and high-order spectra techniques Ahmed and Nandi [2020].

When relying on frequency-domain methods, energy leakage and spectrum overlap are common sources of significant errors. This makes frequency representation functions (FRFs) less sensitive for fault detection and identification at a very defined periodic time Peng and Chu [2004].

The frequency-domain analysis techniques algorithm and the description used for the feature extraction are described in Table 2.2 with important notation. The table describes the continuous-time Fourier transform, discrete-time Fourier transform, fast Fourier transform and power spectral density (PSD) with their fundamental equations and feature extraction capabilities.

Spectrum analysis based on the FFT is one of the most widely used methods of frequency conversion. The principle of spectrum analysis is to obtain the signal's frequency components and look at certain interesting frequency components to find their relationship with the amplitude, the phase, or the power, and then the fault features can be extracted from the signals. The FFT computational efficiency is excellent, and

Table 2.2: Frequency-domain feature extraction techniques for vibration signals

Feature extraction category	**Fundamental equation**	**Feature extraction capability and description**
CFT	$\int_{-\infty}^{\infty} x(t)e^{-j2\pi ft}dt$	Enables signals analysis in frequency content only and requires high computational complexity.
DFT and FFT	$\sum_{n=0}^{N-1}(x(n)e^{\frac{-j2\pi kn}{N}}, k \to 0, 1, \ldots N-1$	Have excellent computational speed and does not indicate localised time-frequency of signals
PSD	$\lim_{x\to N}\frac{(\triangle t)^2}{T}\| \sum_{n=-N}^{N} x_e^{-j2\pi fn\triangle t}\|^2$	Adequately describes the additive noise and does not fully describe the multiplicative noise

it saves time, resources, and energy used during synthesis and analysis. The spectrum analysis mainly includes the amplitude spectrum, power spectrum, Cepstrum spectrum, and Hilbert spectrum. However, when a rotating component has a fault, the vibration signal will become non-stationary and non-linear, and the spectral composition of the vibration signal will often change with time.

FT and FFT are not practical for non-stationary, transient vibration signals to be analysed in the frequency domain, as the power spectrum of the signature gives only delocalised information on the frequency content. Furthermore, since the signal power is averaged on the whole frequency axis, two different vibration signatures may have a very similar power spectrum.

Based on the Boashash [2015], the frequency-domain analysis approaches of two different signals may have similar magnitude spectra, as shown in Figure 2.2. The difference is clearly visible in the time domain (left-hand traces), whereas it is hardly visible in the frequency domain (right-hand traces). The present observation serves to demonstrate that the frequency domain manifests the frequency composition that is contained in the entire signal, irrespective of any temporal influence. This indicates that the frequency content of the signal is not a function of time.

By utilising the properties of the FT, efforts were made to examine the state of the wheel component of Katowice urban trams. The analysis involves collecting vibration signals of rail track by employing a sensor device on a rail track, then processing the collected data through a frequency-domain approach, which entails extracting the spec-

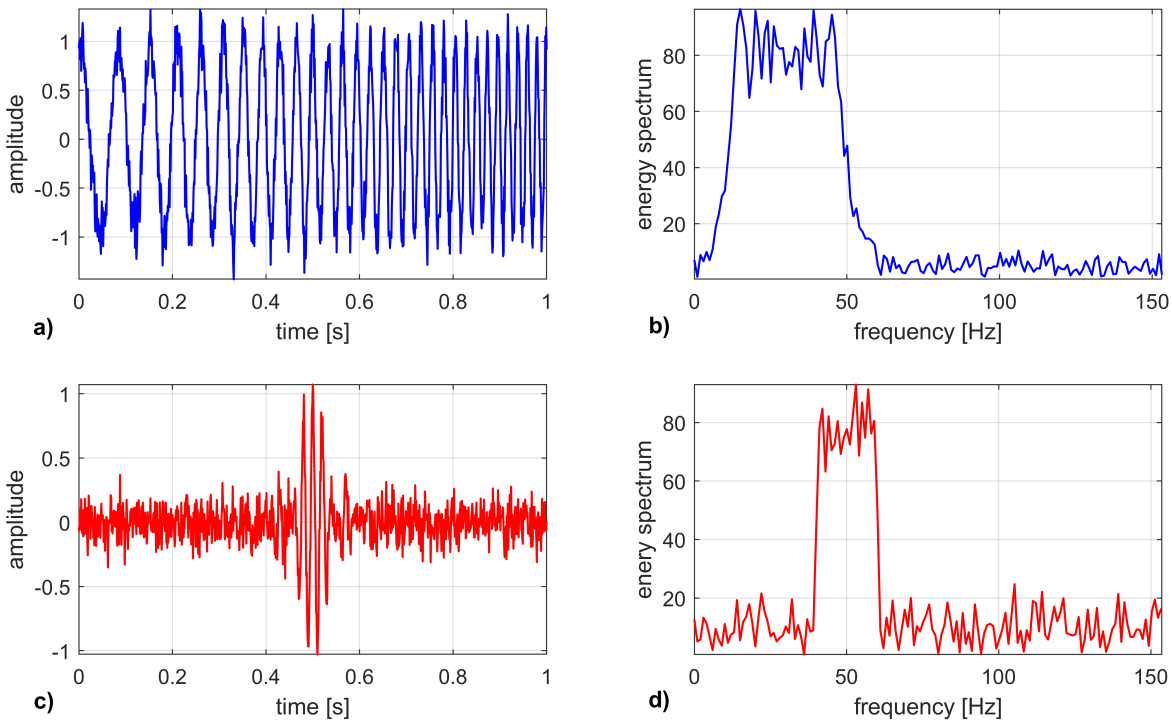

Figure 2.2: Power spectrum of a) a noisy low-frequency modulation signal with an SNR of 16dB and b) its energy spectrum; c) a noisy modulated sinc function with the same SNR and d) its energy spectrum

tral frequency of the rail track signals. Figure 2.3 and Figure 2.4 showcase the power spectral density of the signal under fault and normal wheel conditions respectively.

By closely looking at Figure 2.3, the frequency spectrum of the signals collected under fault-free conditions, the impulsive overshoot of the frequency spectrum resulted within the range of 400 Hz to 450 Hz and experiences huge variation in dispersion. Similarly, in Figure 2.4 for a wheel with fault condition, the impulsive power spectrum of a signal resulted within the ranges of 180 Hz-230Hz. There is a prominent spike around 200 Hz, indicating a significant anomaly or feature at this frequency. This could potentially be associated with a specific type of fault condition on the wheel components.

For both signals, the time-domain information appeared to be similar. However, a shift in the frequency spectrum band was observed during the frequency analysis. One of the challenges encountered in this frequency-domain analysis technique is the inability to determine the exact time at which the spikes of this frequency spectrum occur and to which element of the wheel frequency that indicates fault condition is related. This makes it challenging to distinguish between wheels in good condition and those in poor condition. To enhance the accuracy of fault detection in railway wheels,

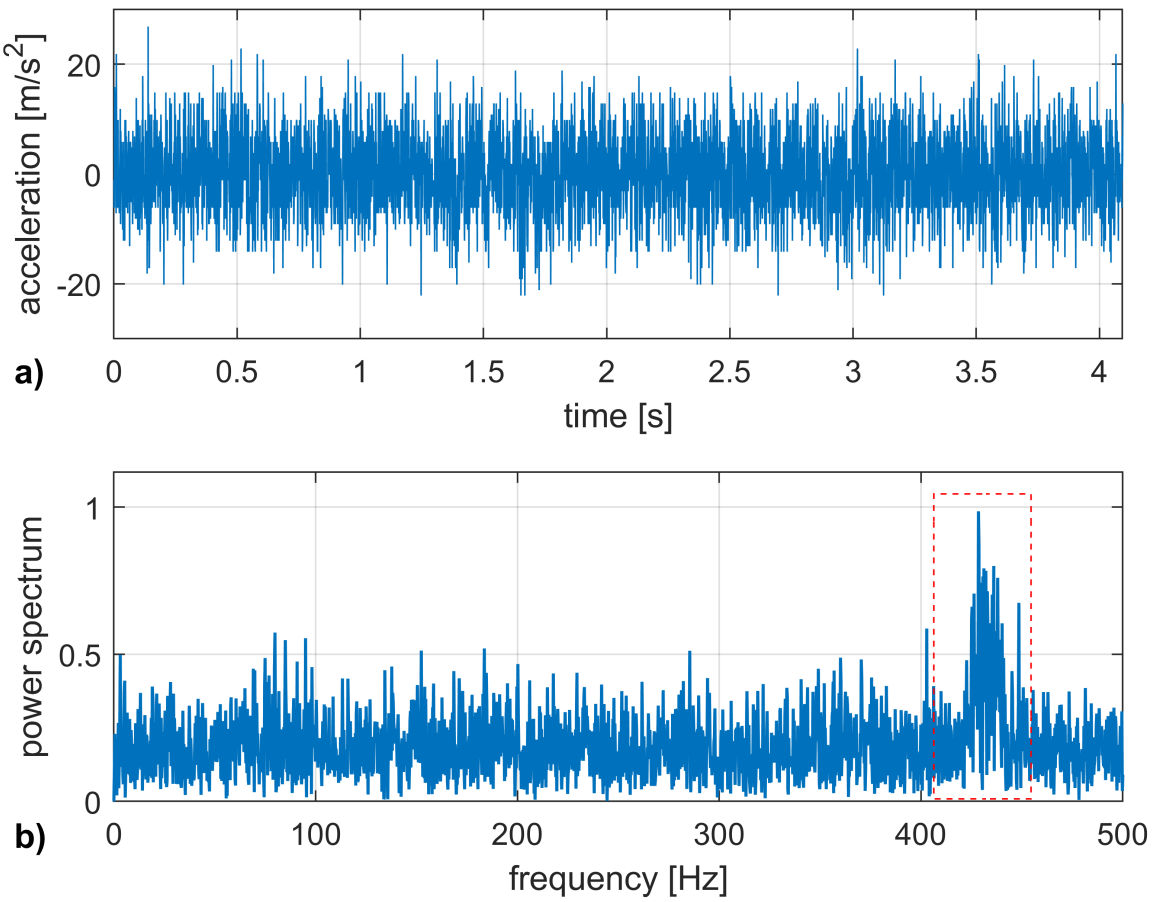

Figure 2.3: a) Time series and b) frequency spectrum of the fault-free wheel signal

this analysis results underscore the need for further signal processing techniques such as time-frequency domain analysis.

Numerous studies have utilised frequency-domain analysis techniques for fault condition monitoring of railway wheels and signal feature extraction. For instance, in a wheel-rail system, researchers have employed the fast Fourier transform to raw data to derive the power spectrum and gain insights into the signal's characteristic frequencies Zhang et al. [2011a].

Shim et al. [2021] discusses vibration signal processing techniques for identifying wheel flats in railway vehicles. They focus on utilising cepstrum analysis, order analysis, and cross-correlation analysis to address challenges posed by varying train speeds and high levels of field noise. However, assessing the flat wheel signal is complicated due to frequent changes in train speed which impact the time cycle of the flat wheel signal. Further research is necessary to refine fault detection and diagnosis accuracy in real-world operational settings.

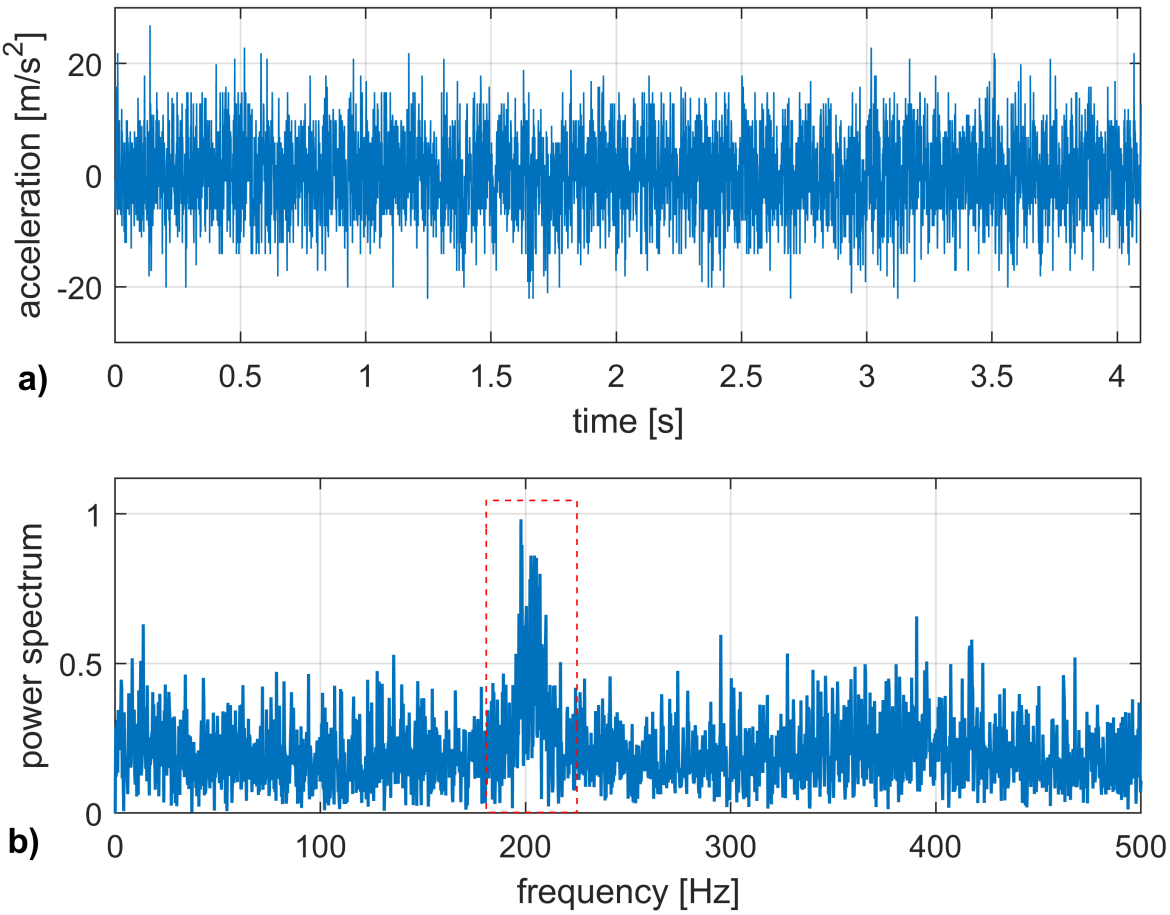

Figure 2.4: a) Time series and b) frequency spectrum of the fault wheel signal

Zhou et al. [2024] presents an experimental study on the detection of wheel flats (WFs) in railway vehicles using the angular domain synchronous averaging (ADSA) method. The ADSA method is shown to effectively detect WFs by averaging axle box acceleration (ABA) signals in the angular domain, reducing the amount of measured data and eliminating interference signals. However, the experimental study focuses on a single-wheel flat with a specific length of 20 mm on a tank wagon, which may not fully represent the range of WFs conditions that can occur in railway vehicles.

Kvasnikov and Stakhova [2022] explores the use of vibration analysis for early identification and prevention of critical machine fault problems. The approach involves examining vibration patterns through the Fourier transform to analyse the output signal connected to a sensor. The findings indicate that spectral analysis, specifically narrowband spectral analysis, is effective in identifying various faults and is vital for equipment monitoring and thorough diagnostics. Additionally, it underscores the significance of considering the relationship between spectrum bandwidth and signal accumulation time to enhance test efficiency. However, while FFT algorithms improve performance by reduc-

ing operations, they may introduce limitations such as resolution, leakage or windowing effects.

Another work that has been done by Atoui et al. [2013] discusses the application of FFT and wavelet transform in detecting faults in rotating machinery, with a focus on rotor unbalance. The approach entails utilising a combined FFT-wavelet transform method to analyse vibration signals collected from accelerometer sensors during experimental investigations on a defective rotor. The findings validate the capability of wavelet transform-FFT to promptly identify fault conditions and their locations.

In summary, FA is ineffective when the acquired signals exhibit non-stationary characteristics, as this method obscures the time localization of local oscillations. Therefore, it is impossible to determine whether the frequencies of the FT exist uniformly across the signal or are focused within specific localised intervals. Providing time-frequency analysis techniques such as a short-time frequency history of the localised signals, i.e. the short-time Fourier transform and wavelet analysis can mitigate some of the Fourier transform's shortcomings. Short-time Fourier transform and wavelet analysis reflect important feature characteristics of localised signals that FA cannot reflect. The details of the time-frequency analysing techniques which are used for processing vibration signals for condition monitoring of railway wheels are presented in detail in the Section 2.5.

2.5 Time-frequency analysis of vibrations signals

Fourier analysis and its related frequency methods have been established based on an ideal linear transformation model, which is a steady-state conversion. Therefore, they are suitable for dealing with linear and stationary signals. However, when industrial and rotating mechanical equipment fails, the vibration signal typically becomes non-stationary. The critical step in processing non-stationary signals requires performing a local time-frequency analysis. Unfortunately, FA has difficulty in processing a nonlinear and non-stationary signal in practical applications. As a result, time-frequency analysis was developed for non-stationary vibration signals analysis purposes.

Time-frequency distributions (TFDs) provide information about non-stationary signals that neither time-domain nor frequency-domain-alone representations can provide.

This includes the frequency of the instantaneous signal. TFDs can be used to classify non-stationary signals by extracting relevant (time, frequency) features as characteristics rather than using all (time, frequency) points as features, which would result in many redundant features, increasing the computational time and cost for analysis of the data.

Two significant deficiencies of the conventional time-domain and spectral analysis techniques include (i) the inability to interpret time dependence between frequency content and time and vice versa; and (ii) the difficulty in representing signals with non-periodic components, such as a transient signal. For example, specific frequency components indicate faults in rotating machines; however, because some of these frequencies are dependent on the rotational speed, it is impossible to determine these frequencies using spectral analysis when the rotating element operates at a variable rotational speed.

In addition, studies have underscored the importance of monitoring railway wheel systems and other rotating machinery during transient states like startup, shutdown, brake down, and acceleration. This is crucial as substantial component failures often occur during these transitional phases. Transient signals can yield important insights into the condition of the wheelset system that are not evident during steady states. Consequently, methods based on the FT may not be suitable for fault diagnosis and condition monitoring under changing time conditions Jardine et al. [2006].

A significant reason to use time-frequency representations (TFRs) and TFDs of signals is that they reveal whether the signal is mono- or multi-component, which cannot be determined easily using conventional frequency analysis, even more so when individual components are also time-varying. In summary, the (time, frequency) representation is more appropriate and intuitive for non-stationary signals.

Numerous time-frequency analysis techniques have been used to diagnose railway wheels faults condition, including short-time Fourier transforms, wavelet transforms, the Hilbert Huang transform, and empirical mode decomposition. The discussion, analysis, and selection of these time-frequency analysis techniques were given greater weight in this research work. More efficient methods other than using the FT and its frequency spectrum features are described for determining the best time-frequency characteristics of a signal. The following section describes each time-frequency technique in detail, including its defined scope, a review of related scope, and finally, the limitations related

to each technique.

2.5.1 Short-time Fourier transform

Cohen [1995] developed the short-time Fourier transform (STFT), which was the first modified version of the Fourier transform that could be used to analyse both stationary and non-stationary signals in the time-frequency domain. Gabor was the one who first introduced this algorithm, Gabor [1946]. Fundamentally, the STFT converts the vibration signal into a two-dimensional (2D) time-frequency function. The following relations give the fundamental equation of STFT for a specific continuous-time signal segment:

$$STFT_{x(t)}(t, w) = \int_{-\infty}^{+\infty} x(t)w(t-\tau)e^{-jwt}d\tau \tag{2.1}$$

Where $w(\tau)$ is a window function and τ is a time variable. For a vibration signal in discrete form, Equation 2.1 above becomes;

$$STFT_{x[n]}(n, w) = \sum_{-\infty}^{+\infty} x(n)w(n-m)e^{-jwt}d\tau \tag{2.2}$$

Instead of computing the discrete Fourier transform of the entire signal, the STFT decomposes the signal into shorter segments of equal length using a time-localised window function, such as a Gaussian or Hamming window and then performs the DFT separately on each windowed segment Sejdić et al. [2009]. This enables the frequency of the defect signal to be determined within a given time window. The time interval used in this method is very critical. By decreasing the window size, it is possible to achieve more accurate representations of signals in terms of time resolution, but this causes an increase in computational time. Furthermore, a longer time interval is required to improve the frequency resolution.

The challenge with using the STFT is that the accuracy of the frequency information extracted is limited by the window's length in relation to the signal's duration. Once the window function is defined, its area in the time-frequency plane (time-bandwidth product) remains constant. This means that the resolutions of both time and frequency

cannot be increased concurrently. STFT can overcome the limitations of FFT-based methods in processing non-stationary signals; however, it does not produce a constant resolution for all frequencies because it uses the same window for the entire signal during processing. Obtaining high-frequency resolution requires the use of wide windows for low-frequency components, which results in a trade-off with the time resolution needed for analysing high-frequency components. Therefore, STFT is suitable for analysing quasi-stationary signals instead of real non-stationary signals.

As a result of using the STFT, the frequency content of a signal can be determined based on its magnitude squared, or spectrogram. Spectrograms are chart representations of a signal that show its energy distribution over a time-frequency domain. The spectrogram of STFT can be mathematically presented using the following relation:

$$SPEC_{x[n]}(n, w) = |STFT_{x(n)}[n, w]^2| \tag{2.3}$$

The STFT technique is pivotal in this analysis as it enables the examination of these frequency components in a time-localised manner. By windowing the signal and transforming these windows into the frequency domain, it is possible to detect transient faults in the wheel that may not be perceptible in a standard FT.

Wigner introduced the Wigner-Ville distribution (WVDs) Ville [1958]. He derived a relationship between the power spectrum and the autocorrelation function for a non-stationary, time-variant process to analyse a signal. WVDs have overcome some limitations of STFT time-frequency resolution. However, when multiple component signals are applied, interference terms between the bi-linear distribution and the real signal overlap, and interpreting the energy distribution of the 2D image is a more challenging task in such a case.

Considering that the STFT does not use windowing functions with varying sizes for all frequency components, fault diagnosis and condition monitoring of rotating machines based on non-stationary signals, which are masked by noises, may need more adaptable and effective techniques than the STFT. Among these adaptable and effective techniques, the commonly used methods are presented in the next subsection. The choice of each technique depends on different factors, and there is no generalised rule. However, what makes these techniques more valuable than STFT is their ability to analyse the non-

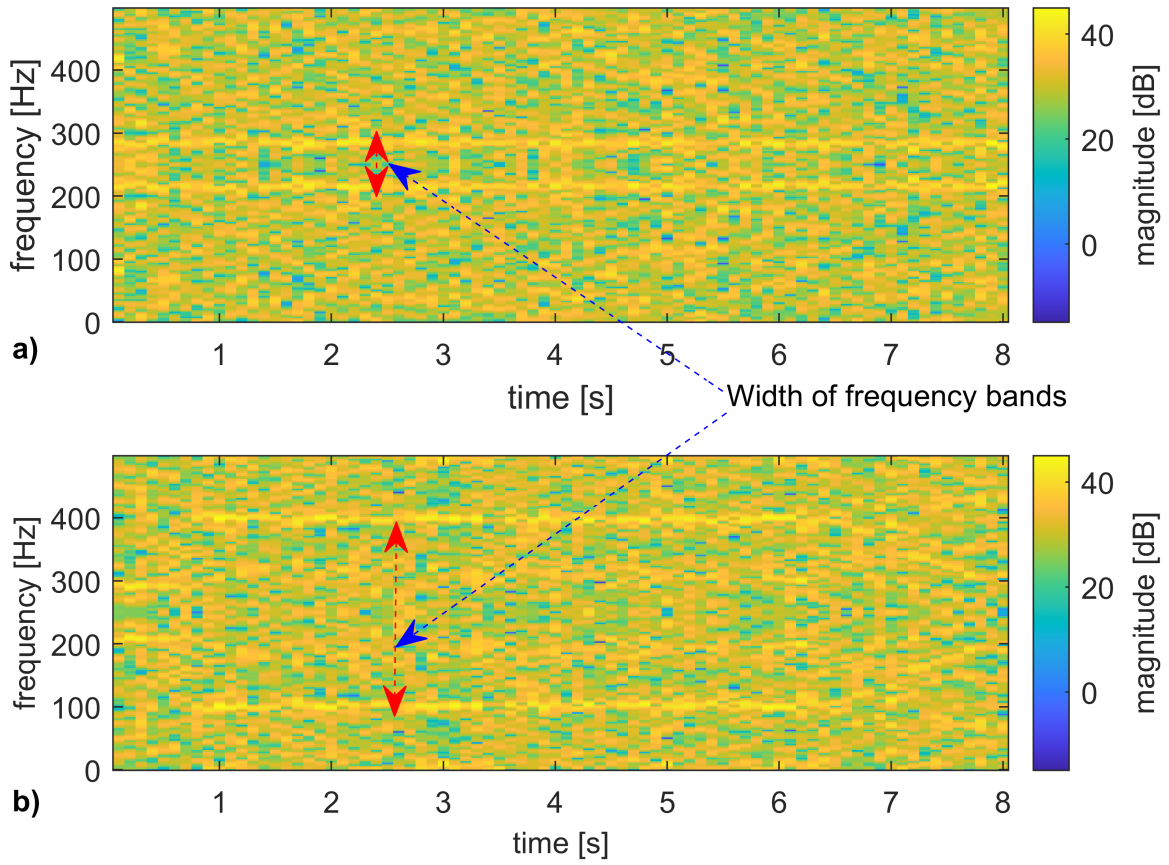

Figure 2.5: Short-time Fourier transform scalogram of wheel vibration signals with a) a normal and b) fault wheel condition

stationary vibration signals within a variable time-frequency window resolution needed for quantification of the content of the slice of a signal.

In the attempt made to analyse the acceleration datasets measured at the Katowice tram depot using the STFT technique, the potential of this technique is evaluated for extracting valuable features that indicate the wheel condition. For instance, Figure 2.5 provides a visual representation that displays two scalograms that illustrate the STFT of signals acquired by a MEMS sensor from a rail track to monitor wheel fault conditions. The STFT technique is utilised to determine the frequency and time characteristics of local segments of a signal.

The first scalogram in Figure 2.5 a) illustrates the frequency distribution of wheel signals collected under fault-free circumstances. The magnitude of the STFT coefficients is represented by a colour gradient ranging from blue to yellow, with yellow denoting higher magnitudes. Noteworthy high-magnitude frequency spectrum characteristic bands of the signals which are identified by red arrows at approximately the entire given time occur

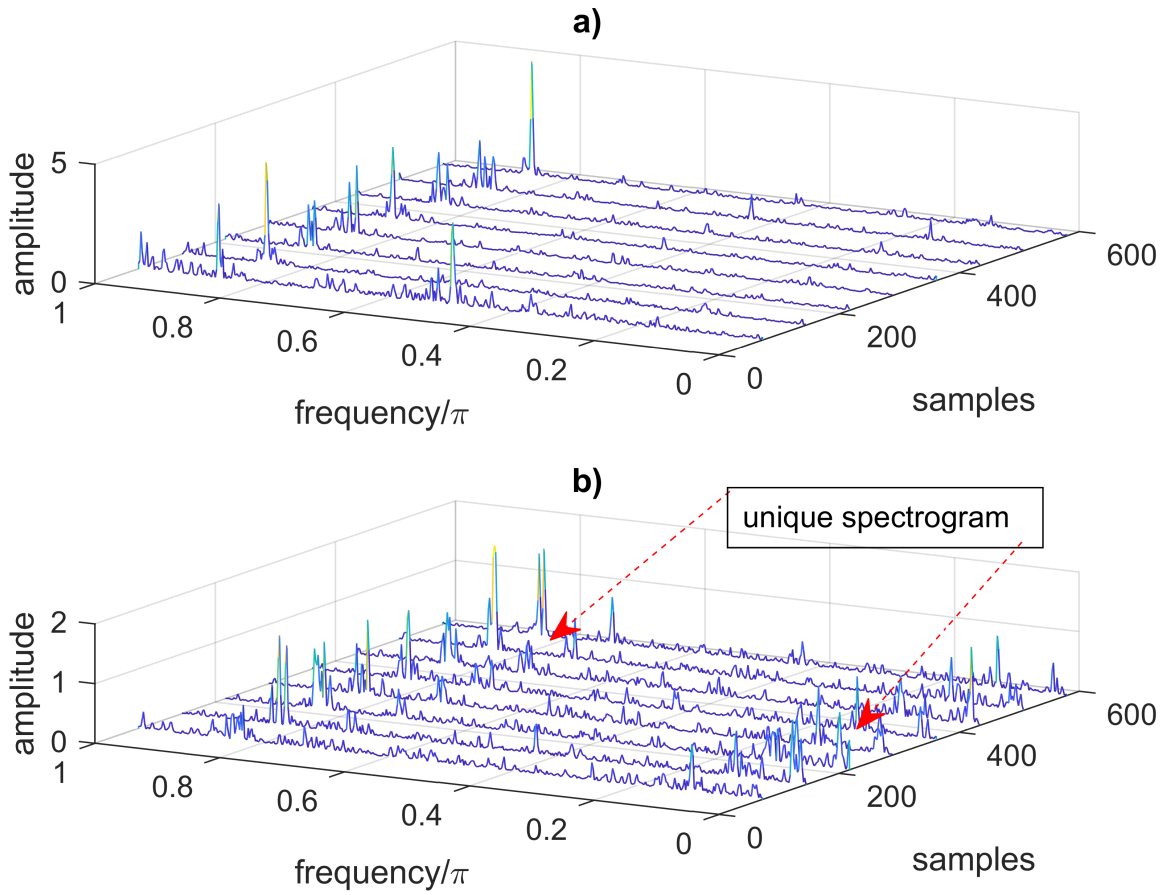

Figure 2.6: Short-time Fourier transform spectrogram of a wheel vibration signals with a) a normal and b) a fault wheel condition

at a frequency bandwidth of 200 Hz-300 Hz, which could potentially signify normal operational characteristics of the wheel.

The second scalogram of Figure 2.5 b) illustrates the frequency distribution of signals collected during a fault condition. Similar to Figure 2.5 a), the colour gradient represents the magnitude of the STFT coefficients. In the presence of prominent signals, at varying times and frequencies bandwidth of a signal is widened from 100Hz-400Hz which is indicated by both red and blue arrows, resulting in distinct types or stages of faults or anomalies compared to normal wheel signals. The STFT technique involves segmenting the signal's data into manageable portions and subsequently computing the FT on each segment individually. This approach yields a time-frequency representation that can be visually analysed as demonstrated in these scalograms.

Figure 2.6 presents a pair of 3D spectrograms of STFT, which are employed to examine the frequency characteristics of a signal over time. Figure 2.6 a) shows STFT spectrogram that displays various frequencies at different sample times. Notable peaks

in amplitude at specific times indicate prominent frequencies. Similarly, Figure 2.6 b) presents a unique spectrogram that marks certain frequencies with red arrows which are not noticeable in Figure 2.6 a). These frequencies could potentially signify abnormal or unexpected frequency components that may indicate a fault condition in the wheel.

In summary, although the STFT is capable of analysing non-stationary signals, it suffers from certain limitations. The fixed window size introduces a compromise between time and frequency resolution. Moreover, spectral leakage, edge effects, and aliasing, spectrum distortion of the original signal resulted due to the windowing function. Consequently, this may impact the accuracy of fault detection analysis. Therefore, alternative time-frequency processing methods become necessary despite the efficiency of the STFT in analysing non-stationary signals.

2.5.2 Wavelet transform

Another linear transform that provides time-frequency analyses is a wavelet transform (WT). A WT is a mathematical tool that converts a signal in the time domain to a different form in the time-scale domain, namely to a series of wavelet coefficients Chan [2011]. An implementation of the wavelet transform requires a wavelet function. A wavelet function is a small wave that exhibits oscillating wave-like characteristics and concentrates its energy in a short period. The difference between a wave (sine cosine, which is typically deterministic and time-invariant or stationary signals) and a wavelet is that a wave is usually smooth and regular in shape and can be infinite, while in contrast, a wavelet may be irregular in shape and normally lasts only for a limited period. The wavelet function is referred to as a mother wavelet or a father wavelet, and subsequent families of wavelet transforms are decomposed from this base function Bhatnagar [2020].

Morlet introduced the wavelet transform, and it quickly developed into a powerful mathematical tool. For N data points, the wavelet transforms computation time is $O(N)$, which is less than the FFT computation time of $O(NlogN)$. Wavelet transform is an adaptive transform that overcomes the STFT's resolution problem. It exhibits fundamental properties such as linearity, translation, dilation, and symmetry. The WT properties are well suited for performing multi-resolution analysis on a non-stationary signal both in the time domain (via translation) and the frequency domain (through

dilation). WT is a type of variable window in which the high and low-frequency components of the signal are analysed using a time interval. WT data can be decomposed into approximation and detail coefficients in a multi-scale manner, making it a more effective algorithm for the analysis of non-stationary signals than FT.

Compared to STFT, wavelets enable effective analysis of multi-scale signals and the extraction of time-frequency characteristics from non-stationary signals. Wavelet analysis is a good alternative to the STFT method because it localises the signal's information in the time-frequency domain via variable spectrograms. The wavelet transform enables time-frequency analysis and the creation of maps with high time resolution at high frequencies, thereby identifying the temporal instants at which transient phenomena occur: the presence of impulses in the vibration signal can be determined using the high-frequency part of the wavelet transform, where the time resolution is comparable to the duration of the analysed events Rubini and Meneghetti [2001].

In contrast to the STFT window, wavelet families such as Haar, Daubechies, Symlets, Morlets, and Coiflets all have fixed shapes. However, the wavelet function is scalable, which means it can be applied to a wide variety of frequency and time-based resolutions. As a result, wavelets are more suitable for analysing non-stationary signals than STFT. Nevertheless, because wavelets are not adaptive, their analysis results depend on the chosen wavelet base function. This may result in a subjective and prior assumption about the characteristics of a signal. In this case, only those characteristics of the signal that correlate well with the shape of the wavelet base function can produce coefficients of high value. Any additional characteristics can be masked or ignored entirely Lei et al. [2013].

Unlike FT and STFT, WT has more options for matching a specific fault symptom, which helps to extract fault features. WT has also proven extremely useful in diagnosing faults in rotating machinery due to its multi-resolution advantage. To improve rotating machinery fault detection and diagnosis, WT is widely used. Its strong time and frequency capabilities have recently been used in rotating machinery fault detection Chen et al. [2016].

The wavelet theory has gained widespread acceptance and rapid development over the past decades, with a wide range of applications. Generally, wavelet transforms were

classified as continuous wavelet transform (CWT), Discrete wavelet transform (DWT), and wavelet packets transform (WPT) Goswami and Chan [2011]. The developments in the discrete wavelet transform (DWT) and the wavelet packets series (WPS) make the wavelet approach more suitable for signal and image processing. The following subsections discuss the fundamental theory underlying each classical wavelet type and the common application capability of each wavelet type.

Continuous wavelet transform

The term continuous wavelet transform (CWT) is an integral wavelet transform (IWT) and unlike the FT, which always uses a sinusoidal wave as its basis for decomposing a signal, wavelet shape allows for the selection of other basis functions based on the signal's characteristics. The scale and translation parameters define the basis function in wavelet analysis Daubechies [1992]. This property enables the representation of non-stationary signals with multiple resolutions analysis that employs a basis wavelet function (mother wavelet), which indicated in the Equation 2.4. The basis function of a wavelet with the order N is denoted by:

$$\psi(n) = c_j \sum_{j=0}^{N-1} (-1)^j (2n + j - N + 1) \tag{2.4}$$

where c_j is a coefficient and the base function, ψ should satisfy the following two conditions. The basis function integrates to zero.

$$\int_{-\infty}^{+\infty} \psi(t)dt = 0 \tag{2.5}$$

and it is square integrable or, equivalently, has finite energy, i.e.

$$\int_{-\infty}^{+\infty} |\psi(t)|^2 dt = 0 \tag{2.6}$$

Equation 2.5 suggests an oscillatory or wave basis function. According to Equation 2.6, the basis function's energy is mostly finite. Orthogonality and bi-orthogonality are important basis function properties. These properties allow for quick coefficient

calculation. There is no redundancy because there is only one wavelet decomposition for the signal. But not all basis functions have these. The term compact support is used as the basis function, which values are non-zero for finite intervals. This property allows for efficient representation of localised signals. Continuous wavelet transform is defined using the following relations.

$$W(a,b) = \frac{1}{\sqrt{a}} \int f(t).\psi^* \left(\frac{t-b}{a} \right) \tag{2.7}$$

where a and b are scale and translation parameters, respectively and ψ^* is the complex conjugate of W. The basis function W is represented as;

$$\psi_{j,k}(t) = 2^{1/2}\psi(2^j t - k) \tag{2.8}$$

The primary uses of the CWT are for analysing the time-frequency characteristics of signals and for filtering out specific frequency components that are localised in time.

Using the acceleration measurement dataset conducted at the Katowice tram depot, the acceleration signals are analysed to test the efficiency of CWT in extracting valuable features, which are insightful for the wheel fault condition monitoring. For example, Figure 2.7 shows the magnitude of the scalogram for a fault-free and fault wheel condition signal.

Figures 2.7 a) and c) illustrates a time-frequency scalogram representation of the signals. The colour intensity indicates the strength of different frequency components over time. Compared to Figure 2.7 a), Figure 2.7 c) scalogram does not provide an informative frequency band due to the fault-free condition of a signal. By closely looking at both figures, the magnitude of the frequency intensity of the scalogram for a fault wheel suspected is greater than that of a fault-free wheel.

A higher frequency intensity for fault wheels results within a narrow frequency band found around 100 Hz whereas wide frequency ranges are registered for wheels in normal condition. However, there is an overlapping and mixing of frequency bands, especially in the characteristic frequency band region, making it difficult to distinctly differentiate or categorise the signals. Figures 2.7 b) and d) show the amplitude of these signals over

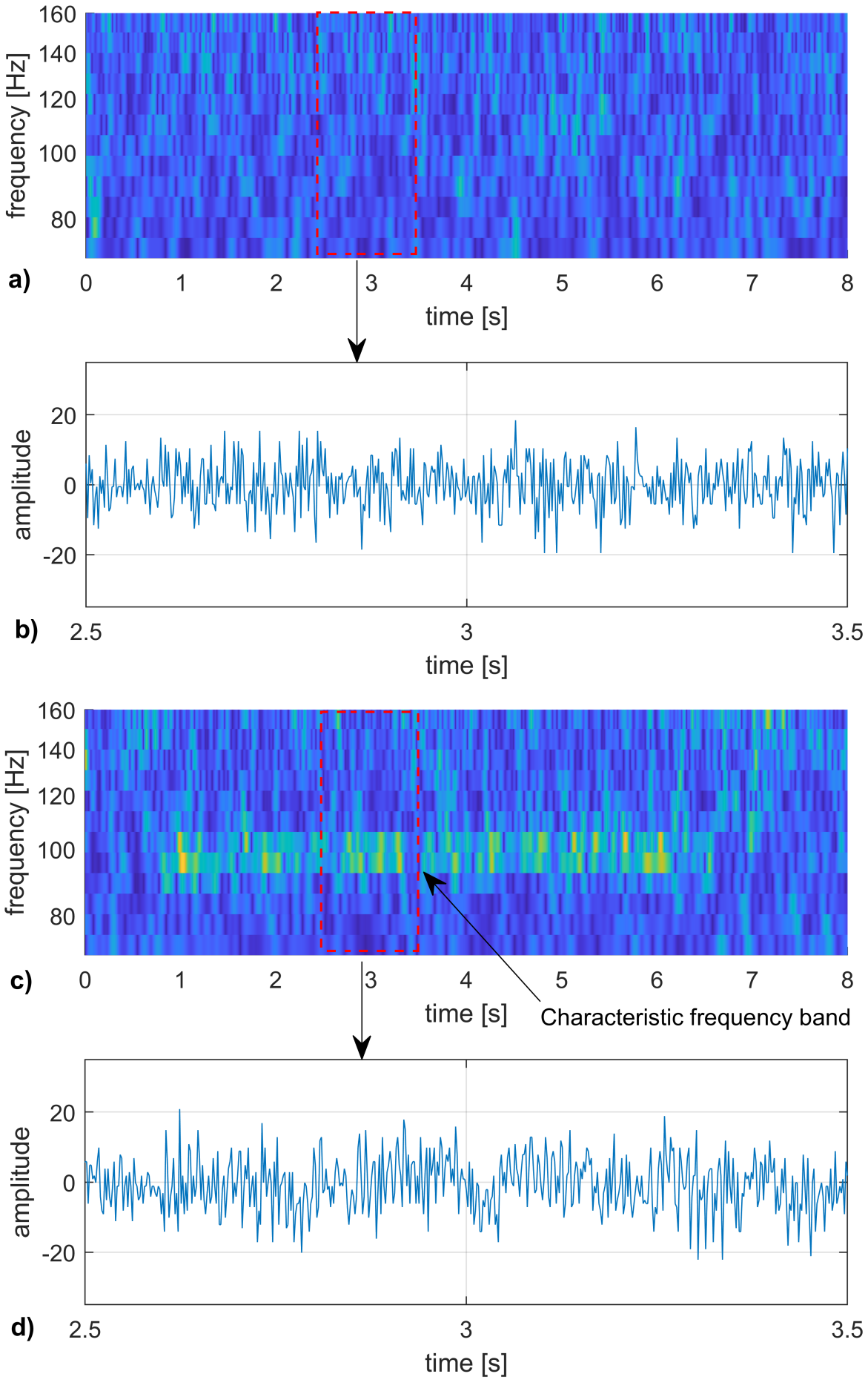

Figure 2.7: CWT time-frequency images of wheel vibration signal; Magnitude of scalogram images of a wheel with normal a), b) and c), d) wheel with faulty conditions

a short time frame that is very similar. It provides a snapshot of the signal's behaviour within a specific time frame marked by an arrow on the top graph.

Despite CWT's capability to handle complex signals, Figure 2.7 shows a challenge in differentiating signals effectively although it does better than STFT. This complexity arises due to the limitation of multi-resolution analysis of CWT, leading to increased difficulty in isolating specific frequency components associated with wheel faults effectively. Thus, while CWT remains a powerful tool, additional processing methods are required to enhance fault detection accuracy in such scenarios.

Discrete wavelet transform

The Discrete wavelet transform (DWT) is a discretised form of a continuous wavelet transform. The most common discretisation is dyadic. On the time-frequency plane of the CWT assigns redundant information Daubechies [1992]. To address these redundant time-frequency deficiencies, DWT was established Yan et al. [2014]. The mathematical expression of DWT is shown as the following:

$$DWT(j,k) = \frac{1}{\sqrt{2^j}} \int f(t).\psi^* \left(\frac{t - 2^j k}{2^j} \right) \tag{2.9}$$

where a and b are scales are replaced by 2^j, and $2^j k$, j, is an integer.

DWT is a multi-resolution analysis transform that analyses a signal at different scales. The Figure 2.8 illustrates the useful application of DWT for multi-resolution analysis step. For this purpose, DWT uses two distinct sets of functions, the scaling functions and wavelet functions, which correspond to low-pass and high-pass filters, respectively. The discrete signal is passed through a high-pass filter (H) and a low-pass filter (L), yielding two vectors at the first level: the approximation coefficient (A1) and the detail coefficient (L).

In the same manner, the same transform is applied to the approximation coefficient (A1), which is further decomposed at the second level into the approximation (A2) and detail (D2) coefficients. Finally, the signal is decomposed into its component parts at the expected decomposition level. The approximations represent the signal's high-scale

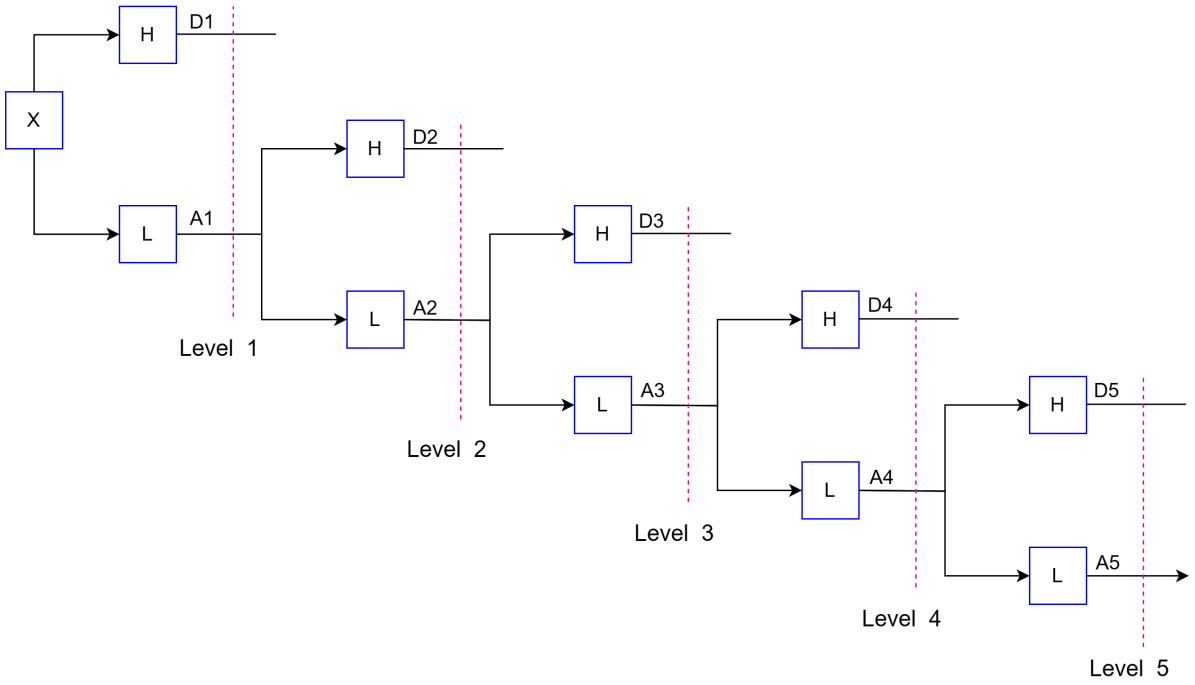

Figure 2.8: Principles of DWT with five decomposition levels

and low-frequency components, while the details represent the signal's low-scale with a high-frequency components.

Figure 2.8 illustrates the discrete wavelet decomposition of level 5. Each vector A_j contains approximately $N/2^j$ coefficients, where N denotes the number of data points in the input signal x, and contains information about the frequency range $[0, fs/2^{j+1}]$, where fs denotes the sampling frequency. The H and L denote the decomposition filters, and each filter is downsampled by two factors Bendjama et al. [2012].

Wavelet packet transform

The wavelet packet transform (WPT) is a modified version of DWT in which every of high-frequency detail obtained by DWT is further decomposed into an approximate and a detail coefficients Shen et al. [2013]. This can be possible because WPT processes a signal by using more filters than those that DWT offers. The following Equations 2.10 yield the WPT decomposition coefficients for a given signal $x(t)$:

$$\begin{aligned} d_{j+1,2n} &= \sum_m (h(m-2k)2_{j,n} \\ d_{j+1,2n+1} &= \sum_m (g(m-2k)2_{j,n} \end{aligned} \tag{2.10}$$

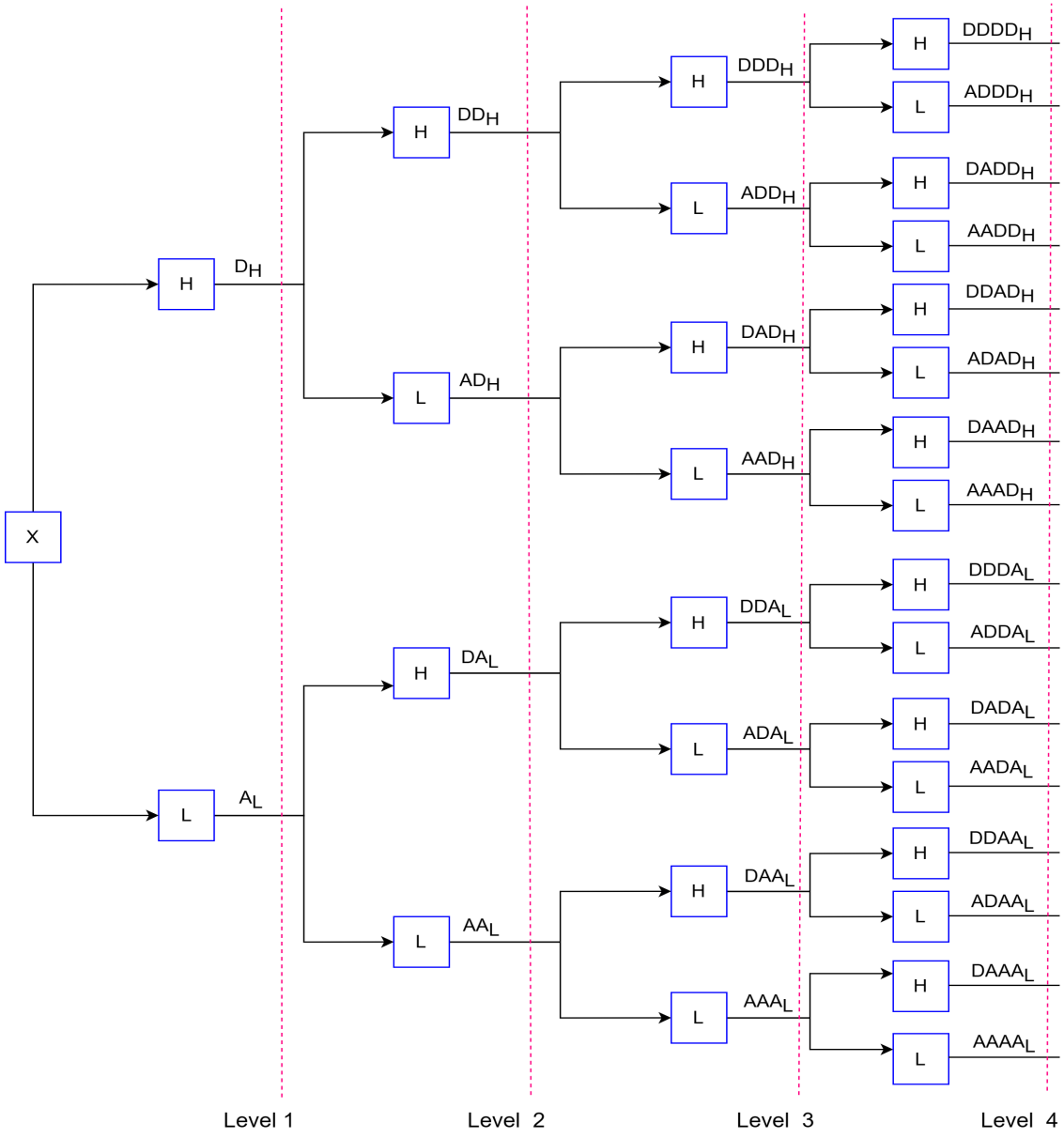

Figure 2.9: Principles of WPT with third decomposition levels

Where, m is the number of coefficients, and $d_{j,n}, d_{j+1,2n}$, and $d_{j+1,2n+1}$ are the wavelet coefficients at sub-bands $n, 2n$, and $2n+1$, respectively. WPT provides a more approximation and detailed representation of extracted frequency components than DWT, which is significantly beneficial Saleh and Rahman [2005]. An approximation and detailed representations of the decomposed signals make the WPT superior to other wavelet transforms. Time-localised wavelet packet basis functions also improve signal approximation and decomposition levels.

The WPT of a discrete signal x involves filtering it with a low-pass filter (L) and high-pass filter (H), resulting in two sub-bands at the first level (i). The first vector represents the approximation coefficient (AL), and the second is the detailed coefficient (DH).

To proceed with the next decomposition, x(ii) applies L and H filters to AL and DH, resulting in approximation coefficients (AAL and ADH) and detailed coefficients (DAL and DDH) at subsequent levels. Figure 2.9 shows the principle of WPT decomposition for the fourth level of decomposition. The drawback of the WPT is the loss of detailed information about the signal due to downsampling by two factors at each H and L filter decomposition.

The MODWPT algorithm, which do not use downsampling techniques to decompose and filter a signal using high and low filters, improve the shortcomings of WPT. MODWPT is a time-invariant and energy-conserving wavelet packet algorithm that can be used to decompose a signal into an approximate and detail coefficient like WPT Percival and Walden [2000]. The difference is that MODWPT does not use the downsampling of a signal at each decomposing filter. Further information about the MODWPT algorithm is discussed and presented in the chapter 3 of this dissertation.

When it comes to the application of WT and STFT time-frequency analysis techniques in the fault detection, diagnosis and condition monitoring, several researchers have used various techniques to identify fault conditions. For instance, Peng and Chu [2004] introduces the first form of a comprehensive review of the application of wavelet transforms in machine fault diagnosis and condition monitoring, with a focus on time-frequency, fault feature extraction, weak signal extraction, and vibration signal compression for system identification. The review summarizes the successful role of wavelet transform in handling multi-scale signals and its potential for analyzing non-stationary signals.

Belotti et al. [2006] developed a flat wheel defect diagnostics technique using wavelet transform. The authors set up an experimental tool for the study of wheel conditions at a variable train speed with accurate speed measurement using a single accelerometer, reducing hardware requirements and providing accurate results. While this approach reduces hardware requirements and provides accurate results, the study identifies the bogie with the defective wheel without explicitly pinpointing the flat wheel element. Additionally, the author highlights that a train's speed has a considerable impact on detecting wheel defects; however, in urban tram systems, factors such as braking frequency due to traffic engineering need to be taken into account. Because trams experience surface defects as a result of frequent brake usage at multiple stop locations, which needs to be

considered but not taken into account by the authors.

An adaptive chirp mode decomposition method for railway wheel flat detection under variable-speed conditions was proposed by Chen et al. [2021b]. The author employed a time-frequency analysis technique to precisely extract the time-varying fault characteristic frequencies and thus successfully detected the fault through simulation and experimental verification. Detecting wheel flats under variable-speed conditions is a difficult task that has only been rarely reported in the scientific literature. Identifying time-varying characteristic frequencies and strong interference that overwhelm the fault signal features are two of the most difficult challenges.

The study conducted by Ding et al. [2014] provides a detailed analysis of the shock experienced by the wheel-rail system in the presence of a wheel flat, focusing on the time-frequency aspects. Based on wheel vertical force measurements from sensors installed on the railway network, two machine learning methods were proposed by Krummenacher et al. [2017] to detect wheel defects automatically.

Dalpiaz and Rivola [1997] assessed the effectiveness and reliability of vibration techniques and wavelet transform fault detection and diagnostics in a cam mechanism of an automatic packaging machine. The study found that the wavelet transform is better at detecting and diagnosing faults in non-stationary, transient (different impulsive phenomena) signals than other vibration assessing techniques like amplitude probability density, power spectral density , and time-synchronous averaging.

Zhang et al. [2017] proposed an adaptive blind source separation (BSS) approach based on the theory of adaptive time-frequency distributions to address the non-stationary blind separation problem and applied it to the diagnosis and monitor the wheel defects condition. Quantitative metrics of inter-symbol interference and experimental work validated the proposed method, concluding that BSS can separate weak fault sources from various source mixtures.

An online wheel tread defect detection system using wayside fibre bragg gratings (FBG) was developed by Liu et al. [2019]. As part of the analysis, the author employed a Bayesian blind source separation approach to obtain the component that contains defect-sensitive features by decomposing the rail response signal. The method was then verified by testing a train with defective wheels. However, numerous variables, such as

train speed variation, temperature effects on strain gauge measurements, and location of the FBG sensor with respect to sleepers that could influence defect detection results, are not considered in the method.

Wan et al. [2023] studied the detection of train wheel anomalies utilising short-time Fourier transforms combined with unsupervised learning algorithms for monitoring passenger train wheel conditions. The authors used STFT to extract time-frequency features from the vibration signal collected with a pair of fibre bragg grating sensors during normal operating hours. In addition, they illustrated the efficiency of the proposed method of the FBG sensor signal samples and the STFT in inspecting the condition of the wheel by reprofiling the wheel circumference using turning operations.

Zhang et al. [2011b] proposed wavelet-based online flange thickness measurement using laser displacement sensors and discovered that the wavelet method outperforms FFT in non-stationary signal analysis. The author measured practical data with optical-electronic sensors and found that the measurements were noise-contaminated, so they used the Wavelet tool to denoise the data. When the laser displacement sensor method was compared to the manual measurement method, the result obtained by the laser displacement sensor method was not significantly different from the manual method. This suggests that further signal processing, such as wavelet analysis, is required to identify the actual wheel conditions online.

Bian et al. [2013] investigated impact analysis induced by wheel flats and found that wheel flat presence significantly increases dynamic impact forces on the rail and sleeper and also increases the size of wheel flats. However, the study does not indicate the exact size, and when a significant wheel condition emerged in the wheel portion during in-service operations, several studies were conducted to investigate the relationship between the impact forces and the wheel flat sizes.

Experimental investigation of essential features of polygonal wear of locomotive wheels performed by Yang et al. [2020] revealed that high-order polygonal wear is the root cause of locomotive vibration and contributes to another type of residue. However, due to its complexity and universality, the source of high-order polygonal wear remains unknown and unsolved. As a result, more experimentation and theoretical research are required.

Bai et al. [2023] review the effectiveness of time-frequency analysis in diagnosing faults

in rotating machinery by capturing transient signal information. They discussed time-frequency transformation methods and their development, emphasizing their importance in vibration signal fault diagnosis. Time-frequency analysis has improved machinery fault detection and has the potential for further research. In addition, the authors discuss the development and future of data analysis technology with time-frequency transformation.

2.5.3 Empirical mode decomposition

Empirical mode decomposition (EMD) is a self-adaptive signal processing method that can be applied to non-linear and non-stationary signals. EMD is used to decompose and process the time-domain signal $x(t)$ into different scales called intrinsic mode functions (IMF) Huang et al. [1998]. The EMD method was formulated under the assumption that every signal consists of distinct intrinsic modes of oscillations, which can be either linear or non-linear. An IMF meets two conditions: (i) the number of extrema and zero crossings must be equal or differ by one across the dataset, and (ii) the mean value of the envelope defined by the local maxima and minima must be zero at any point Huang [2014]. The EMD employs a recursive and repetitive decomposition technique to systematically extract the IMFs of a signal at different levels. For a signal $x(t)$, the EMD decomposition process can be described as follows.

i) Determine all the local extrema and then link all the local maxima using a cubic spline as the upper envelope.

ii) Repeat the procedure for local minima to create the lower envelope. The lower and upper envelopes should cover all data between them.

iii) Define m_1 as the mean of upper and lower envelope values, and h_1 as the difference between signal $x(t)$ and m_1, which is the IMF, ideally the first component of $x(t)$.

$$h_1 = x(t) - m_1 \tag{2.11}$$

iv) If h_1 is not an IMF, treat it as the original signal and repeat the above steps, then

$$h_{11} = h_1 - m_{11} \tag{2.12}$$

where m_{11} is the mean of the upper and lower envelope values of signal h_1.

v) For a repeated shift up to k times, h_{1k} becomes an IMF, such that:

$$\begin{aligned} h_{1k} &= h_{1(k-1)} - m_{1k} \\ C_1 &= h_{1k} \end{aligned} \tag{2.13}$$

Where C_1 is the first IMF component from the data.

The stoppage criterion for the repeated shifting process must be selected to guarantee that the IMF components retain enough physical sense of amplitude and frequency modulation Huang et al. [1998]. Reducing the standard deviation (SD) from two consecutive sifting results can accomplish this. The following equation defines the normalised SD between two successive shifting operations:

$$SD_k = \sum_{t=0}^{T} \frac{|(h_{1(k-1))}(t) - h_{1k}(t)|^2}{h^2_{1(k-1)}(t)} \tag{2.14}$$

The standard deviation is commonly assigned a value within the range of 0.2 to 0.3. Shifting stops if SD_k is less than a predetermined value of SD. Once the first IMF is found, the remaining IMF components can be generated from the original signal x(t) by using the repeated shifting algorithms as indicated in the following equation:

$$\left.\begin{aligned} r_1 &= x(t) - C_1 \\ r_2 &= r1 - C_2 \\ \vdots &\qquad \vdots \\ r_j &= r_{j-1} - C_j \end{aligned}\right\} \tag{2.15}$$

Where r_1 and r_2 are residues treated as the new signals for the first and second shifting processes, this procedure may be repeated up to r_j's, where $r = 1, 2, 3, \ldots n$. Mathematically, summing up the equation above, we can get the original signal $x(t)$ using the following equation:

$$x(t) = \sum_{j=1}^{n} C_j + r_n \tag{2.16}$$

EMD has been utilised by a multitude of researchers for analysing vibration signals for machine fault diagnosis purposes. For instance, Zhao et al. [2012] introduces the use of EMD for condition monitoring of rotating machinery. Lei et al. [2013] presented a review of EMD research and development in rotating machinery fault diagnosis to provide

comprehensive references and aim at helping researchers identify new research topics. The authors describe the highlights of EMD fault diagnosis applications for rotating machinery components like rolling element bearings, gears, and rotors. They also indicated the EMD's unsolved fault diagnosis problems and future research directions.

Li et al. [2016] established an improved empirical mode decomposition (EMD) approach for the detection of railway wheel flats. The proposed method investigates the axle box vibration response caused by wheel flats. The experimental results show that an improved EMD extracts wheel fault characteristics effectively. However, EMD may not correctly extract the desired fault signals in complex excitation due to inherent limitations such as mode mixing, end effects, and noise robustness. Moreover, axle box vibration signals are always contaminated by track irregularity, vehicle speed variation, and noise. Furthermore, extracting fault-relevant characteristics using the axle box vibration signals is difficult.

Jiang and Lin [2018] proposed wheel flat fault diagnosis based on the EMD-Hilbert envelope spectrum. Wang et al. [2018] proposed an improved EMD method using second-generation wavelet interpolation. Li et al. [2016] established an improved empirical mode decomposition (EMD) approach for the detection of railway wheel flats. The proposed method looks into the vibration response of the axle box due to wheel flats. The experimental results show that an improved EMD extracts wheel fault characteristics. However, EMD might not be able to correctly pull out the fault signals that are needed in complex excitations because of built-in problems like mode mixing, end effects, and noise robustness. Additionally, track irregularities, vehicle speed variations, and noise are always contaminating axle box vibration signals. Furthermore, extracting fault-relevant characteristics using the axle box vibration signals is difficult.

For example, for this study, the analysis of samples of dataset measurement conducted at the Katowice tram depot has utilised the EMD to check the applicability of this transform in the fault identification for assessing the condition of railcar wheels. Figure 2.10 illustrates the EMD of the signals collected from a rail track for monitoring the fault condition of the wheels.

Figures 2.10 a) and b) show 3 out of 4 IMFs derived from the signal. Each IMF is represented as a waveform pattern against sample points. The amplitude variations are

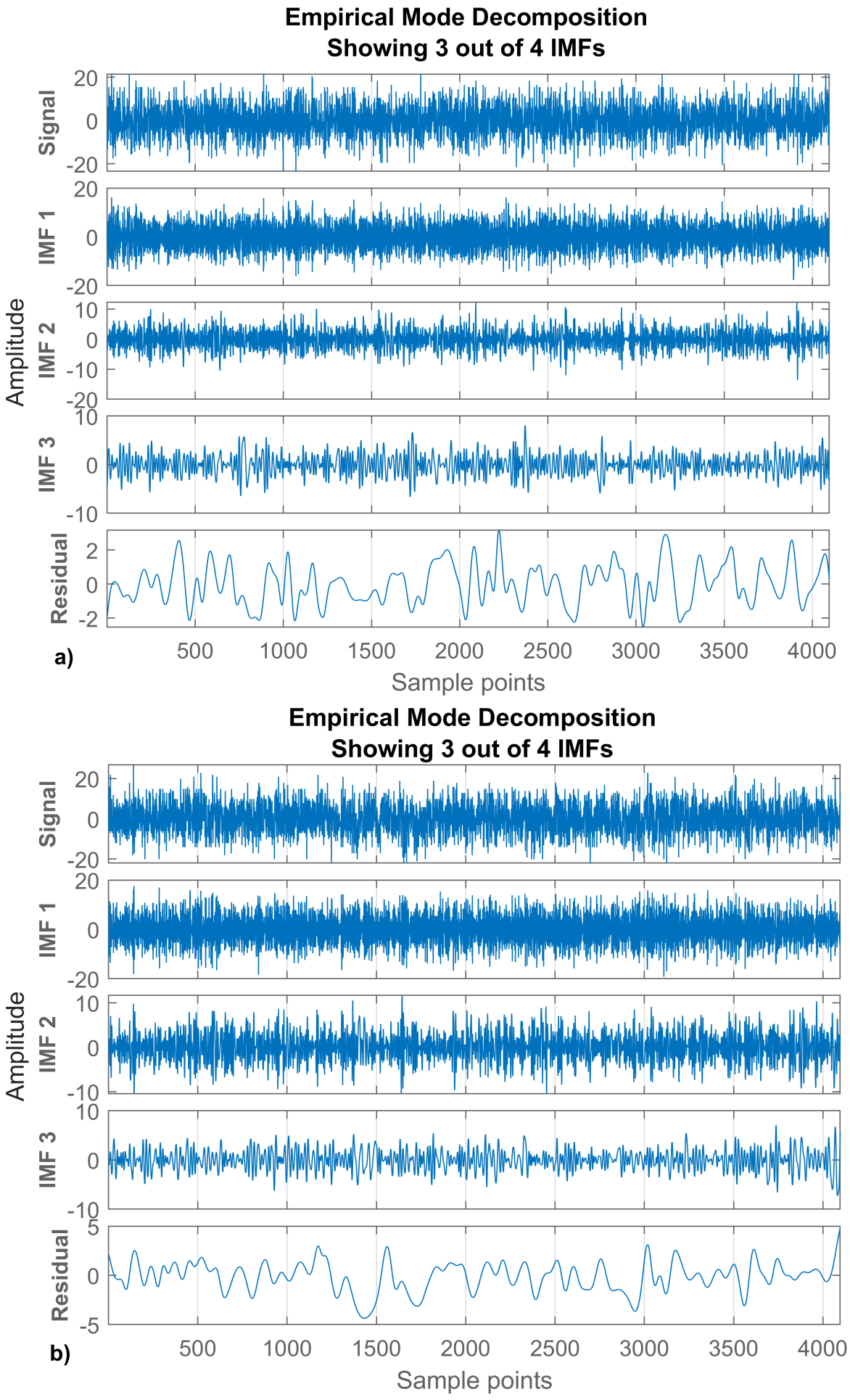

Figure 2.10: Empirical mode decomposition of a wheel with a) fault-free and b) fault wheel signal

visible but show similarities across different IMFs, making differentiation challenging. For both signals, the residual component at the bottom exhibits a waveform pattern but with less frequency variation compared to IMFs.

Despite EMD's adaptability in handling complex signal patterns, the Figure 2.10 underscores a challenge in differentiating signals effectively. This indicates that while EMD is adept at isolating intrinsic oscillatory modes embedded within complex signals, distinguishing between normal and anomaly conditions necessitates further analytical approaches to enhance diagnostic precision.

2.5.4 Hilbert-Huang transform

The Hilbert-Huang transform (HHT) is a time-frequency technique that has been widely applied to analyse vibration signals in the field of fault diagnosis of rotating machinery Shan et al. [2010]. The HHT consists of two main operations: the EMD and Hilbert transform. EMD can decompose a signal into an IMF Chandra and Sekhar [2016]. Once IMFs are produced by EMD, the application of the Hilbert transform to each IMF, helps for calculating the instantaneous frequency and amplitude corresponding to each IMF Fan and Zuo [2006]. The Hilbert transform of a signal $x(t)$ can be defined as its complex conjugate $y(t)$.

$$y(t) = \frac{p}{\pi} \int_{-\infty}^{+\infty} \frac{x(t)}{t-\tau} d\tau \tag{2.17}$$

Where P is the principal value of the singular integral. With the help of HT, the analytic signal $z(t)$, which is an imaginary complex signal part, is the Hilbert transform of its real part; $x(t)$ can be expressed mathematically in the following equation:

$$\begin{cases} z(t) = & x(t) + iy(t) = a(t)e^{i\varphi(t)} \\ a(t) = & \sqrt{x^2(t) + y^2(t)} \\ \varphi(t) = & arctan(y(t)/x(t)) \end{cases} \tag{2.18}$$

where $a(t)$ is the instantaneous amplitude of $x(t)$, which reflects how the energy of $x(t)$ varies with time t and $\varphi(t)$ is the instantaneous phase of $x(t)$. If the signal $x(t)$ is monocomponent, then the time derivative of the instantaneous phase $\varphi(t)$ will be the instantaneous frequency $\omega(t)$ of the signal $x(t)$. The instantaneous frequency $\omega(t)$ is

given as

$$\omega(t) = \frac{d\varphi(t)}{dt} \tag{2.19}$$

For a signal $x(t)$ having an N number of IMFs created by EMD, by applying HHT, the instantaneous amplitude $a(t)$ and frequency $\omega(t)$ determined can be integrated to produce the original signal $x(t$ using the following equation:

$$x(t) = \sum_{n=1}^{N} a_n(t) exp\left(i \int_n^N \omega_n(t) dt\right) \tag{2.20}$$

Thus, utilising the IMFs derived from EMD, the Hilbert transform represents the signal $x(t)$ in terms of its time-frequency-energy distribution.

The utilisation of the Hilbert transform in fault diagnosis, specifically in analysing vibration signals, has been extensively researched, and numerous studies have been published by various scholars. For instance, Lei and Zuo [2009] introduced an improved HHT based on ensemble empirical mode decomposition (EEMD) fault diagnosis of rotating machinery using sensitive IMFs. The authors analysed the vibration signals using intrinsic mode functions extracted using EMD. However, the drawback of EMD is that it cannot reveal the signal characteristics accurately because of the problem of mode mixing.

This problem was alleviated by introducing EEMD. The findings of the work proved that improved HHT based on EEMD performed superior to HHT based on the EMD fault diagnosis technique. Feldman [2011] presented a detailed application of the Hilbert transform in vibration analysis. The author relies on many examples to demonstrate how the Hilbert transform can be used in machine diagnostics, mechanical system identification, and signal component decomposition.

Furthermore, Nowakowski et al. [2019] used Hilbert's transform to detect tram wheel flats; the analysis was performed for identifying good and bad wheel condition responses. The authors used an experimental investigation randomly that placed a tram wheel with a flat spots. However, the fault wheel was not carefully chosen from the rest of the wheels with unique characteristics. Also, the author assumed the vehicle accelerations to be a basic physical quantity, though tram wheel acceleration is low, at 15-20 km/hr relative to other trains.

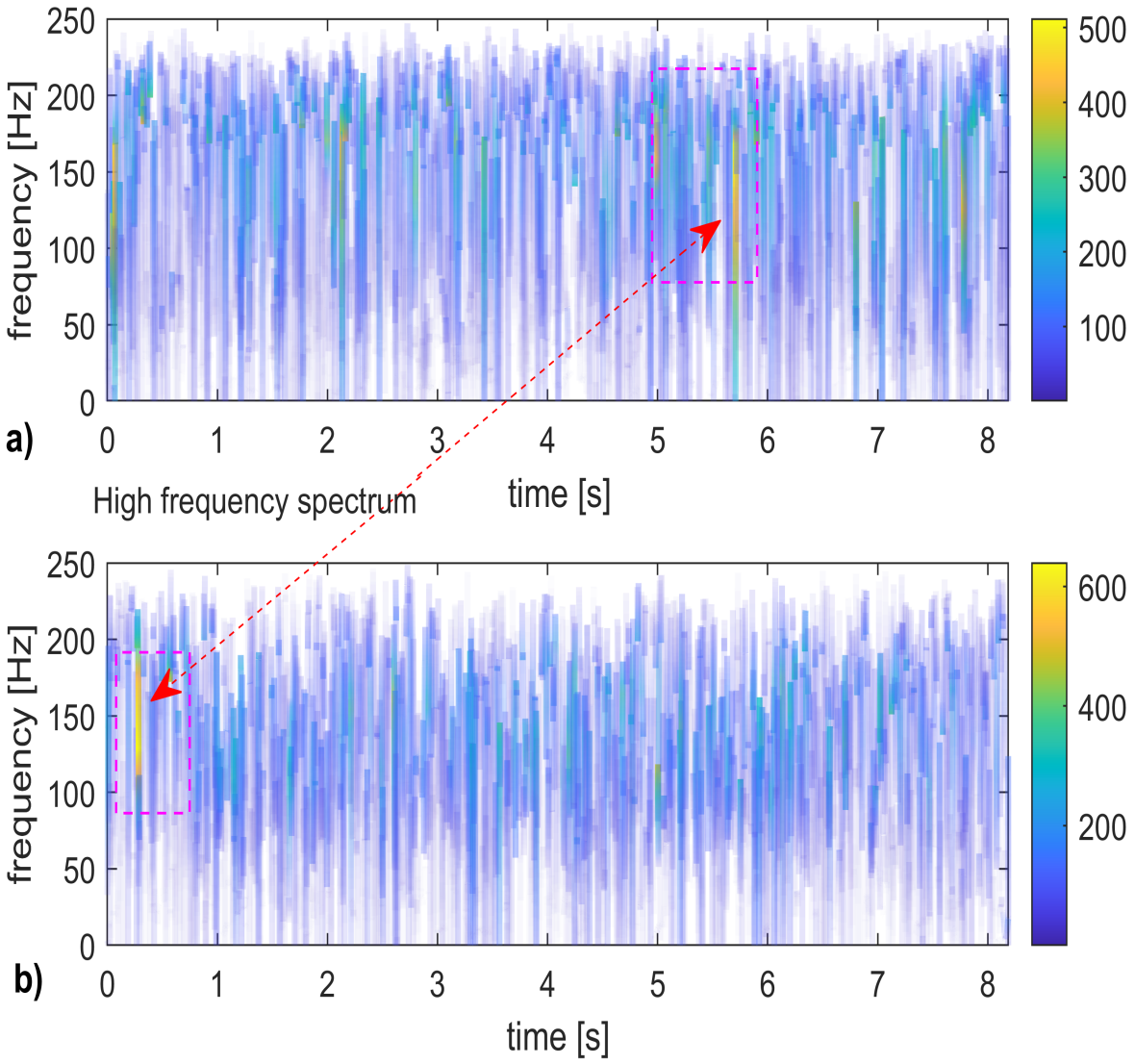

Figure 2.11: Hillbert Huang transform spectrum for a signal with a) fault-free and b) fault wheel condition

The analysis of acceleration datasets measurement obtained from Katowice tram depot is conducted by employing the HHT technique to assess its applicability in deriving meaningful insights from these datasets. For instance, Figure 2.11 presents high-frequency spectrums obtained through the HHT. HHT is a powerful tool for analyzing nonlinear and non-stationary signals, which seems to be the case with these signals that were collected from rail track sensors to monitor wheel fault conditions.

Figure 2.11 a) shows a high-frequency spectrum with varying intensities over time, indicating a mix of frequencies. The complexity of these signals makes it difficult to isolate specific frequency components associated with distinct fault conditions. Figure 2.11 b) exhibits a similar pattern with slight variations in intensity distribution. The presence of multiple overlapping signals further complicates the task of signal differentiation.

While HHT is renowned for its adaptability in handling complex signal patterns, the complexity of the presented data underscores the need for supplementary analytical tools or methodologies to enhance signal differentiation and fault identification precision.

2.6 Time-frequency methods comparison

As mostly described in detail in the previous section, the time-frequency analysis techniques are utilised to analyse non-stationary signals and extract valuable features such as frequency spectral content at each respective time point. The Table 2.3 below compares various time-frequency analysis techniques utilised for fault detection in the railway wheels and other field of applications. Each technique offers unique advantages and limitations. For instance, the STFT excels in providing a well-defined time-frequency localization but struggles with non-stationary signals Shaikh et al. [2023], Fu et al. [2023].

On the other hand, DWT and WPT techniques offer multi-resolution analysis capabilities, enabling the extraction of smooth trends and spaced frequencies while preserving energy Liang et al. [2013], Yuejian et al. [2014]. The EMD method stands out for its adaptability to nonlinear and non-stationary signals, making it suitable for capturing localised transient events Zhang et al. [2017], Liu et al. [2016]. However, it is sensitive to noise and may encounter mode mixing issues. The principles of each technique presented also aid in understanding the scenarios of fault detection applicability. In summary, the specific characteristics of the signals and the desired features for fault detection determine the choice among these techniques, every technique has a unique set of benefits and limitations.

Moreover, the MODWPT is a highly effective choice for non-stationary signal analysis and fault detection, boasting a range of valuable properties such as exceptional time-frequency resolution and the ability to mitigate boundary effects through its maximal overlap approach Walden and Cristan [1998]. By combining the benefits of wavelet packet decomposition and overlap processing, MODWPT can accurately capture localised transient events, greatly enhancing fault detection capabilities in railway wheel systems Peng et al. [2005].

Furthermore, MODWPT is adept at extracting smooth trends and spaced frequencies

Table 2.3: Summary of time-frequency techniques comparison

Time-frequency	**Base equation**	**Important parameter**	**Fundamental principle**	**Pros**	**Cons**
STFT	$x(t)(t,w) = \int_{-\infty}^{+\infty} x(t)w(t-\tau)e^{-jwt}d\tau$	Window length, Overlap ratio	Time-frequency localization	Provides frequency resolution and simple implementation	Fixed time-frequency resolution trade-off
CWT	$W(a,b) = \frac{1}{\sqrt{a}}\int f(t).\psi^*\left(\frac{t-b}{a}\right)$	Wavelet function, Scale range	Multi-resolution analysis	Variable time-frequency resolution and effective for non-stationary signals	Computational complexity and selection of appropriate wavelet
DWT	$DWT(j,k) = \frac{1}{\sqrt{2^j}}\int f(t).\psi^*\left(\frac{t-2^jk}{2^j}\right)$	Wavelet type, Decomposition levels	Signal decomposition and reconstruction	Multi-resolution analysis and Efficient implementation	Discrete nature introduces artifacts and Limited frequency resolution
WPT	$d_{j+1,2n} = \sum_m(h(m-2k)2_{j,n}, \quad d_{j+1,2n+1} = \sum_m(g(m-2k)2_{j,n}$	Wavelet type, Decomposition levels	Frequency localization	Provides detailed frequency information and energy compaction	Increased computational complexity and redundancy in representation
EMD	$x(t) = \sum_{j=1}^{n} C_j + r_n$	Number of intrinsic mode functions (IMFs)	Intrinsic mode functions (IMFs)	Adaptive time-frequency representation and suitable for nonlinear and non-stationary signals	Sensitivity to noise and mode mixing phenomenon
HHT	$y(t) = \frac{p}{\pi}\int_{-\infty}^{+\infty}\frac{x(t)}{t-\tau}d\tau$	Number of intrinsic mode functions (IMFs), EMD parameter	Empirical Mode Decomposition (EMD)	Adaptive time-frequency representation and no preassumption on signal stationarity	Sensitivity to noise and mode mixing phenomenon
MODWPT	$W_{1,j,k} = \sum_{l=1}^{L-1} f_{j,l}W_{i-1,\left\lvert\frac{j}{2}\right\rvert,(k-2^{(j-1)}l)\ mod\ N}$	Wavelet type, Decomposition levels	Overlap in time-frequency domain	Improved time-frequency resolution and reduced boundary effects	Increased computational complexity and redundancy in representation

while preserving energy, ensuring a comprehensive analysis that doesn't compromise crucial signal features Gómez et al. [2020], Yang [2021]. Its versatility in handling complex signals, coupled with its ability to balance computational efficiency with high-resolution analysis, makes MODWPT a valuable tool for fault detection tasks. With a wide range of time-frequency analysis techniques to choose from, MODWPT is chosen in this study, as it emerges as an optimal solution for addressing the multifaceted challenges inherent in railway wheel fault detection.

Therefore, this research primarily aims to utilise MEMS-based sensors for acquiring acceleration and MODWPT for analysing the acceleration signals to detect faults in railway wheels. Conventional vibration measurement techniques encounter difficulties in promptly detecting transient faults and have limited diagnostic sensitivity. MEMS-based sensors and MODWPT signal analysis could provide improved monitoring capabilities that exceed the limitations of traditional methods.

Additionally, the current real-time wheel defect detection techniques require enhancement, and MEMS-based sensors could offer more cost-effective, low-power, precise, and timely data measurements for identifying wheel faults. There is a clear indication of further efforts to improve existing detection methods by employing MEMS-based sensors. Incorporating MEMS-based sensors and the MODWPT algorithm has the potential to lead to significant advancements in railway wheel condition monitoring and fault detection.

3

MODWPT-Based Wheel Condition Assessment

The use of MEMS-based acceleration sensors limits the scope of available measurement data for processing and requires a careful approach for extracting diagnostic details, which are beneficial for evaluating wheel conditions. The study assumes that wheel conditions irregularities produce disruptions in the frequency spectrum of recorded accelerations and these irregularities can be used to derive information on the condition of wheels. The rail vibration energy in the characteristic frequency bands is chosen as the measure of the wheel condition. The properties of MODWPT favour its application for determining the properties of the collected data. These prerequisites curb the design of the method for assessing wheel condition.

This chapter provides details of the MODWPT algorithm; the proposed method for analysing the condition of wheel fault signals. The proposed MODWPT analysis tech-

nique employed for the wheel condition assessment outlines three key steps: i) vibration data measurement, ii) processing of the data, and iii) analysis of MODWPT coefficients to identify fault conditions in the wheels. In addition, the samples of results gained using the proposed method are thoroughly presented and discussed in this chapter. Furthermore, a discussion of the solution search limits for processing requirements for assessing the wheel conditions of a moving railcar is presented.

3.1 Concept of the proposed method

The proposed method is essentially aimed at achieving an efficient interpretation of vibration signals with the goal of detecting indications of the wheel condition. The proposed method involves the use of MEMS-based acceleration sensors, which are highly sensitive and capable of measuring the parameters of vibration signals with a great accuracy. In addition, the MODWPT signal processing technique is proposed as a robust method for processing the acquired acceleration signals. The combination of these techniques promises to facilitate the processing of acceleration signals and yield a precise interpretation of vibration signals. By leveraging these techniques, it is expected that the proposed method will serve as a reliable means of detecting the wheel condition at the workshop and maintenance operation centres of the tram vehicle.

The processing steps and overall concept of the proposed method are illustrated in Figure 3.1. A selective framework is designed to offer a comprehensive analysis of the state of railcar wheels during railroad drive operations. This framework employs a systematic approach that aims to identify any potential issues with the wheels, allowing for prompt maintenance, and ensuring a safety of railcars during railroad drive operations. In brief, the processing steps that are used for the detection of the wheels condition are presented as the following.

1. Data collection.

   The method begins with the collection of vibration signals from railway tracks using MEMS-based accelerometer sensors. These signals, which represent track vibration are represented by acceleration signals in three axes. The measurement data is saved in embedded memory or radio transmitted to a local repository.

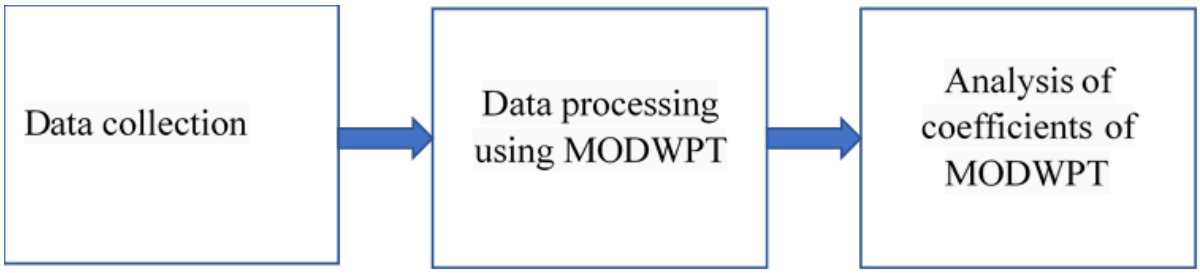

Figure 3.1: Processing steps of the method

2. Data processing.

   The collected data is then processed using MODWPT. MODWPT is applied to the collected acceleration data to extract informative frequency bands. The parameters of MODWPT are derived from field tests carried out on rail tracks during railroad drives.

3. Analysis of MODWT coefficients.

   By analysing the MODWPT coefficients, the MODWPT assesses vibration energy within the characteristic frequency bands which are used as the measure of anomalies of the vibration signals. Anomalies in these bands serve as indicators of wheel condition, allowing for the detection of wheel faults.

3.2 Application of MEMS-based sensors

The first step of the proposed method relies on the effective collection of vibration data. Preliminary tests show that accelerations of the rail track correctly map the vibration signal. Accelerations in the three axes are measured in order to include the effects of different kinds of wheel fault conditions which may cause movements in the specific axis of the track. The condition of the track, sleeper type and ground parameters affect the vibration image. Damaged sleepers and loose ground contribute to the spectrum of vibrations in various ways, especially by increasing the amplitude of vibrations. In order to account for such acceleration deviations, the acquisition process needs to be carefully devised.

For instance, hardware-based filtering in the frequency domain is commonly used to reduce or alleviate interference signals corrupting the measured physical quantity. However, hardware filtering of signals in the frequency domain may delete significant

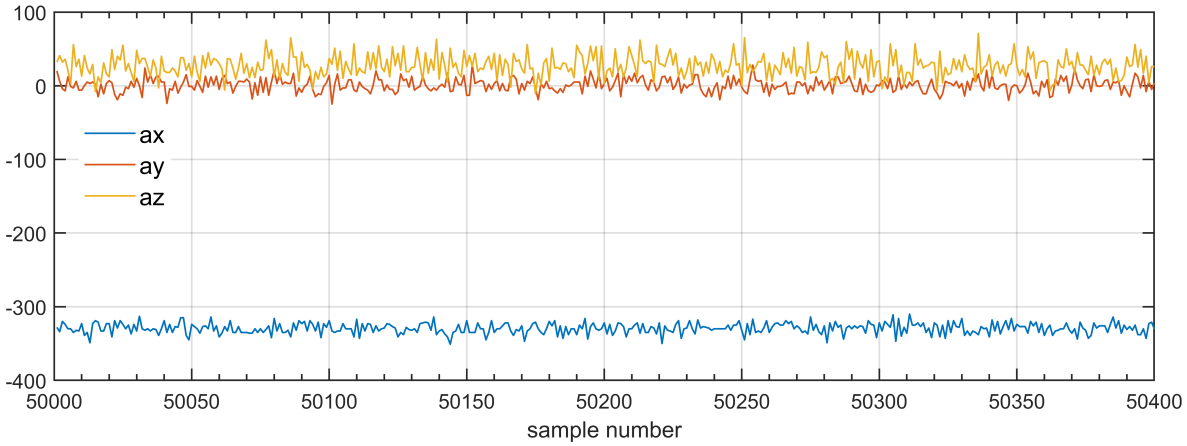

Figure 3.2: Raw acceleration data from an acceleration sensor

indications of vibration anomalies. Increasing the resolution of collected data, in place of filtering can enable to retain of details masked by the disrupting sources. Higher resolution brings the ability to analyse superimposed signals with large differences in values. It also enhances the accuracy of processing for correct calculation of the transform coefficients when the technical track conditions are poor.

Preliminary studies show that the frequency bandwidth of vibrations signal that significant for evaluating the condition of wheels falls within a few hundred Hz. The limited ranges of such vibration frequencies open up a great opportunity for applying MEMS-based sensors, particularly in wheel fault condition monitoring. MEMS devices that are widely accessible have the capability to capture acceleration data at a frequency of several thousand times per second. The measured acceleration values span across ranges that surpass hundreds of $[m/s^2]$ Murphy [2017]. These devices can provide analogue output signals representing accelerations or digital outputs streaming data containing measured acceleration values. Data streams can be treated as discrete-time-series signals.

For instance, the Figure 3.2 presents an excerpt of a graph of raw acceleration data collected by an accelerometer during a railroad drive. The accelerometer is mounted on the rail track and measures accelerations in three axes (x, y, z). The x-axis values are gravity-biased because the sensor was attached to the web of the rail. Each sample number corresponds to a specific point in time during the railroad drive when the vibration data was collected.

The list of parameters of the MEMS sensors that can be used for collecting vibration is elaborated in Table 3.1. These are examples of sensors for applications in robotics,

Table 3.1: Examples of MEMS-based acceleration sensors suitable for measuring track vibrations caused by railcars

Manufacturer	Device series	Measuring range, sampling rate	Resolution $[m/s^2]$
Analog Devices	ADXL357	±10g, 4kHz	0,0002
STMicroelectronics	LIS2DUX12	±8g, 800Hz	0,002
STMicroelectronics	**AIS3624DQ**	**±6g, 1kHz**	**0,03**
Bosch	BMA400	±8g, 800Hz	0,04
Kionix	KX132-1211	±8g, 1600Hz	0,002

condition monitoring and for use in the Internet of Things (IoT) devices. The highest resolution equals $1/2^{20}$ of the measurement range (the sensor incorporates a 20-bit ADC) and if the range is ±10g it means the sensor has the ability to distinguish acceleration values of 0,0002 $[m/s^2]$. Some sensors incorporate 16-bit ADCs which give resolutions of 0,002 $[m/s^2]$. The most common sensors are equipped with 12-bit ADC (the bold row series of sensor in the Table 3.1 giving lower resolutions which are adequate for obtaining and processing vibration data for identifying the wheels condition. For this study, the STMicroelectronics, AIS3624DQ sensors with a measuring range and sampling rate of ±6g, 1 kHz and with a resolution of 0.03 is considered.

Figure 3.3 illustrates the scaled example of the acceleration data collected by a MEMS sensor at the precise moment when the wheelset passes over the sensor. The accelerations of the rail are quantified through the deployment of a sensor positioned beneath the track, which records data as the tram progresses at an approximate speed of 2 $[m/s]$. The sampling rate is set to 1 kHz. The values of the lateral accelerations are shown and the raw data is converted to absolute acceleration values. There are two distinct scenarios of lateral acceleration signals (wheel impact signals and rolling wheels signal) collected by the sensor from a railway wheel during a railroad drive:

Figure 3.3 a) shows significant spikes in the lateral acceleration signals at specific instances (around 503 [s] and 525 [s]) due to wheel impact at the rail joint. The wheel impacts cause a sudden increase in lateral acceleration due to the physical interaction between the wheel and the rail joints. This could be indicative of potential anomalies resulted on wheels surface due to rail joints.

Figure 3.3 b) shows a more consistent yet fluctuating pattern of lateral acceleration signals between the impacts. This may represents the normal operation of rolling wheels

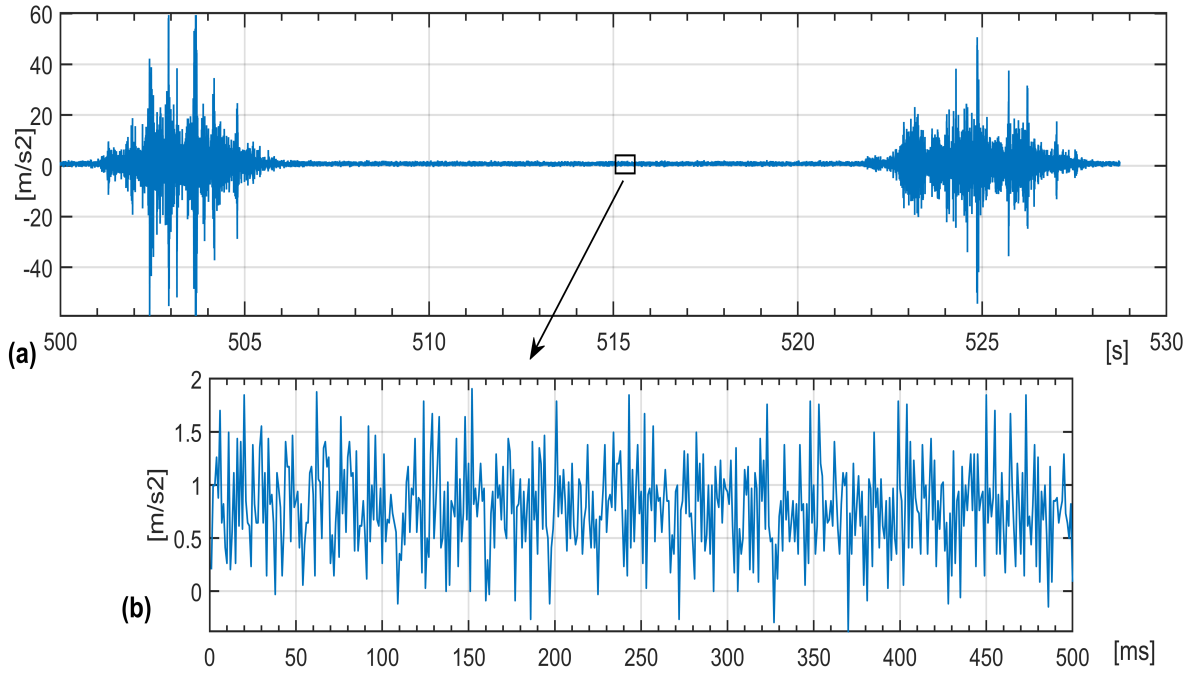

Figure 3.3: Samples of acceleration data collected by MEMS sensor (a) wheel impacts at rail joints; (b) rolling wheels

where no direct impacts like those at rail joints are occurring. This indicates that the vibration signals has strong relations with the operating condition of the wheels.

To analysis the vibration signals of the railcar wheels, the measurement data is saved in embedded memory or radio transmitted to a local repository. In order to facilitate efficient processing and to retain accuracy it is advisable to keep the raw format of the measurements.

3.3 Maximal overlap discrete wavelet packets transforms

The wheel fault irregularities produce disruptions in the frequency spectrum of recorded acceleration signals. The acceleration signals generated under such circumstances exhibit non-stationary behaviour, and the analysis based on the Fourier transform is restricted in its ability to effectively extract the characteristic frequency spectrum of these signals. A maximal overlap discrete wavelet packet-based approach is proposed for processing the acceleration data collected under such a scenario.

The MODWPT is a powerful technique utilised for exploring the frequency charac-

teristics of data. Its advantages include time-frequency localization, energy compaction, multi-resolution analysis, and noise reduction. This approach enables the examination of signals at various resolutions, making it well-suited for analyzing signals with diverse scales or frequencies. Furthermore, MODWPT can identify signal faults as it offers a precise and concise representation of signals, which can be used to describe anomalies.

The MODWPT is a transform method that remains unchanged over time and breaks down an input signal into numerous coefficients. Unlike other discrete wavelet transforms, the MODWPT does not reduce the input signal by half or lose its coefficients at various decomposition levels Walden and Cristan [1998], Shrifan et al. [2021]. This implies that all the decomposition coefficients are directly linked to their respective time series, ensuring consistent pass-band duration at each stage of decomposition. The length of the resulting coefficients matches the length of the input signal. To decompose the input signal, the low and high-pass filters are used in the MODWPT to produce a uniform frequency output bands.

The acceleration measurement registered for the rolling wheel sample data points looks the same making it difficult to distinguish fault wheel acceleration data from good wheel condition. To discern the contrast between these sets of sample data, it is imperative to pinpoint a unique eyeglass and thoroughly examine the signal in the other window.

MODWPT is chosen as the tool for processing these samples of data. This transform algorithm enables gaining a more comprehensive understanding of the underlying patterns and variations in the data. This transformation exhibits resilience against the absence of translation invariance by maintaining invariance to circular shifts within the data samples. This attribute is particularly beneficial for the identification of signal anomalies, ensuring that the detection process is not hindered by the positioning of the data points.

The mathematical representation of MODWPT entails a series of procedures. MODWPT is the analysis method that breaks down a signal into smaller sub-bands by repeatedly applying the discrete wavelet transform. The initial phase involves using the DWT on the input signal, followed by organizing the resulting coefficients into a binary tree structure called the wavelet packet tree, which represents different sub-bands as shown

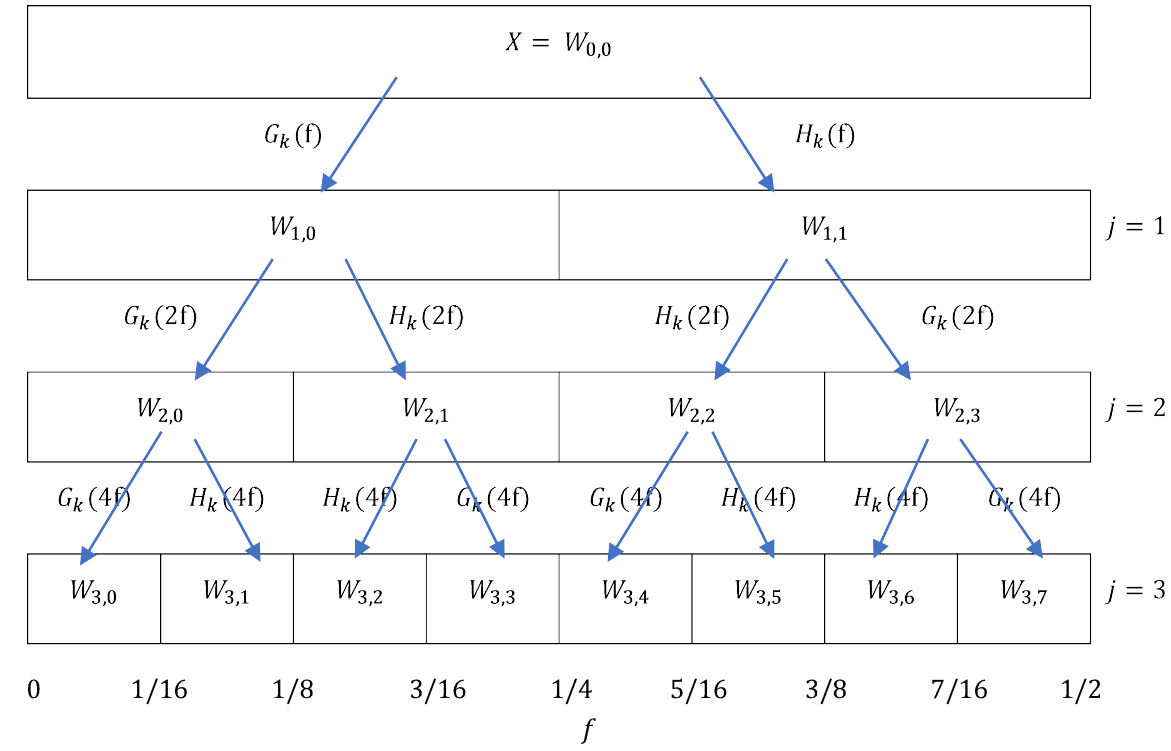

Figure 3.4: Undecimated wavelet packet tree coefficients for a signal X at the 3rd level of decomposition using MODWPT.

in Figure 3.4.

At each node in this tree diagram, MODWPT identifies the sub-band with the highest energy and applies another DWT to it. This recursive process continues until a specific decomposition level is achieved. The details of the MODWPT algorithm is demonstrated in the undecimated wavelet packet tree of the Figure 3.4.

For a discrete-time sequence X=$\{x_0, x_1, x_2, \ldots, x_{N-1}\}$ comprising N samples obtained from the MEMS sensor at sampling rate f_s, the MODWPT decomposition coefficient is computed by convolving X with a subset of low-pass scaling filter $(g_k : k = 0, 1, \ldots L-1)$ and its quadrature mirror high-pass wavelet filter $(h_k : k = 0, 1, \ldots L-1)$. Here, L denotes the length of the filter and must be lesser than or equal to N. The two filters are interrelated according to the Equation 3.1.

$$h_k = (-1)^k g_{L-K-1}, \quad g_k = (-1)^k h_{L-K-1} \tag{3.1}$$

The filters are scaled by a factor of $\frac{1}{\sqrt{2}}$ to maintain energy conservation. The mathematical representation of these scaled filters is given as $h_k = h_k \frac{1}{\sqrt{2}}$ and $gk = g_k \frac{1}{\sqrt{2}}$. The relationship between the corresponding transfer functions of the scaled filters is expressed

as follows:

$$G_k(f) = \sum_{k=0}^{L-1}(-1)g_k e^{-j2\pi fk}, H_k(f) = \sum_{k=0}^{L-1}(-1)h_k e^{-j2\pi fk} \tag{3.2}$$

The MODWPT coefficients are computed using an iterative method, as illustrated in Figure 3.4. Initially, X undergoes circular processing and filtering through g_k with its corresponding transfer function $G_k(f)$ to produce the initial set of scaling coefficients, denoted as $W_{1,0} = \{W_{(1,0,k)}k = 0, 1, \ldots, N-1\}$. Similarly at this stage, X is subjected to circular processing and filtering through h_k, along with its respective transfer function $H_k(f)$ to yield the first set of wavelet coefficients given by $W_{1,1} = \{W_{(1,1,k)} : k = 0, 1, \ldots, N-1\}$.

Subsequently, for levels j greater than or equal to 1, the filters at each level is extended by inserting $2^{(j-1)} - 1$ zeros between the coefficients of low and high pass filters (g_k, h_k) respectively. The placement of $2^{(j-1)} - 1$ zeroes in between the filter coefficients takes into account that there is no downsampling. The alteration of the transfer function representing the sequence-ordered changes with a level of decomposition is determined by the relationship between $G_k(2^{(j-1)}f)$ and $H_k(2^{(j-1)}f)$ correspondingly. This computation is iterated to obtain the next level of wavelet coefficients: $W_{2,0}, W_{2,1}, W_{2,2}, W_{2,3}$. This process continues until it reaches a desired level of decomposition.

The MODWPT coefficients at node (j, n) are;

$$W_{j,n,m} = \sum_{k=0}^{L-1} f_{n,k} W_{j-1,} \left|\frac{n}{2}\right|, (m - 2^{(j-1)}k) \; mod \; N \tag{3.3}$$

where,

$$f_{n,k} = \begin{cases} g_k & \text{if n mod 4=0 or 3} \\ h_k & \text{if n mod 4=0 or 3} \end{cases} \tag{3.4}$$

At each decomposition level, there are a total of $2^{(j-1)}$ frequency bands, n- refers to the specific frequency band number at that level and 'mod' means modulus after division.

The energy of a signal captured by the MEMS sensor is expressed using MODWPT coefficients at j^{th} level of decomposition and the values of the energy at a given level is

calculated using the following equation:

$$||X|| = \sum_{k=0}^{2^j-1} ||W_{j,n}||^2 \tag{3.5}$$

The norm vector, $||X||$ represents the total energy across all frequency bands in the sensor samples. The sampling rate f_s establishes both the frequency ranges of the bands b_n^j at a specific decomposition level j, and it also determines the resolution of the frequency analysis for signals.

$$b_n^j = \left\{ n\left(\frac{f_s}{2^j}\right), (n+1)\left(\frac{f_s}{2^j}\right) \right\} \tag{3.6}$$

The energy levels of the signal within specific frequency ranges provide insights into potential faults in the wheels. The objective of conducting MODWPT signal analysis is to identify high-energy frequency bands or frequency bands with extraordinary energy values. For a normal wheel, the baseline vibration energy level is determined as the average of frequency band energies, thereby representing typical operating conditions on the analysed rail track. Identifying the frequency band with the highest energy can serve as an indication of any wheel faults arising from irregularities on its surface. By monitoring these peak positions throughout tram journeys, it becomes possible to map out the instances of faulty wheel elements during operation.

Base wavelet for vibration energy calculation

The sensor registers vibrations in the rail caused by the rolling tram wheels and much higher vibrations caused by impacts of the wheels at rail joints. The rail segments at the depot are not welded together so the segments, during the tram passage, warp generating high amplitude accelerations of the rails that effectively mask the effects of wheel faults Figure 3.3 a). Cutting out the impacts from the collected sensor dataset gives data for assessing wheel conditions Figure 3.3 b).

The energy of vibration in characteristic frequency bands is chosen as the measure for assessing the condition of wheels. The MODWPT properties are defined by the base wavelet in consequence this sets up the energy evaluation. The base wavelet defines the ability to efficiently approximate particular behaviour of the vibration signal with few nonzero wavelet coefficients. The candidates for evaluation are Daubechies

wavelets, Symlets and Coiflets. Wavelets with 3 vanishing moments are used for evaluation. MODWPT with such wavelet bases can be efficiently calculated using modest processing resources.

The 9^{th} level of decomposition is arbitrarily chosen for the comparison of the energy calculation properties using MODWPT with different base wavelets. At this level of decomposition, when the sampling rate equals 1 kHz, the resolution of frequency analysis is about 1 Hz which is common in vibration analysis tasks. The ability to resolve the difference between wheels in good and bad condition is adopted as the appraisal criterion.

A random pair of datasets mapping fault-free wheels and wheels in bad condition is transformed using MODWPT with Daubechies, Coiflets and Symlets base wavelets. Datasets contain 4096 acceleration samples mapping the vibrations. The resultant coefficients are used for calculating the vibration energy in the frequency bands determined by the level of decomposition.

Figure 3.5 a) presents the vibration energy spectrum of a fault-free wheel. There are small peaks of vibration energy at 160, 166 and higher peaks at 432, 437, and 442 Hz. Their values do not exceed 0.015. Figure 3.5 b) indicates the fault condition, with a distinct peak of energy at 421 Hz reaching 0.02. This peak signifies resonant frequencies where excessive vibrations occur due to bad wheel conditions. Figure 3.5 c) superimposes the energy spectra of both fault-free and fault conditions for comparison. It is evident that there is a significant increase in energy at specific frequencies when a fault is present, indicating abnormal vibrations."Bad wheels" can be clearly identified as the energy peaks do not overlap.

The energy values obtained using MODWPT with Daubechies and Symlets base wavelets coincide, whereas Coiflets give higher values and steeper peaks. MODWPT with Coiflet3 base wavelet gives 40% higher energy values focused in single frequency bands of the decomposition. The energy peaks are distinct and steep. Other pairs of collected vibration data give similar results.

The MODWPT with the Coiflet base wavelet approximates better the behaviour of the vibration signal of the rails generated during railcar drives. Regardless of the type of wavelet, the extraction of vibration energy based on the MODWPT coefficients yields comparable outcomes. For the same level of decomposition, changing the base wavelet

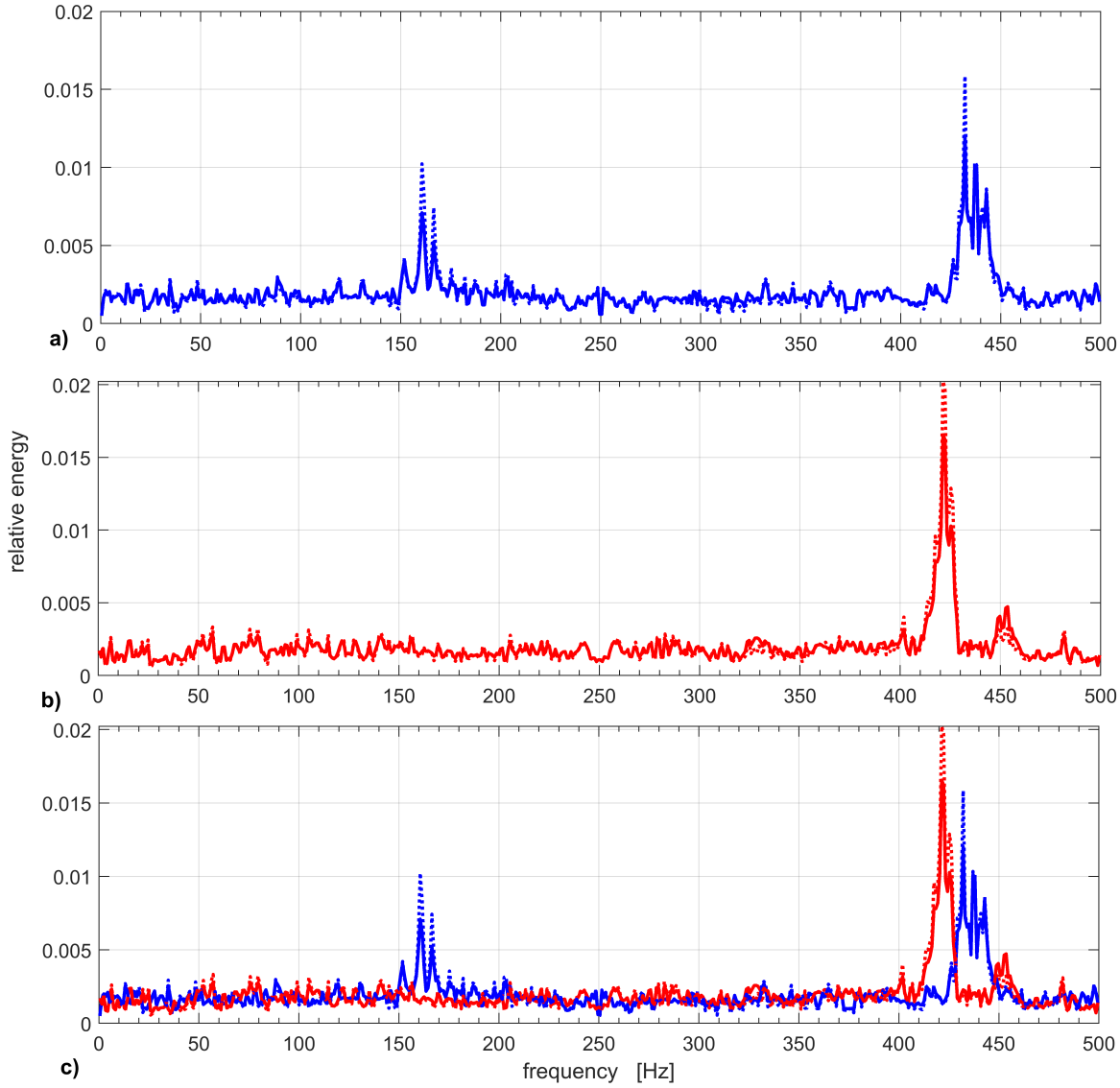

Figure 3.5: Relative energy of the vibrations a) fault-free wheel, b) "bad" wheel, c) both fault-free and "bad" wheel. Marked by: solid line - Daubechies base wavelet, dotted line - Coiflet base wavelet, dashed line - Symlet base wavelet.

does not alter the frequency bands characteristic for describing the wheel conditions.

3.4 Analysis of signal anomalies - wheel fault indications

The properties of the MODWPT coefficients are determined by the base wavelet type and the level of decomposition. Different wavelets such as Daubechies wavelets, Coiflets, and Symlets can be considered for use due to their distinct characteristics. The frequency

resolution of the analysis is defined by the chosen level of decomposition. The important optimisation criterion is the complexity of calculations as the signals from MEMS sensors are usually processed using microcontrollers.

The task of finding the energy frequency band and parameters of MODWPT which most distinctly distinguish the condition of the wheel is the base of the analysis. It can be formulated as a discrete optimisation problem as the variables are discrete. The weighted difference, DW between values of energy in the frequency band for a wheels in the fault condition, E_f and for a wheels in the good condition, E_n is proposed as the measure of the ability to distinguish the wheels condition.

$$DW = \frac{E_f - E_n}{E_n} \tag{3.7}$$

It is assumed that the wheels in bad condition generate higher energy values in characteristic frequency bands than wheels in good condition. The energies are calculated using MODWPT coefficients determined by the transform parameters. These are base wavelet type - w, decomposition level - i and the number of the frequency band of the decomposition - n. The width of the frequency band may be advantageously extended to take into account the behaviour and characteristics of the signal in neighbouring bands of the decomposition. The largest extension may cover the whole spectrum of frequencies. The extended width is defined as the number - k of combined frequency bands at the current decomposition level.

The resulting search has four parameters which depend on the condition of the rails at the depot, the kind and size of wheel faults which require maintenance and the speed of travelling of the tram. The goal is to find the parameters defining the frequency bandwidth and the largest difference of energies between normal and faulty wheels, using vibration data from tests at the tram depot. The tests are representative of the standard operating procedures for the arrival and departure of trams.

The objective function is:

$$DW(w,i,k,n) = \frac{E_f\big(n(\frac{f_s}{2^i}),(n+k)(\frac{f_s}{2^i})\big) - E_n\big(n(\frac{f_s}{2^i}),(n+k)(\frac{f_s}{2^i})\big)}{E_n\big(n(\frac{f_s}{2^i}),(n+k)(\frac{f_s}{2^i})\big)} \tag{3.8}$$

expressed using wavelet coefficients:

$$DW(w,i,k,n) = \frac{\sum_{j=n}^{n+k} \|w_{i,l,f}\|^2 - \sum_{j=n}^{n+k} \|w_{i,l,n}\|^2}{\sum_{j=n}^{n+k} \|w_{i,l,n}\|^2} \tag{3.9}$$

where: $w-$ base wavelet of the transform, $i-$ decomposition level, $k-$ number of neighbouring (slots) frequency bands, $n-$ width of the frequency band. Each MODWPT coefficients of wheels in a good ($w_{i,l,n}$) and in a fault conditions ($w_{i,l,f}$) are calculated using Equation (3.3) and the absolute vibration energy values of each variable is computed using Equation (3.5).

The solution defines the parameters of calculating the MODWPT, for determining the indicative frequency band, using a set of samples from a MEMS-based acceleration sensor. This solution takes into account the conditions of performing tests that represent the real-world dispatch or arrival of trams at the tram depot. The mid value between the minimum energy of fault wheels ($minE_f$) and maximum energy of normal wheels ($maxE_n$) in the obtained frequency band, is taken as a threshold (TH) for detecting the fault wheels condition.

$$TH = \frac{minE_f(\frac{nf_s}{2^i}) + maxE_n(\frac{nf_s}{2^i})}{2} \tag{3.10}$$

The energy of vibration, in the frequency band, above the threshold TH signals a faulty wheels condition. The resultant detection threshold is determined by the state of the rails at the tram depot which defines the vibration image registered by the MEMS sensor. Consequently, the implementation of the method may necessitate updates in response to alterations in the wheels-rail conditions at the tram depot.

The optimisation problem is subjected to the following constraints:

- wavelet types: $w = \{Db, coif, sym\}$,
- N - number of frequency bands at decomposition level i,
- number of decomposition levels: $i = \{1, \ldots, \log_2(N)\}$,
- number of combined frequency bands: $k = \{0, \ldots, N\}$,
- frequency band number: $n = \{0, \ldots, N\}$.

3.4.1 Length of sensor datasets

The length of sensor datasets used for fault detection is another factor determining the success of analysis using MODWPT. Small datasets limit the permissible decomposition level and this decreases the frequency resolution of the transform. Wide frequency bands may lose indications of the fault conditions. The length of time required for sample collection is based on the volume of samples being processed. This time frame is limited by the time gap between consecutive impacts of the tram wheels, which in turn relies on the speed of the tram and the distance between rail joints. When manoeuvring at a tram depot, the number of samples can reach thousands when utilising a sensor sampling rate set at 1 kHz.

In the first step, to limit the search for the solution, the frequency resolution is restricted to 1 Hz. This value is common for describing the vibration properties of objects. Taking into account the distance between rail joints and the manoeuvring speeds the time lapse between rail joint impacts can fall in the range of 6 to 12 seconds. This observation and the use of 1 kHz sampling rate determine the number of samples, in the dataset, to be in the interval of 6000 to 12000, which can be used for describing the wheels condition. The size of the dataset in turn determines the possible range of decomposition levels which can be applied to obtain MODWPT coefficients and calculate vibration energy.

At a defined decomposition level the dataset size determines the number of samples used for computing a single coefficient. A small number of samples gives a coefficient sensitive to signal disruptions. The smallest number of samples for applying MODWPT at the 9^{th} level of decomposition is $2^9 = 512$.

Figure 3.6 illustrates the changes in the value of DW which is the measure of the ability to distinguish the condition of wheels, for different dataset sizes and a range of decomposition levels. The base wavelet of the MODWPT is coif3 as this gives the best vibration energy evaluation. The dataset samples size is limited to 12000, which accounts for the largest time intervals between rail joint impacts.

The DW values for decomposition levels 4 to 6 are small and change little in the whole range of sensor data sizes. These decomposition levels give frequency resolutions in the

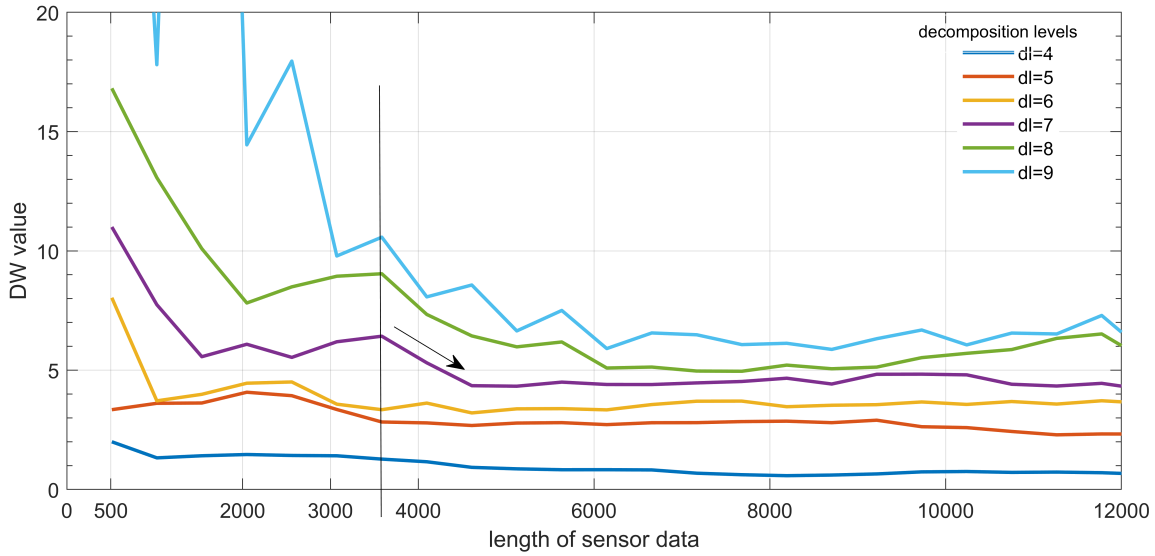

Figure 3.6: DW values relative to the level of decomposition - dl, calculated using MODWPT with coif3 base wavelet

range of 32 - 8 Hz which may be inadequate for distinguishing the wheels' condition. Higher decomposition levels give larger DW values, but decrease with the sample data size, up to the sample data size equal to 6000, from there on the DW graphs behave in a similar way as in the case of the lower decomposition levels. The DW value fall starts about the dataset size equal to 3600. The behaviour of the DW for the 9^{th} decomposition level is volatile.

In order to obtain stable evaluations of the DW function, the 7^{th} or 8^{th} level of decomposition is appropriate. The dataset size can be set to 3600. This size safeguards at least 28 or 14 samples for calculating a single coefficient at the determined decomposition levels. A large set of samples effectively suppresses signal disruptions. The collection of a set of 3600 samples is done in approximately 4 seconds, which is suitable for conducting a real-time diagnosis of the wheels condition.

3.4.2 Number of vanishing moments of the wavelet filters for vibration energy calculation

In the next step, the idea of combining the vibration energy of neighbouring frequency bands is abandoned. This approach reduces the number of variables of the objective function $DW(w, i, k, n)$ to 3: w - wavelet type, i- is the level of decomposition, n – number of the frequency band and reduces the complexity of the optimisation task. The

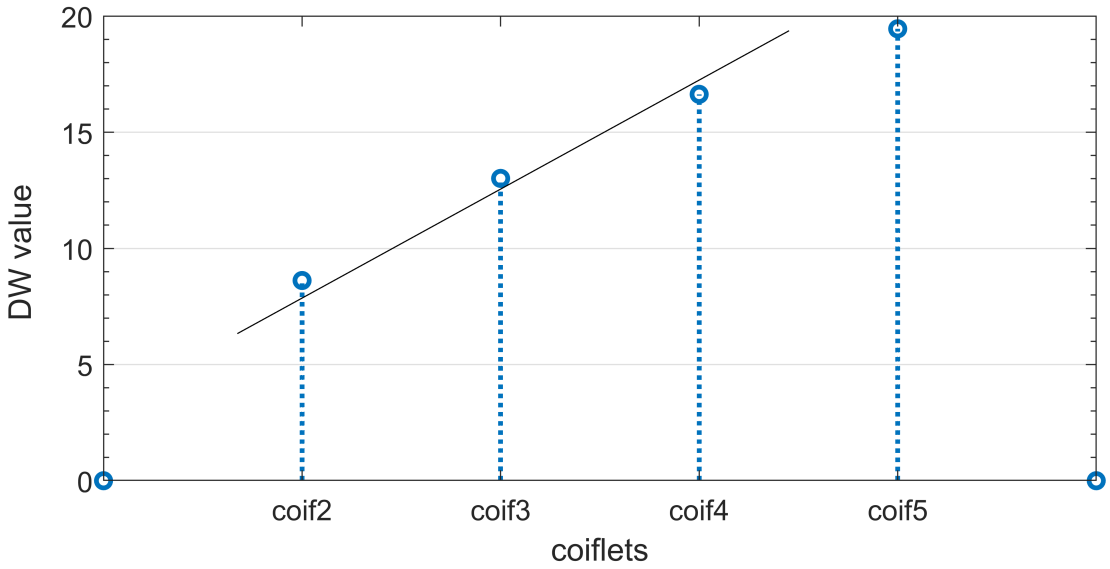

Figure 3.7: DW function values for the changing number of vanishing moments of the Coiflet base wavelet

number of the frequency band, in the decomposition, indicates the range of frequencies of the band.

Description of the vibration signal using MODWPT, with Coiflet3 base wavelet, coefficients, gives the best results, a question arises as to whether this can be improved. Modification of the base wavelet by increasing the number of vanishing moments brings "smoother" approximations of the vibration signal which can be advantageous in calculating the vibration energy and DW value. The comparison of DW values for evaluating the impact of vanishing moment change of the base wavelet - Coiflet, is done.

The stem plot in Figure 3.7 illustrates the change of DW in the function of the number of vanishing moments of the Coiflet base wavelet. The 8^{th} level of decomposition is applied and the dataset consists of 3600 samples. There is a slight flattening increase of the DW value as the number of vanishing moments grows. This increase aids in distinguishing between signals from good and faulty wheels. At this point, it becomes evident that the vibration energy difference between signals varies, with the faulty wheel energy consistently higher.

Increasing the number of vanishing moments of the wavelets filters improves the DW value but at the cost of computational complexity which may be prohibitive when the calculation is done and implemented in an embedded microcontroller-based device. The preferred wavelet base is Coiflet with 3 vanishing moments - coif3.

3.4.3 Level of decomposition for vibration energy calculation

In the final step of limiting the search for the solution, the level of decomposition comes under scrutiny. Commonly a 1 Hz resolution of analysis is used so it implies the use of the 9^{th} level of decomposition when a 1 kHz sampling rate is used. As the graph in Figure 3.6 shows the 9^{th} level of decomposition gives volatile results when calculating the DW value. Other candidates are the 7^{th} and 8^{th} level of decomposition which give a 4 and 2 Hz resolution.

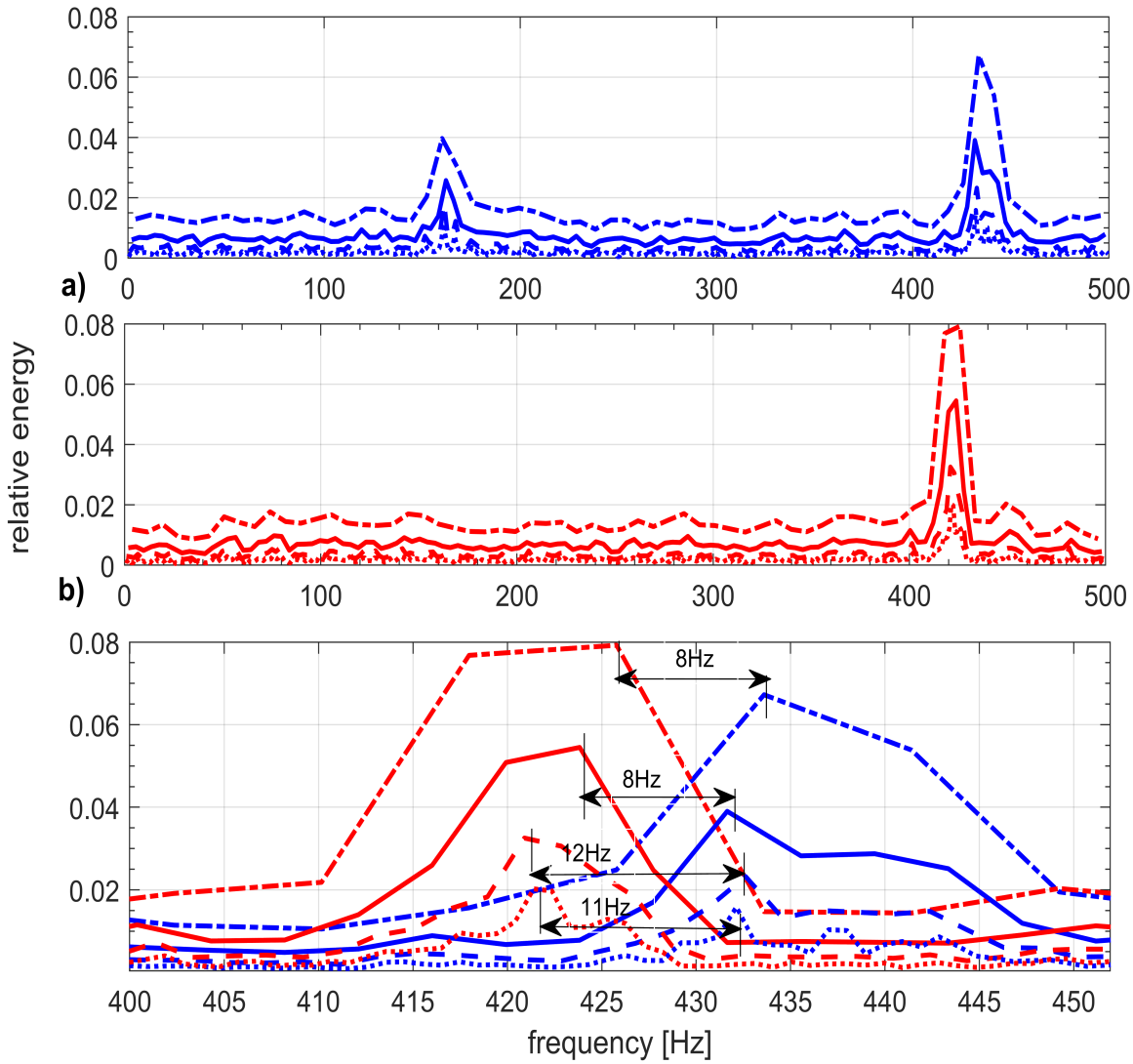

Figure 3.8: Relative energy of the vibrations a) fault-free wheel, b) "bad" wheel, c) both fault-free and "bad" wheel. Decomposition levels marked by: dash-dotted line - 6^{th}, solid line - 7^{th}, dashed line - 8^{th}, dotted line - 9^{th}.

The comparison of results of using different decomposition levels for evaluating the wheel conditions is presented in Figure 3.8. Relative energy graphs calculated using 6^{th}

to 9^{th} decomposition levels illustrate the ability to distinguish good and bad wheels. Figures 3.8 a), b) show energy islands with widths equal to the width of frequency bands resulting from the decomposition level. This confirms that abandoning the idea of combining neighbouring frequency bands is justified.

The enlarged excerpt of the spectrum Figure 3.8 c) details the intervals characteristic for separating the wheel conditions. In the case of the 6^{th} level of decomposition the interval is equal to one frequency band of the decomposition which is 8 Hz. Similarly the 7^{th} level gives also an 8 Hz separation but this represents 2 frequency bands by filtering the bands using a dyadic filters $(2^i, i = 0, 1, 2, 3)$ starting from the ninth level of decomposition.

At the 8^{th} and 9^{th} decomposition levels, the generated frequency interval for the separations wheel conditions are much larger, specifically 12 Hz and 10 Hz, which in turn corresponds to 6 and 10 frequency bands. This means that the signals are broken down into smaller and distinct frequency ranges, allowing for a more detailed analysis of the signal. Table 3.2 contains the frequency description for differentiating the wheel conditions.

Table 3.2: Wheel condition description

Decomposition level	Peak frequency [Hz] fault-free	"bad" wheel	Distance Δ [Hz]	freq. bands	DW
6	433	425	8	1	3
7	431	423	8	2	6
8	433	421	12	6	9
9	432	422	10	10	10

When evaluating the condition of wheels, it is important to take into account the frequency bands that separate the wheels in good and bad condition. A larger number of frequency bands makes it easier to differentiate between the two conditions, as it allows for a more precise evaluation. However, it is important to note that small errors in energy calculation may cause changes in the peak energy frequency bands, which can affect the accuracy of the evaluation. To ensure a more robust evaluation, it is recommended to have a large number of separating frequency bands, as this provides a more rugged margin of evaluation.

The level of decomposition in the MODWPT significantly influences the resolution

of the signal and therefore affects the ability to assess the wheel condition. The higher levels of decomposition enable finer resolution in frequency bands, which is essential for identifying sharp changes in vibration signals. With an increased level of decomposition, the width of frequency bands decreases, allowing for more detailed frequency information to be captured. This detail is crucial for extracting specific anomaly frequencies that may indicate wheel defects.

In contrast, lower decomposition levels result in wider frequency bands that can blend various components together, making it difficult to distinguish between normal and faulty wheel conditions as distinctive features might be masked. In short, the wider frequency bands at a lower decomposition level may lead to decreased resolution, making it more challenging to accurately identify wheel conditions.

The findings prove that the 8^{th} decomposition level utilising coif3 wavelets base offers an optimal combination of computational efficiency and reliable condition assessment capability.

4

Validation of the Method Using Field Test Data

The proposed method is validated at the main tram depot of Tramwaje Śląskie, S.A., which is the largest tramway operator in the Silesian Region in Poland. The company provides tram services for the Upper Silesia Region in Poland. The depot is responsible for the maintenance of more than 130 trams. The company strives to enhance the operational maintenance of its tram fleet. The primary objective is to tune the parameters of the proposed method to obtain a robust solution for assessing the condition of wheels of dispatched and arriving trams.

Figure 4.1 presents the block diagram of the actions used for the validations of the method. A prototype recording device based on a MEMS acceleration sensor is used to collect vibration data. The collected data is transformed using MODWPT with parameters determined in the course of the design of the proposed method by selecting

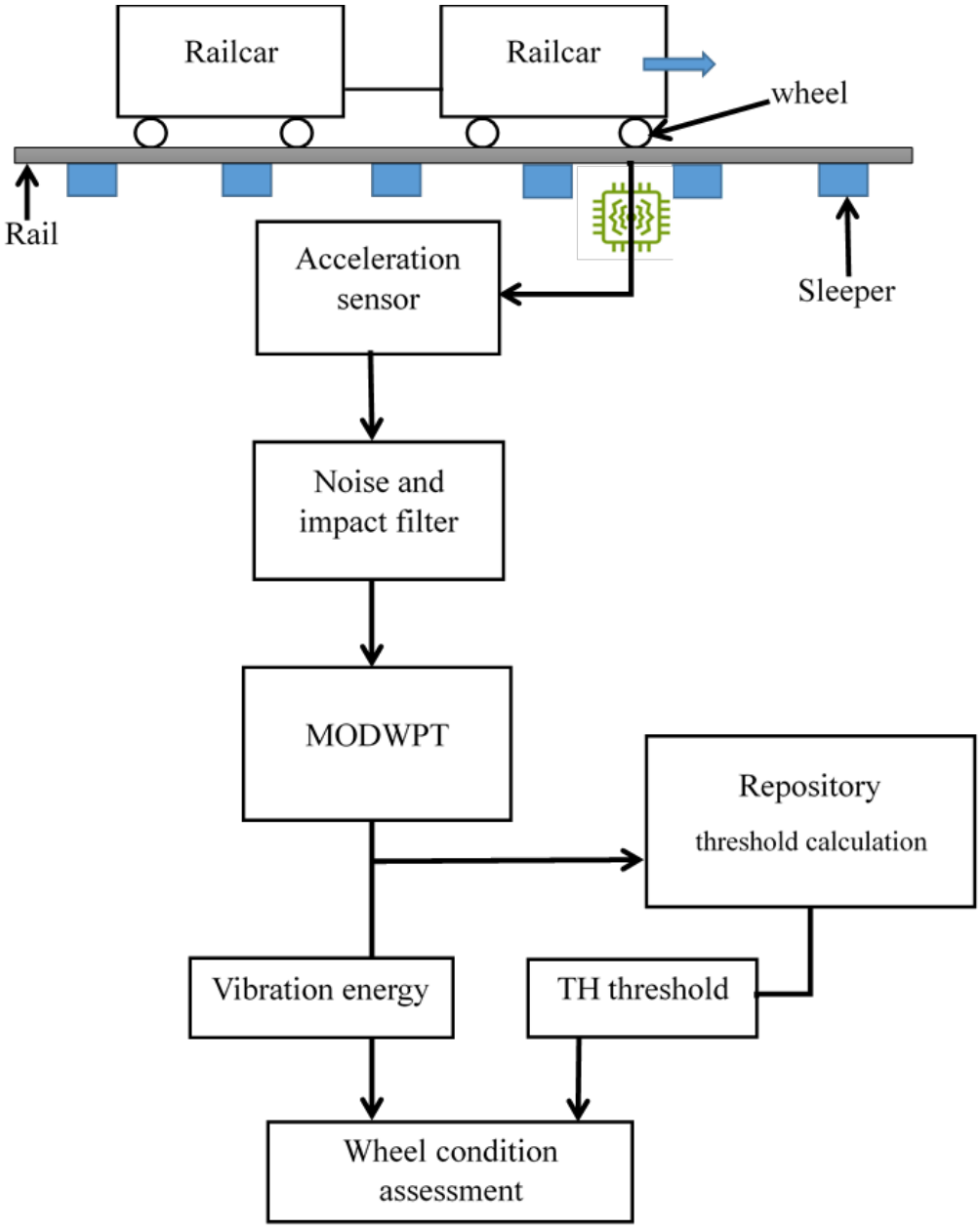

Figure 4.1: The block diagram for validating the wheel condition assessment method

the most valuable base wavelet. These base wavelet of the transform is mainly the Coiflet with 3 vanishing moments, the 8^{th} level of decomposition is applied, and the characteristic frequency band of 420 – 422 Hz clearly determines the condition of wheels within which fault conditions experienced.

The coefficients of the transformed acceleration data are used to calculate the energies of the vibration in frequency bands of the decomposition. The energy values are stored in the repository and are used to calculate the threshold for detecting faulty wheels. A number of drives with known wheel conditions are done to set up TH - the reference threshold. The value of the threshold is henceforth updated every new railroad drive

of the dispatched or arriving trams. This value is used to evaluate the condition of the wheels. If the current energy value in the characteristic frequency band surpasses, the threshold of a wheel fault is signalled. The size of the DW can be a measure of the wheel condition. A higher DW value indicates a more serious condition requiring manual inspection.

4.1 Test site and the acceleration sensor

The tram depot includes repair workshops, test tracks and complex facilities for re-generating wheelsets of trams. The process of regenerating wheelsets involves different machining operations (molding, turning, facing, drilling) for evaluation of the condition of the wheels, reconstruction of damaged wheels and testing. The depot has a very long history of operation and the staff is experienced in inspecting, repairing and maintaining overall operations of tram vehicles. Their attitude favours testing new solutions for enhancing the depot's operation. A large spectrum of faulty wheels is available for testing and a suitable piece of track is ready for tests.

The tram depot is equipped with several rail tracks, which are utilised to effectively organise the movement of trams within the premises. The chosen rail track for the tests consists of grooved rails type 59R1 (Ri59) 18 m long placed on concrete sleepers. Consecutive rails are not welded so the track vibrations transferred from rail to rail are highly dampened. The prototype vibration recording device containing a MEMS-based acceleration sensor is attached to the foot of the rail - Figure 4.2 b). A special metal bracket is used for reliable vibration transfer. The device may also be attached, using a strong magnet, to the web of the rail Figure 4.2 a).

The prototype vibration recording device contains a 3-axis MEMS accelerometer sensor. The measurement ranges are ±6g, ±12g and ±24g. The accelerometer has been qualified according to AEC-Q100 standards, making it suitable for operating in challenging environmental conditions. The MEMS prototype is self-powered and it is able to record acceleration measurements for several weeks. Through various testing procedures, the most effective measurement range was established. The established measurement range is ±6g and this range enables the registration of impacts at rail joints without "overloading" the sensor and also, this ranges gives large signal values

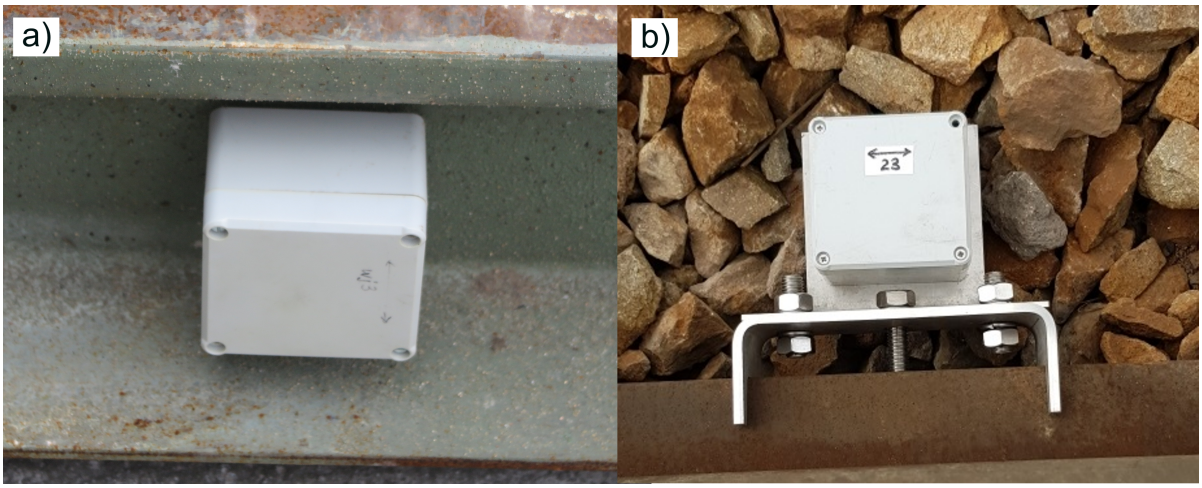

Figure 4.2: Sensor prototype mounted a) on the web of the rail, b) on foot of the rail

during wheel rolling operation. The accelerometer has a digital output and provides a stream of data with a resolution of $1/2^{12}$ of its range. The highest sampling rate equals 1 kHz.

4.2 Data filtering

The stream of acceleration data is stored in an embedded memory or it may be radio transmitted to a repository. During the tests, the option of local storage is used. Several recording sessions were carried out. A recording session is performed during a railroad drive of a tram on the test track. Trams with wheelsets in different conditions were driven. Figure 4.3 shows the results of a recording session with graphs of acceleration values for wheelsets in good condition (a) and wheelsets with "flat" wheels (b).

The graphs present rolling vibrations alternated with impact images when the tram wheels pass rail joints. The amplitude of the impact vibrations is much higher than rolling. The acceleration values are raw data from the ADC of the sensor. The sensor contains a 12-bit ADC providing values in the range [-2048, 2047] which covers the measuring range in the tests that are ±6g.

Figure 4.4 presents a 0,1 [s] excerpt with data converted to absolute acceleration values. The sensor is mounted to the web of the rail in such a way that the x-axis data is biased by the earth's gravity and maps up-down accelerations of movements of the rail, y-axis data maps accelerations along the rail, whereas z-axis values represent

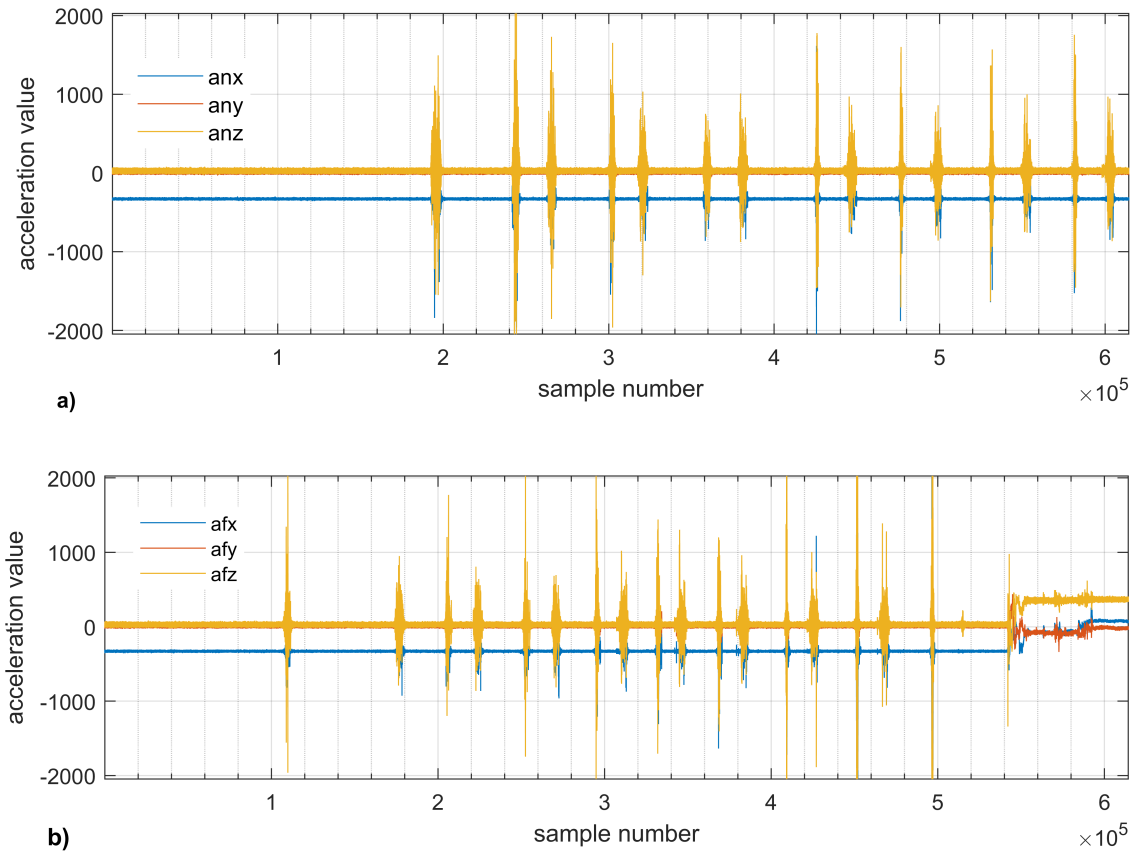

Figure 4.3: Samples of acceleration values for wheelsets; a) good condition and b) wheelsets with "flat" wheels

accelerations of movements perpendicular to the length of the rail. The values do not exceed 2 $[m/s^2]$ which is about 1/60 of the measuring range.

The perpendicular accelerations have the highest amplitudes as illustrated in the Figure 4.4 c) surpassing twice the accelerations in other axes. The source of these vibrations is not clear it may originate from the side movements of the wheelsets during the drive.

Damaged wheels especially with deformations of the wheel surface act on the rail in a hammer-like way causing up-down movements which are visible in the x-axis acceleration data as demonstrated in the Figure 4.4 a). This stream of data is the candidate for extraction of wheel condition indications. Comparable acceleration values are measured in the y-axis, shown in Figure 4.4 b).

The employed MEMS-based acceleration sensor includes an advanced noise-filtering circuit which adapts the cut-off frequency to the programmed sampling rate. This ensures

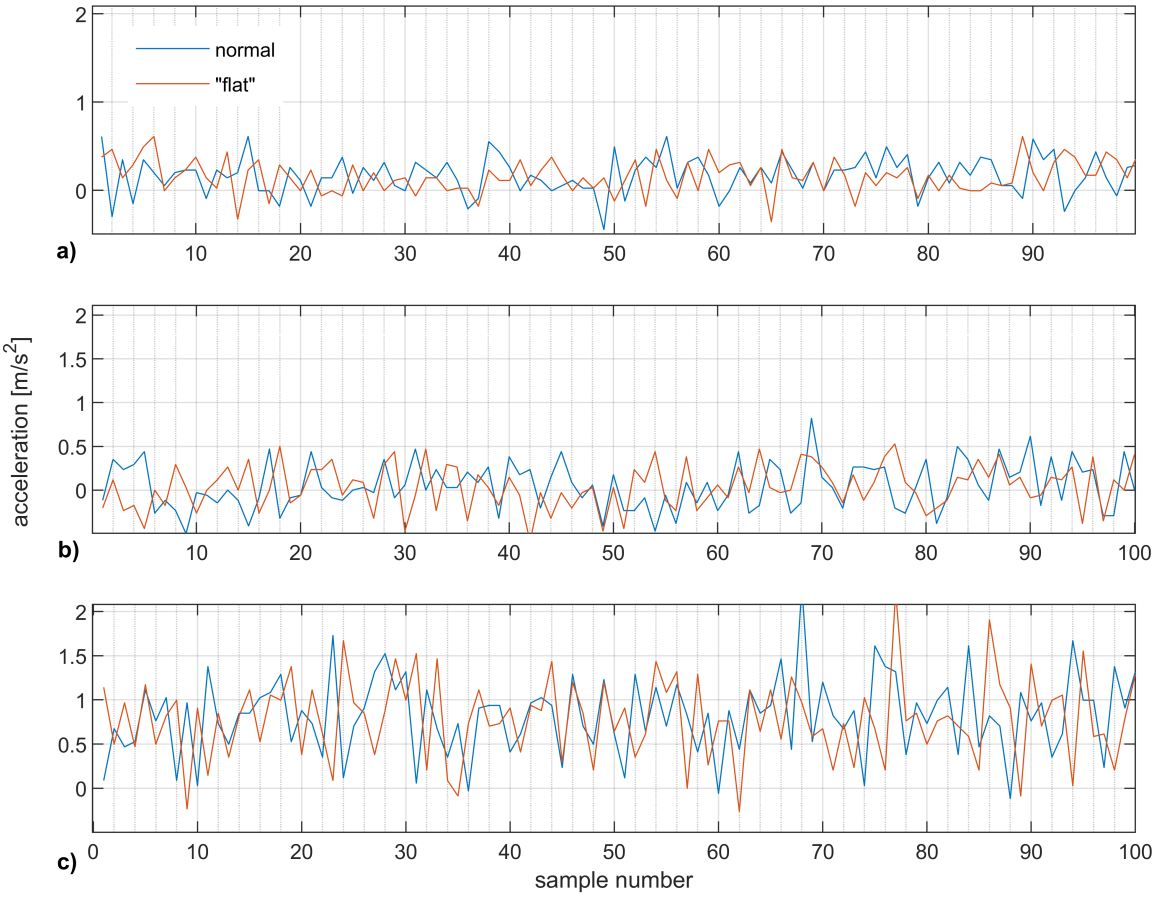

Figure 4.4: Samples of acceleration values for wheelsets; a) x-axis b) y-axis c) z-axis

a reliable conversion of accelerations using the embedded ADC.

The elapsed time between rail joint impacts varies in the time bracket 6 to 12 seconds that is 6000 to 12000 samples when the sampling rate equals 1 kHz. The size of the time bracket depends on the tram's speed during the railroad drive and on the distances between the wheelsets of the tram and on the distance of wheels of the wheelsets. Complying with the results of the search for the best dataset length in order to safeguard a "clean set" of rolling vibration data and to obtain a high DW value, 3600 samples are cut out of the data stream between impacts.

A moving average of the incoming acceleration values is used as an indication of the start of the rolling period. The length of averaging the incoming samples is chosen to match the size of the impact. A number of tests were carried out and the value of 1000 proved satisfactory. During the tests, a rolling threshold was also determined. When the average of the previous 1000 samples falls below the rolling threshold it signals the start of rolling data. The start signal triggers the assembly of the dataset for the MODWPT.

The next set is assembled when the average sustains a rise and falls again. The collected sets of data - packets are passed to the MODWPT calculation step. The packets contain 3600 samples of x-axis acceleration values.

4.3 MODWPT-based energy results for test drives

The goal of transforming the data packets is to obtain vibration energy values in frequency bands which describe the properties of the vibration signal. The vibration energy proves credibility for assessing wheel anomalies such as faults. MODWPT is applied to obtain description coefficients which are used to calculate energy values. The proposed method defines the appropriate base wavelet of the transform and the necessary decomposition level in order to achieve effective results for describing the energy characteristics.

MODWPT with base wavelet coif3 is applied to the collected data packets. The MODWPT coefficients at the 8^{th} level of decomposition are used to calculate energy values of the vibration signal in the frequency bands of the decomposition. Railroad drive tests were done using different trams.

Figures 4.5 and 4.6 present energy variation of the rolling data calculated using the MODWPT coefficients for two exemplary test drives sessions. Theses test drives sessions were carried out using trams with different wheels and wheelsets condition. The sampling rate is 1 kHz so the width of the frequency bands comes to about 2 Hz. In these figures, the normal wheel data and "flat" wheel data are graphed. The relative energy graphs presented in these figures map data from packets collected during the two test sessions. Each test drive session consist of a sets of tram drive for the diagnosis of wheels conditions. These sets of drives have 10-12 packets of characteristic frequency which is represented with the specific tram and wheels as graphed in the following figures.

The superimposed graphs of the relative energy illustrate the behaviour of the rails due to rail - wheel contacts during the drive. The graphs slightly differ but retain the characteristics. The relative energies values are related to the total vibration energy in the measured frequency spectrum. The selected trams for test drive had "flat" wheels and wheelsets in different conditions. There are characteristic high energy islands in frequency bands at 150-230 Hz and at 400-460 Hz in test session I as illustrated in

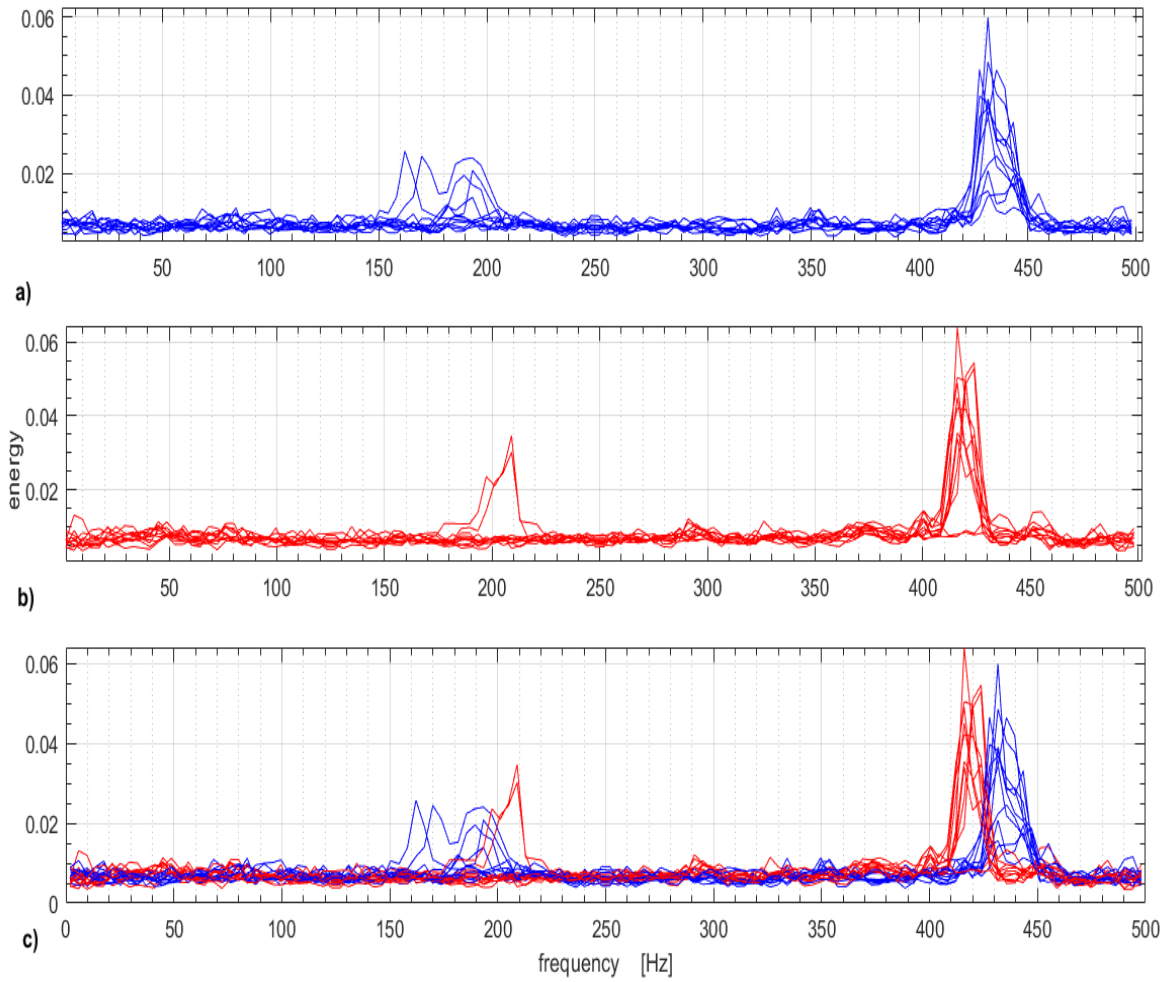

Figure 4.5: Relative energy of the sensor samples (test session I): a) normal wheels, b) "flat" wheels, c) superimposed normal and "flat"

Figure 4.5. In test session II there is an island at 70 – 110 Hz with twice the energy and also an island with smaller energy at 170 – 230 Hz and again at 400 – 460 Hz Figure 4.6.

The lower frequency band energies of normal and "flat" wheels, obtained in both test sessions, almost cover each other, no distinct differences can be extracted. The energy volatility may be assigned to the wheelset conditions. The test track condition may also add energy islands with characteristic frequencies.

In the case of the higher frequency band, the "flat" wheels have an energy peak in the frequency band 420 – 422 Hz, whereas normal wheels are 12 Hz further on. This complies with the results of determining the frequency band with the highest DW value. The damaged wheel frequency images appear independent from the frequency spectrum generated by the conditions of wheelsets.

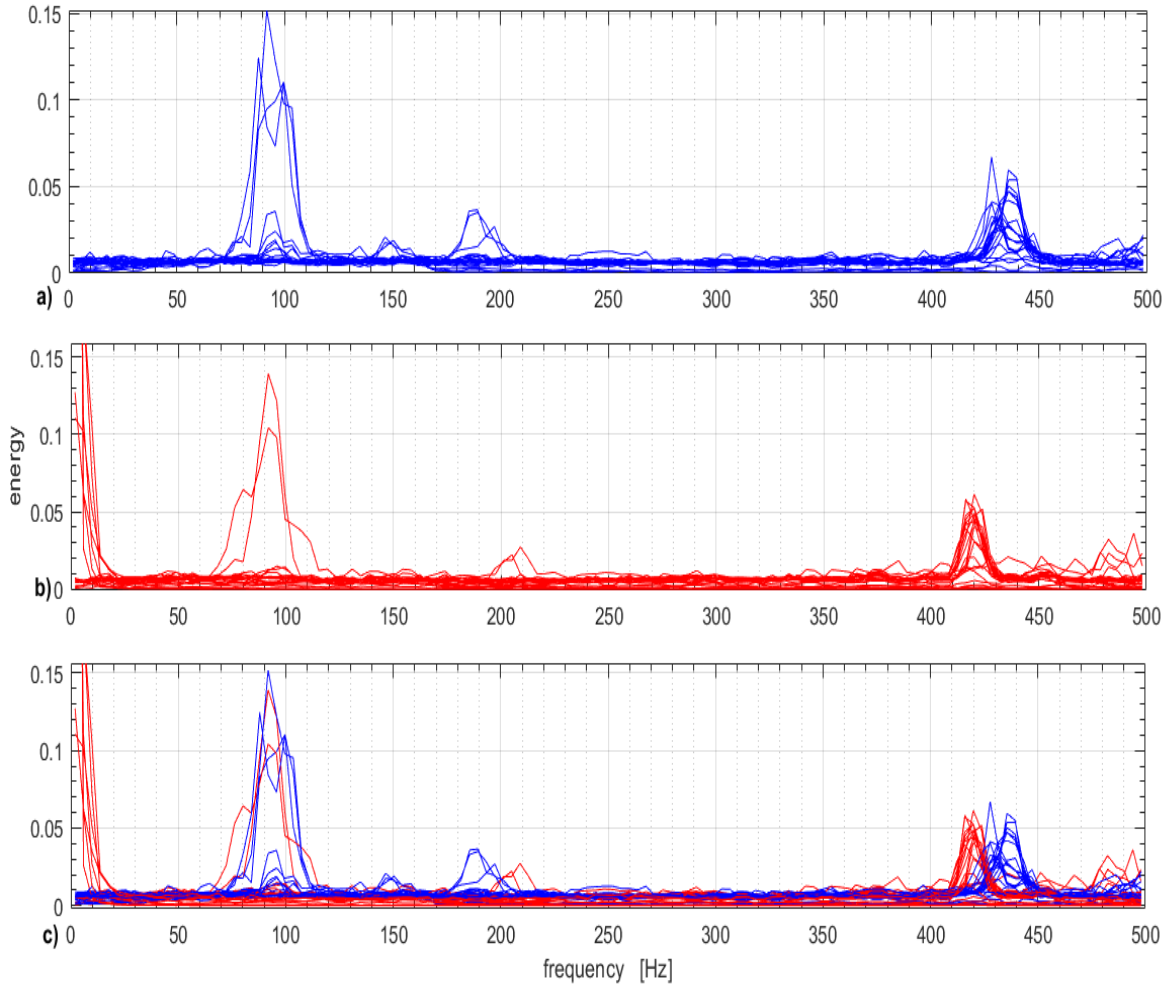

Figure 4.6: Relative energy of the sensor samples (test session II): a) normal wheels, b) "flat" wheels, c) superimposed normal and "flat"

4.4 Wheel condition assessment

The obtained energy values for each of the data packets are used for the calculation of TH - the threshold for determining the wheel condition. A number of railroad drives are carried out with trams which have "flat" wheels to determine the reference TH. The way the drives are carried out and the conditions of the trams influence the value of TH. The reference value is chosen to satisfy the worst testing condition for "flat" wheels.

Figure 4.7 presents the characteristics of the test drives session I. The DW values and energies are calculated for the energy peak of "bad" wheels frequency band 420 – 422 Hz using datasets with 3600 samples. The DW values fall in the range 2 – 9 and the vibration energy values correspond to the DW values. Taking into account that the

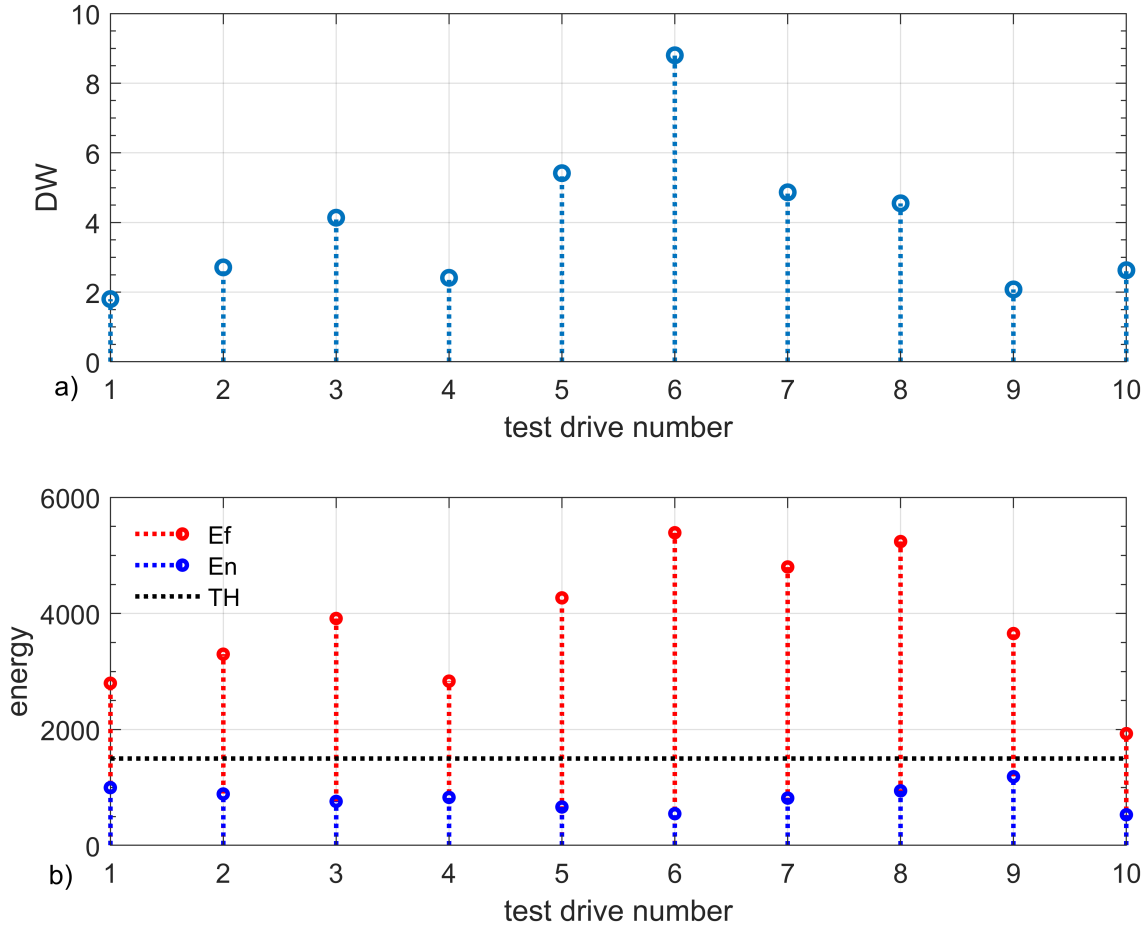

Figure 4.7: Characteristics of the test drives (session I) a) DW values, b) energies En - good condition, Ef - bad condition and bad condition threshold - TH

rolling energy of wheels in good condition does not change much, because the test drives are carried out on the same test track, the higher energies may indicate the size of surface damages of the wheels.

Table 4.1 demonstrates the energies during test drives session I. The vibration energy of wheels in good condition is more than twice as small as that of the "bad" wheels. The scattering of energy values in the case of wheels in good condition does not surpasses 23% whereas for the "bad" wheels reaches up to 30%.

Table 4.1 demonstrates an analysis of vibration energies of ten specific tram vehicles' wheels during test drives. Wheels in faulty conditions were intentionally mounted on the tram vehicle. Test drives were conducted on the same length of rail track, and repeated measurements were analysed. The maximum energy resulting from the faulty wheel was registered at test number six, whereas the minimum energy was registered during test

Table 4.1: Wheel energies characteristics for a test drives session I

Test drives session I	1	2	3	4	5	6	7	8	9	10
DW	2	3	4	3	6	9	5	5	2	3
E_f	2800	3300	3915	2835	4270	5390	4800	5240	3655	1930
E_n	1000	890	760	830	665	550	820	940	1190	530
$E_f - E_n$	1800	2410	3155	2005	3605	4840	3980	4300	2465	1400

drive number ten.

For a normal wheel, the same measurement was conducted simultaneously, and the all-wheel energies registered were much smaller compared to faulty wheel energies. The variation in wheel energy is significant for faulty wheel conditions. A huge variation of energy is registered for test drive numbers 5 to 8. An examination conducted verified the presence of the wheels with worse conditions, which confirmed that high vibration energy may be generated by the very bad condition of the wheels.

For the same set of test drives session I, a reference TH is calculated using Equation 3.10 and indicated in the Figure 4.7 b). The range of "flat" wheel energies is significantly larger. TH is calculated as the mid-value between the highest normal wheel energy and the lowest "bad" wheel energy. The size of the difference between the threshold and "bad" wheel energy may be a measure of the wheel tyre damage or wheel fault condition.

Similarly, in the test drives session II - Figure 4.8, the vibration energy of selected tram vehicles was registered and analysed to identify differences in vibration energy resulting from normal and faulty wheel conditions. The numerical values illustrated in Figure 4.8 b) confirmed similar conclusions derived from session I. The DW values range increased up to 15 without affecting the TH value assigned for the separation condition of the wheels. The increase in the DW values supports the differentiation of signal energy resulting from a faulty wheel, and it enhances monitoring operations. Therefore, the results gained from test drives session II confirm that a faulty wheel induces much higher vibration compared to a normal wheel.

Table 4.2 illustrates the vibration energy registered and analysed for a typical fleet of tram vehicles which are considered in the test drives session II. In this session, the fleet of tram vehicles is randomly chosen and ordered for the railroad drive test. Likewise the first session drive test, the higher vibration energy resulted from the faulty wheel-

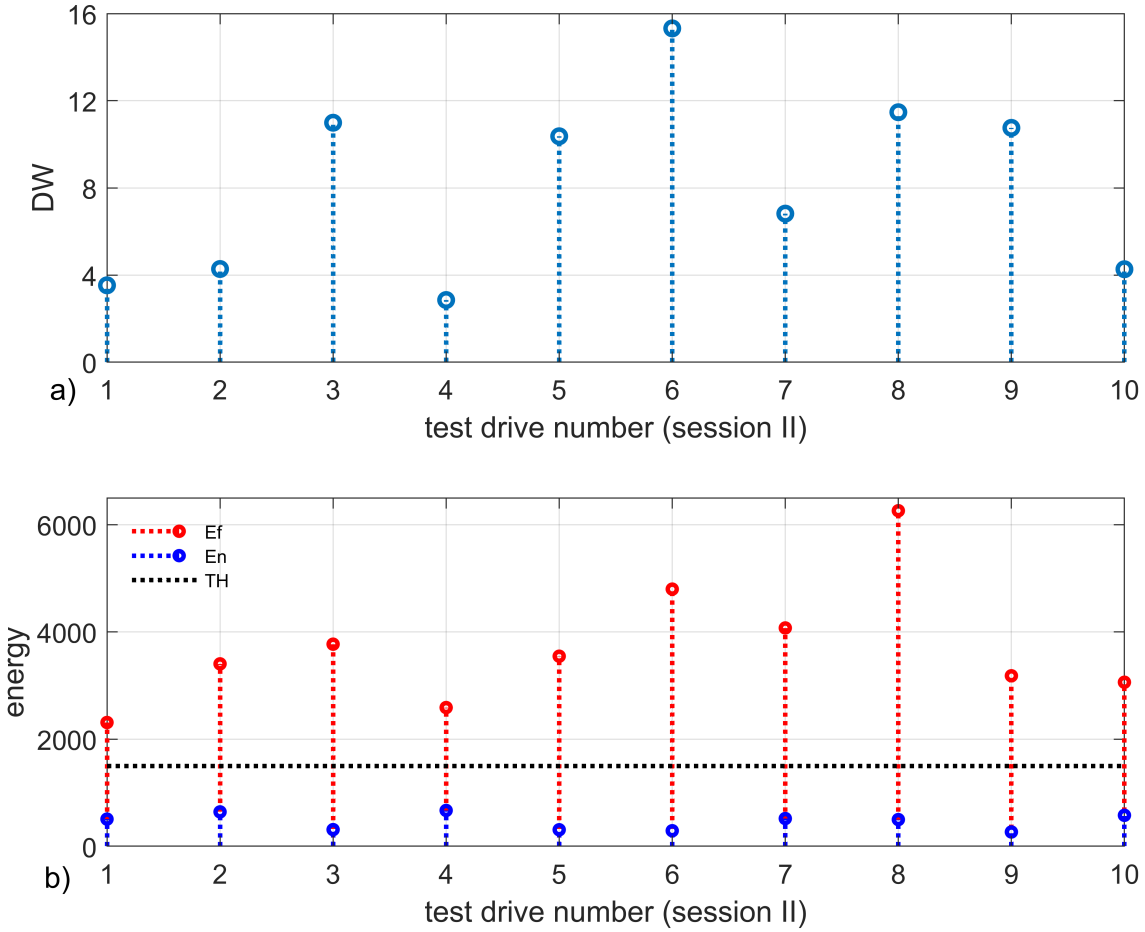

Figure 4.8: Characteristics of the test drives (session II) a) DW values, b) energies En - good condition, Ef - bad condition and bad condition threshold - TH

mounted tram vehicle.

For a fault wheel-mounted tram vehicle, the maximum energy was registered at test drive number 8, whereas the minimum energy was registered during test drive number 1. Higher energy value variations are registered at test numbers 3, 5, 6, 8 and 9. By closely looking at the DW value, the maximum DW value of 15 is registered at 6^{th} test drive number although the maximum energy of the signal is registered for test drive number 8. This show that for DW>0, after a certain limit, the peak DW values are not always proportional to the peak energy resulting from the signal.

Faulty wheels detection tests using the threshold also prove that the threshold value is robust to variation of tram speed in the range of 2-7 $[m/s]$ which covers the range of speeds of manoeuvring trams in the tram depot.

The threshold value for the detection of faulty wheels is susceptible to the conditions

Table 4.2: Wheel energies characteristics for a test drives session II

Test drives session II	1	2	3	4	5	6	7	8	9	10
DW	3	4	11	3	10	15	7	11	10	4
E_f	2300	3405	3770	2590	3545	4800	4075	6260	3180	3060
E_n	510	645	315	670	310	295	520	500	270	580
$E_f - E_n$	1790	2760	3455	1920	3235	4505	3555	5760	2910	2480

of the rail tracks within the tram depot area. Poorly maintained rail joints and damaged sleepers produce substantial vibration signals when trams are in motion, which can adversely affect the collected vibration data. Consequently, this leads to distorted energy values in frequency bands that do not align with the actual conditions of the wheels.

Wheel energy values and TH values are stored in the repository. The reference TH obtained in test drives is updated when there is an indication that new data describes "flat" wheels. The indication may be entered by staff or it may come from the condition assessment stage when the evaluated energy surpasses the threshold TH.

The tram depot where the tests were conducted maintains a large fleet of trams in different technical conditions. The tests were carried out for trams with flat wheels. The reference threshold TH was applied for the calculated energies in the tests and every flat wheel was detected. The reference threshold is independent of the vibration spectrum generated by the conditions of wheelsets. Calculated DW values in the test could be used to assess the severity of the wheel damage. The results prove that more damaged wheels have higher values of the DW and generate much higher vibration energies.

5

Sensor Node for Wheel Condition Monitoring

Validation of the proposed wheel condition assessment method proves that the application of MEMS-based acceleration sensors is effective for obtaining the spectrum image of vibrations. Collected acceleration data can be transformed using MODWPT and the resultant coefficient values can be used to describe with sufficient accuracy the condition of wheels. The practical implementation of the proposed method is determined by the tram depot resources. The goal is to provide reliable information, for the personnel responsible for maintaining the tram fleet, on the conditions of being dispatched or arriving trams.

A least invasive, into the infrastructure of the depot, implementation is highly recommended. This implies the reduction of wiring needs which involves designing and putting some cables in the ground within the manoeuvring rail network. Power supply for functioning may be difficult to deliver same as carrying out of the transfer of vibration data for processing. The proliferation of IoT solutions is a chance to satisfy such limitations of the implementation.

An IoT solution of the sensor node for wheel condition monitoring determines a circuit optimised for energy consumption, efficient wireless communication and for least maintenance requirements. This gives a construction based on an embedded solution integrating a transceiver, microcontroller, sensor and power supply. The transceiver may be combined with the microcontroller, the sensor will be a MEMS-based device and the power supply must ensure long periods of operation and easy charging.

The energy balance of a sensor node consists of a transceiver, computing and sensing energy. The transceiver energy consumption dominates as it determines the reliability of exchanging vibration data within the tram depot which may have a very noisy electromagnetically environment. Such environments require higher transmitter energies to sustain error-free communications.

Radio platforms available for developing wireless communications can be split into licensed platforms strictly governed by radio operators and free-to-use platforms using proprietary or standardised transmission technologies. Preferable are license-free platforms such as WiFi, Bluetooth LE, LoRa and Zigbee. Transceiver energy consumption is reduced by selecting the right mode of transceiver operation to ensure the required range and error rate. The application of sleep/wake and cycling is noted as the most effective approach for saving power.

The transceiver must comply with radio regulations that limit the transmission power at the antenna. The necessary power for transmitting depends on the modulation schema and on the efficiency of the transceiver circuit. The efficiency of the transceiver circuit highly depends on the construction of its antenna and matching components. Table 5.1 lists the maximum power requirements of transmissions meeting the radio regulations. LoRa platform has the lowest power demand and it also has the longest transmission range. This platform uses spread spectrum modulation which is very resistant to ambient radio noise.

Table 5.1: Radio platforms power requirements mW

Platform	WiFi 2.4GHz	BLE 2.4GHz	LoRa subGHz	Zigbee 2.4GHz
Tx	940	640	150	200
Rx	300	83	33	92

A design is proposed which meets the presented limitations for the construction.

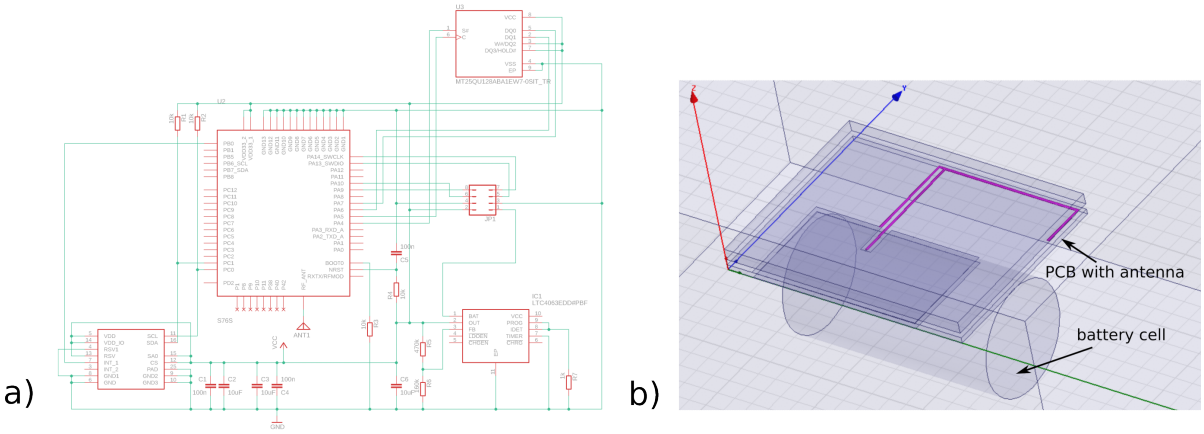

Figure 5.1: Sensor node: a) schematics, b) antenna model

LoRa radio platform is chosen as the communication basis. MEMS-based sensor qualified for automotive use is chosen for enduring the harsh environment at the tram depot and the power supply is provided by a Li-ion cell. Additionally, the work parameters of the device are registered in a flash memory for potential analysis of its performance. The functioning and data processing is controlled using a microcontroller.

Microcontrollers are based on CMOS technology and their power requirements are highly related to the clock frequency. Low-power 32-bit microcontrollers consume about 300µW/MHz which gives around 15 mW at the highest clock frequencies. Such components are capable of calculating MODWPT coefficients. Microcontrollers with integrated LoRa transceivers are available on the market. These devices can greatly reduce the component count of the sensor node design.

The proposed design consists of a microcontroller with an integrated LoRa transceiver, a low-power MEMS 3-axis acceleration sensor, a flash memory and a power supply monitoring component to protect the Li-ion battery which supplies energy for the operation of the sensor node. Figure 5.1 a) presents the schematics. All components are placed on one side of the PCB the transceiver uses a printed inverted F antenna as shown in Figure 5.1 b). The transmission range reaches a few hundred meters, satisfying the needs of operation in the tram depot.

The functionality of the construction is defined by firmware stored in the microcontroller. The construction can function as a transmitter or as a receiver. The transmitter collects vibration data from the MEMS sensor and calculates vibration energy values using MODWPT, the resultant data stream is sent out. The proposed solution incorporates the receiver connected to a PC at the tram depot. The received stream of vibration

energy values is processed and the condition of the wheels is evaluated, the results are presented on the PC. Additional PC software can monitor the behaviour of the sensor node and the operation of the receiver.

Tests of the prototype - Figure 4.2 prove that it can function for several months with an 18Wh Li-ion battery transmitting data to a second prototype which functioned as a repository of vibration data.

6

Conclusions

The analysis of vibration energy content in different frequency bands proves successful for assessing the condition of wheels. The condition is manifested by values of vibration energy in specific frequency bands. The highest vibration frequencies, at low speeds of vehicle movements, do not surpass the frequency bandwidths of commonly available MEMS sensors. The most common sensors equipped with 12-bit ADCs are adequate for obtaining, and useful for processing, vibration data for assessing the wheel conditions.

The provisional research hypotheses are successfully confirmed. The hypotheses constitute the basis of the proposed method for assessing the condition of the wheels of wheelsets of railcar during a railroad drive. The method defines the action steps for deriving the indications of wheel damage using vibration data collected on the rails during the drives. Vibration data is collected using a MEMS-based acceleration sensor mounted on the rail on which the railcar moves. The vertical movement acceleration of the rail track measurements is transformed to obtain the energy of vibrations. MOD-WPT with an appropriate base wavelet that is Coiflet with 3 vanishing moments, is used

for calculating the transform coefficients. The study proves that the 8^{th} decomposition level provides coefficients effective for indicating damaged wheels. The frequency range 420-422 Hz is the characteristic band for assessment of the condition of the wheels.

The use of MEMS sensor devices for measuring acceleration signals by mounting on rail tracks allows for a convenient design of a wheel fault detection system. Highly integrated MEMS-based sensor devices are small sized, can be attached using brackets or magnets to the rail track. The calculation of the MODWPT coefficients for the 8^{th} level of decomposition, utilising the coif3 wavelet, does not impose excessive requirements on the computation resources. Therefore, an embedded system incorporating the MEMS sensor and an advanced microcontroller can effectively handle the stream of acceleration measurements and derive the wheel condition description.

The changes in vibration characteristics mark the initiation of faults within the wheel systems of railcars. Therefore, vibration-based condition monitoring of railway wheels is considered to be a vital approach in the conduct of maintenance services. This approach facilitates early detection of potential problems with wheel systems, enabling timely maintenance interventions to avoid severe accidents.

The application of MODWPT effectively provides a description of MEMS sensor acceleration signals. The values of vibration energy, calculated using the transform coefficients in the frequency bands defined by the decomposition level, indicate potential anomalies of the railroad drive. The anomalies are generated by the technical conditions of the wheels, wheelsets and rails. Careful analysis is required to appropriately assign the frequency bands to the sources of anomalies. This study maps the condition of wheels to the energy in the frequency band 420-422 Hz. It is important to draw attention to the overall circumstances of the railroad drive. A bad condition of the rail track, loose sleepers, and high speed of the railcar may change the characteristic frequency band for assessing the wheel condition.

Future studies can investigate the mapping of other than wheel conditions, sources of vibration energy anomalies to characteristics frequency bands. The problem of evaluating the size and type of wheel damage is challenging and it may require supplementary measuring tools besides the MEMS accelerometers.

Furthermore, the following future research works are promising and they can be used as additional thoughts for researchers interested in this field.

1. Frequency Band Analysis:
   The study of frequency bands can provide valuable insights into the nature of vibration energy anomalies. Different types of wheel damage may produce unique frequency signatures, which could be used to identify and classify the damage. Advanced signal processing techniques, such as wavelet transform, or wavelet scattering, could be employed to extract these frequency characteristics.

2. Sensors Integration:
   While MEMS accelerometers are effective at capturing vibration data, the use of integrating various sensors type could provide a more comprehensive understanding of wheels, wheelsets systems and overall railcars conditions. For instance, acoustic sensors could be used to detect audible changes associated with wheel damage, and temperature sensors could identify overheating issues.

3. Machine Learning Approaches:
   Machine learning algorithms could be trained to recognize patterns in the sensor data that correspond to specific types of wheel damage. This could potentially allow for real-time detection and classification of wheel damage, improving maintenance efficiency and preventing further damage.

4. Damage Simulation:
   To better understand the relationship between wheel conditions and vibration energy anomalies, it might be beneficial to conduct controlled experiments or simulations. By intentionally introducing different types and sizes of damage to wheels in a controlled environment, researchers could directly observe the resulting changes in vibration energy and frequency characteristics.

5. Collaboration with Industry Experts:

   Collaboration with industry experts could provide practical insights into the real-world challenges of wheel damage evaluation. Their experience could guide the design of experiments and the interpretation of results.

In conclusion, the field of vibration analysis for condition monitoring of the wheels of wheelsets of railcar is a complex and multidisciplinary, involving aspects of physics, engineering, and data science. Therefore, a comprehensive approach that incorporates various methods and perspectives will likely yield the most meaningful results.

Bibliography

Anam Abid, Muhammad Tahir Khan, and Javaid Iqbal. A review on fault detection and diagnosis techniques: basics and beyond. *Artificial Intelligence Review*, 54(5): 3639–3664, 2021. doi:10.1007/s10462-020-09934-2.

Hosameldin Ahmed and Asoke K Nandi. *Condition monitoring with vibration signals: Compressive sampling and learning algorithms for rotating machines*. John Wiley & Sons, 2020.

Alireza Alemi, Francesco Corman, and Gabriel Lodewijks. Condition monitoring approaches for the detection of railway wheel defects. *Proceedings of the Institution of Mechanical Engineers, Part F: Journal of Rail and Rapid Transit*, 231(8):961–981, 2017. doi:10.1177/0954409716656218.

Jérôme Antoni. The spectral kurtosis: a useful tool for characterising non-stationary signals. *Mechanical Systems and Signal Processing*, 20(2):282–307, 2006. doi:10.1016/j.ymssp.2004.09.001.

Jérôme Antoni and R.B. Randall. The spectral kurtosis: application to the vibratory surveillance and diagnostics of rotating machines. *Mechanical Systems and Signal Processing*, 20(2):308–331, 2006. doi:10.1016/j.ymssp.2004.09.002.

Issam Atoui, Hazem Meradi, Ramzi Boulkroune, Riad Saidi, and Azzeddine Grid. Fault detection and diagnosis in rotating machinery by vibration monitoring using fft and wavelet techniques. In *2013 8th International Workshop on Systems, Signal Processing and their Applications (WoSSPA)*, pages 401–406, 2013. doi:10.1109/WoSSPA.2013.6602399.

Yihao Bai, Weidong Cheng, Weigang Wen, Yang Liu, et al. Application of time-frequency analysis in rotating machinery fault diagnosis. *Shock and Vibration*, 2023, 2023. doi:10.1155/2023/9878228.

Jyoti Barman and Durlav Hazarika. Linear and quadratic time–frequency analysis of vibration for fault detection and identification of nfr trains. *IEEE Transactions on Instrumentation and Measurement*, 69(11):8902–8909, 2020. doi:10.1109/TIM.2020.2998888.

Vittorio Belotti, Francesco Crenna, Rinaldo C Michelini, and Giovanni B Rossi. Wheel-flat diagnostic tool via wavelet transform. *Mechanical Systems and Signal Processing*, 20(8):1953–1966, 2006. doi:10.1016/j.ymssp.2005.12.012.

Hocine Bendjama, Salah Bouhouche, and Mohamed Seghir Boucherit. Application of wavelet transform for fault diagnosis in rotating machinery. *International Journal of machine Learning and computing*, 2(1):82–87, 2012.

Ellen Bergseth, Martin Höjer, Yezhe Lyu, Rickard Nilsson, and Ulf Olofsson. A wear detection parameter for the wheel–rail contact based on emitted noise. *Tribology Transactions*, 62(3):496–503, 2019. doi:10.1080/10402004.2019.1576957.

Esteban Bernal, Maksym Spiryagin, and Colin Cole. Onboard condition monitoring sensors, systems and techniques for freight railway vehicles: a review. *IEEE Sensors Journal*, 19(1):4–24, 2018. doi:10.1109/JSEN.2018.2875160.

Nirdosh Bhatnagar. *Introduction to wavelet transforms*. Chapman and Hall/CRC, 2020.

Jian Bian, Yuantong Gu, and Martin Howard Murray. A dynamic wheel–rail impact analysis of railway track under wheel flat by finite element analysis. *Vehicle System Dynamics*, 51(6):784–797, 2013. doi:10.1080/00423114.2013.774031.

Boualem Boashash. *Time-frequency signal analysis and processing: a comprehensive reference*. Academic press, 2015.

Massimiliano Bocciarelli, Giuseppe Cocchetti, and Giulio Maier. Shakedown analysis of train wheels by fourier series and nonlinear programming. *Engineering structures*, 26 (4):455–470, 2004. doi:10.1016/j.engstruct.2003.11.002.

Nicola Bosso, Antonio Gugliotta, and Nicolò Zampieri. Wheel flat detection algorithm for onboard diagnostic. *Measurement*, 123:193–202, 2018. doi:10.1016/j.measurement.2018.03.072.

S. Braun. The synchronous (time domain) average revisited. *Mechanical Systems and Signal Processing*, 25(4):1087–1102, 2011. ISSN 0888-3270. doi:10.1016/j.ymssp.2010.07.016.

J. Brizuela, C. Fritsch, and A. Ibáñez. Railway wheel-flat detection and measurement by ultrasound. *Transportation Research Part C: Emerging Technologies*, 19(6):975–984, 2011. doi:10.1016/j.trc.2011.04.004.

Wahyu Caesarendra, Buyung Kosasih, Kiet Tieu, and Craig AS Moodie. An application of nonlinear feature extraction-a case study for low speed slewing bearing condition monitoring and prognosis. In *2013 IEEE/ASME International Conference on Advanced Intelligent Mechatronics*, pages 1713–1718. IEEE, 2013. doi:10.1109/AIM.2013.6584344.

Andrew K Chan. *Fundamentals of wavelets: theory, algorithms, and applications*. John Wiley & Sons, 2011.

N. Harish Chandra and A.S. Sekhar. Fault detection in rotor bearing systems using time frequency techniques. *Mechanical Systems and Signal Processing*, 72-73:105–133, 2016. doi:.1016/j.ymssp.2015.11.013.

Jinglong Chen, Zipeng Li, Jun Pan, Gaige Chen, Yanyang Zi, Jing Yuan, Binqiang Chen, and Zhengjia He. Wavelet transform based on inner product in fault diagnosis of rotating machinery: A review. *Mechanical systems and signal processing*, 70:1–35, 2016. doi:10.1016/j.ymssp.2015.08.023.

Long Chen, Yat-Sze Choy, Kai-Chung Tam, and Cheng-Wei Fei. Hybrid microphone array signal processing approach for faulty wheel identification and ground impedance estimation in wheel/rail system. *Applied Acoustics*, 172:107633, 2021a. doi:10.1016/j.apacoust.2020.107633.

Shiqian Chen, Kaiyun Wang, Chao Chang, Bo Xie, and Wanming Zhai. A two-level adaptive chirp mode decomposition method for the railway wheel flat detection under variable-speed conditions. *Journal of Sound and Vibration*, 498:115963, 2021b. doi:10.1016/j.jsv.2021.115963.

Jie Chao Cheng. *The comparison of the methods based on Wavelet Transform and Hilbert-Huang Transform in fault diagnosis of rotating machinery*. PhD thesis, Concordia University, 2014.

Leon Cohen. *Time-frequency analysis*, volume 778. Prentice Hall PTR Englewood Cliffs, 1995.

Giorgio Dalpiaz and A Rivola. Condition monitoring and diagnostics in automatic machines: comparison of vibration analysis techniques. *Mechanical Systems and Signal Processing*, 11(1):53–73, 1997. doi:10.1006/mssp.1996.0067.

Ingrid Daubechies. *Ten lectures on wavelets*. SIAM, 1992.

Jianming Ding, Jianhui Lin, Guangming Wang, and Jie Zhao. Time-frequency analysis of wheel-rail shock in the presence of wheel flat. *Journal of Traffic and Transportation Engineering (english edition)*, 1(6):457–466, 2014. doi:10.1016/S2095-7564(15)30296-8.

Takeshi Emoto, Ankit A. Ravankar, Abhijeet Ravankar, Takanori Emaru, and Yukinori Kobayashi. Automatic dimensional inspection system of railcar wheelset for condition monitoring. In *2022 61st Annual Conference of the Society of Instrument and Control Engineers (SICE)*, pages 899–904, 2022. doi:10.23919/SICE56594.2022.9905812.

Xianfeng Fan and Ming J. Zuo. Gearbox fault detection using hilbert and wavelet packet transform. *Mechanical Systems and Signal Processing*, 20(4):966–982, 2006. doi:10.1016/j.ymssp.2005.08.032.

Michael Feldman. Hilbert transform in vibration analysis. *Mechanical Systems and Signal Processing*, 25(3):735–802, 2011. doi:10.1016/j.ymssp.2010.07.018.

Wenjie Fu, Qixin He, Qibo Feng, Jiakun Li, Fajia Zheng, and Bin Zhang. Recent advances in wayside railway wheel flat detection techniques: A review. *Sensors*, 23 (8):3916, 2023. doi:10.3390/s23083916.

Dennis Gabor. Theory of communication. part 1: The analysis of information. *Journal of the Institution of Electrical Engineers-part III: radio and communication engineering*, 93(26):429–441, 1946. doi:10.1049/ji-3-2.1946.0074.

Feng Gan, Huanyun Dai, Hao Gao, and Maoru Chi. Wheel–rail wear progression of high speed train with type s1002cn wheel treads. *Wear*, 328:569–581, 2015. doi:10.1016/j.wear.2015.04.002.

Run Gao, Qixin He, Qibo Feng, and Jianying Cui. In-service detection and quantification of railway wheel flat by the reflective optical position sensor. *Sensors*, 20(17):4969, 2020. doi:10.3390/s20174969.

B Gapiński, B Firlik, TG Mathia, et al. Characteristics of tram wheel wear: Focus on mechanism identification and surface topography. *Tribology International*, 150:106365, 2020. doi:10.1016/j.triboint.2020.106365.

Chayan Ghosh, Anshul Verma, and Pradeepika Verma. Real time fault detection in railway tracks using fast fourier transformation and discrete wavelet transformation. *International Journal of Information Technology*, pages 1–10, 2021. doi:10.1007/s41870-021-00784-x.

María Jesús Gómez, Cristina Castejón, Eduardo Corral, and Juan Carlos García-Prada. Railway axle condition monitoring technique based on wavelet packet transform features and support vector machines. *Sensors*, 20(12):3575, 2020. doi:10.3390/s20123575.

Jaideva C Goswami and Andrew K Chan. *Fundamentals of wavelets: theory, algorithms, and applications*. John Wiley & Sons, 2011.

Norden E Huang, Zheng Shen, Steven R Long, Manli C Wu, Hsing H Shih, Quanan Zheng, Nai-Chyuan Yen, Chi Chao Tung, and Henry H Liu. The empirical mode decomposition and the hilbert spectrum for nonlinear and non-stationary time series analysis. *Proceedings of the Royal Society of London. Series A: mathematical, physical and engineering sciences*, 454(1971):903–995, 1998. doi:10.1098/rspa.1998.0193.

Norden Eh Huang. *Hilbert-Huang transform and its applications*, volume 16. World Scientific, 2014.

Anastasija Ignjatovska, Zlatko Petreski, Simona Domazetovska, and Damjan Pecioski. Time-domain analysis of vibration signals of rotating machinery with defects under varying load conditions. In *2023 International Conference on Control, Automation and Diagnosis (ICCAD)*, pages 1–6. IEEE, 2023. doi:10.1109/ICCAD57653.2023.10152458.

Andrew KS Jardine, Daming Lin, and Dragan Banjevic. A review on machinery diagnostics and prognostics implementing condition-based maintenance. *Mechanical systems and signal processing*, 20(7):1483–1510, 2006. doi:10.1016/j.ymssp.2005.09.012.

Hua Jiang and Jianhui Lin. Fault diagnosis of wheel flat using empirical mode decomposition-hilbert envelope spectrum. *Mathematical problems in engineering*, 2018:1–16, 2018. doi:10.1155/2018/8909031.

Yue Jianhai, Qiu Zhengding, and Chen Boshi. Application of wavelet transform to defect detection of wheelflats of railway wheels. In *6th International Conference on Signal Processing, 2002.*, volume 1, pages 29–32. IEEE, 2002. doi:10.1109/ICOSP.2002.1180975.

Zhenzhen Jin, Deqiang He, Rui Ma, Xueyan Zou, Yanjun Chen, and Sheng Shan. Fault diagnosis of train rotating parts based on multi-objective vmd optimization and ensemble learning. *Digital Signal Processing*, 121:103312, 2022. doi:10.1016/j.dsp.2021.103312.

Pawel Komorski, Tomasz Nowakowski, Grzegorz M Szymanski, and Franciszek Tomaszewski. Application of time-frequency analysis of acoustic signal to detecting flat places on the rolling surface of a tram wheel. In *Dynamical Systems Theory and Applications*, pages 205–215. Springer, 2017. doi:10.1007/978-3-319-96601-4_19.

Mariusz Kostrzewski and Rafał Melnik. Condition monitoring of rail transport systems: A bibliometric performance analysis and systematic literature review. *Sensors*, 21(14): 4710, 2021. doi:10.3390/s21144710.

Gabriel Krummenacher, Cheng Soon Ong, Stefan Koller, Seijin Kobayashi, and Joachim M Buhmann. Wheel defect detection with machine learning. *IEEE Transactions on Intelligent Transportation Systems*, 19(4):1176–1187, 2017. doi:10.1109/TITS.2017.2720721.

Tomasz Kuminek, Krzysztof Aniołek, and Jakub Młyńczak. A numerical analysis of the contact stress distribution and physical modelling of abrasive wear in the tram wheel-frog system. *Wear*, 328:177–185, 2015. doi:10.1016/j.wear.2015.02.018.

V. P. Kvasnikov and A. P. Stakhova. Spectral analysis of vibration signal using fourier transform. *Collection of scientific works of the Odesa State Academy of Technical Regulation and Quality*, 21(2):28–33, Dec. 2022. doi:10.32684/2412-5288-2022-2-21-28-33.

Francesco Lanza di Scalea and John McNamara. Wavelet transform for characterizing longitudinal and lateral transient vibrations of railroad tracks. *Research in Nondestructive Evaluation*, 15(2):87–98, 2004. doi:10.1080/09349840490443658.

Yaguo Lei and Ming J Zuo. Fault diagnosis of rotating machinery using an improved hht based on eemd and sensitive imfs. *Measurement Science and Technology*, 20(12): 125701, 2009. doi:10.1088/0957-0233/20/12/125701.

Yaguo Lei, Jing Lin, Zhengjia He, and Ming J Zuo. A review on empirical mode decomposition in fault diagnosis of rotating machinery. *Mechanical systems and signal processing*, 35(1-2):108–126, 2013. doi:10.1016/j.ymssp.2012.09.015.

Yifan Li, Jianxin Liu, and Yan Wang. Railway wheel flat detection based on improved empirical mode decomposition. *Shock and Vibration*, 2016, 2016. doi:10.1155/2016/4879283.

Yifan Li, Ming J. Zuo, Jianhui Lin, and Jianxin Liu. Fault detection method for railway wheel flat using an adaptive multiscale morphological filter. *Mechanical Systems and Signal Processing*, 84:642–658, 2017. doi:10.1016/j.ymssp.2016.07.009.

Bo Liang, SD Iwnicki, Yunshi Zhao, and David Crosbee. Railway wheel-flat and rail surface defect modelling and analysis by time–frequency techniques. *Vehicle System Dynamics*, 51(9):1403–1421, 2013. doi:10.1080/00423114.2013.804192.

Xiao-Zhou Liu, Chi Xu, and Yi-Qing Ni. Wayside detection of wheel minor defects in high-speed trains by a bayesian blind source separation method. *Sensors*, 19(18):3981, 2019. doi:10.3390/s19183981.

Yongbin Liu, Qiang Qian, Yangyang Fu, Fang Liu, and Siliang Lu. Wayside acoustic fault diagnosis of railway wheel-bearing paved with doppler effect reduction and eemd-based diagnosis information enhancement. In *2016 10th International Conference on Sensing Technology (ICST)*, pages 1–5. IEEE, 2016. doi:10.1109/ICSensT.2016.7796264.

J Madejski and A Gola. Tram wheel geometry monitoring system. *WIT Transactions on The Built Environment*, 89, 2006. doi:10.2495/UT060401.

Khakoo Mal, Imtiaz Hussain, Tayab Din Memon, Dileep Kumar, and Bhawani Shankar Chowdhry. Modern condition monitoring systems for railway wheel-set dynamics: Per-

formance analysis and limitations of existing techniques. *Sir Syed University Research Journal of Engineering & Technology*, 12(1):31–41, 2022. doi:10.33317/ssurj.419.

R. Keith Mobley. Chapter 28 - synchronous time averaging. In R. Keith Mobley, editor, *Vibration Fundamentals*, pages 259–264. Newnes, Woburn, 1999. ISBN 978-0-7506-7150-7. doi:10.1016/B978-075067150-7/50065-3.

Araliya Mosleh, Pedro Montenegro, Pedro Alves Costa, and Rui Calçada. An approach for wheel flat detection of railway train wheels using envelope spectrum analysis. *Structure and Infrastructure Engineering*, 17(12):1710–1729, 2021. doi:10.1080/15732479.2020.1832536.

Chris Murphy. Choosing the most suitable mems accelerometer for your application—part 2. *50 Maximize the Run Time in Automotive Battery Stacks Even as Cells Age*, page 5, 2017.

Tomasz Nowakowski, Paweł Komorski, Grzegorz M Szymański, and Franciszek Tomaszewski. Wheel-flat detection on trams using envelope analysis with hilbert transform. *Latin American Journal of Solids and Structures*, 16, 2019. doi:10.1590/1679-78255010.

Hany Osman and Soumaya Yacout. Condition-based monitoring of the rail wheel using logical analysis of data and ant colony optimization. *Journal of Quality in Maintenance Engineering*, 29(2):377–400, 2023. doi:10.1108/JQME-01-2022-0004.

ZK Peng and FL Chu. Application of the wavelet transform in machine condition monitoring and fault diagnostics: a review with bibliography. *Mechanical systems and signal processing*, 18(2):199–221, 2004. doi:10.1016/S0888-3270(03)00075-X.

Z.K. Peng, Peter W. Tse, and F.L. Chu. A comparison study of improved hilbert–huang transform and wavelet transform: Application to fault diagnosis for rolling bearing. *Mechanical Systems and Signal Processing*, 19(5):974–988, 2005. doi:10.1016/j.ymssp.2004.01.006.

Donald B Percival and Andrew T Walden. *Wavelet methods for time series analysis*, volume 4. Cambridge university press, 2000.

Riccardo Rubini and U Meneghetti. Application of the envelope and wavelet transform

analyses for the diagnosis of incipient faults in ball bearings. *Mechanical systems and signal processing*, 15(2):287–302, 2001. doi:10.1006/mssp.2000.1330.

S.A. Saleh and M.A. Rahman. Modeling and protection of a three-phase power transformer using wavelet packet transform. *IEEE Transactions on Power Delivery*, 20(2): 1273–1282, 2005. doi:10.1109/TPWRD.2004.834891.

Ervin Sejdić, Igor Djurović, and Jin Jiang. Time–frequency feature representation using energy concentration: An overview of recent advances. *Digital Signal Processing*, 19 (1):153–183, 2009. doi:10.1016/j.dsp.2007.12.004.

Muhammad Zakir Shaikh, Zeeshan Ahmed, Bhawani Shankar Chowdhry, Enrique Nava Baro, Tanweer Hussain, Muhammad Aslam Uqaili, Sanaullah Mehran, Dileep Kumar, and Ali Akber Shah. State-of-the-art wayside condition monitoring systems for railway wheels: A comprehensive review. *IEEE Access*, 2023. doi:10.1109/ACCESS.2023.3240167.

Pei-Wei Shan, Ming Li, et al. Nonlinear time-varying spectral analysis: Hht and modwpt. *Mathematical Problems in Engineering*, 2010, 2010. doi:10.1155/2010/618231.

Changqing Shen, Dong Wang, Fanrang Kong, and W Tse Peter. Fault diagnosis of rotating machinery based on the statistical parameters of wavelet packet paving and a generic support vector regressive classifier. *Measurement*, 46(4):1551–1564, 2013. doi:10.1016/j.measurement.2012.12.011.

Zhongjie Shen, Zhengjia He, Xuefeng Chen, Chuang Sun, and Zhiwen Liu. A monotonic degradation assessment index of rolling bearings using fuzzy support vector data description and running time. *Sensors*, 12(8):10109–10135, 2012. doi:10.3390/s120810109.

Xiao-zhen Sheng, Ming-hua Li, CJC Jones, and DJ Thompson. Using the fourier-series approach to study interactions between moving wheels and a periodically supported rail. *Journal of Sound and Vibration*, 303(3-5):873–894, 2007. doi:10.1016/j.jsv.2007.02.007.

JaeSeok Shim, GeoYoung Kim, ByungJin Cho, and JeongSeo Koo. Application of vibration signal processing methods to detect and diagnose wheel flats in railway vehicles. *Applied Sciences*, 11(5):2151, 2021. doi:10.3390/app11052151.

Nawaf HMM Shrifan, Muhammad Firdaus Akbar, and Nor Ashidi Mat Isa. Maximal overlap discrete wavelet-packet transform aided microwave nondestructive testing. *NDT & E International*, 119:102414, 2021. doi:10.1016/j.ndteint.2021.102414.

Ying Song, Lei Liang, Yanliang Du, and Baochen Sun. Railway polygonized wheel detection based on numerical time-frequency analysis of axle-box acceleration. *Applied Sciences*, 10(5):1613, 2020. doi:10.3390/app10051613.

Tomasz Staskiewicz and Bartosz Firlik. Influence of tram wheel profile geometry on wear intensity. *Procedia engineering*, 192:1006–1011, 2017. doi:10.1016/j.proeng.2017.06.173.

Qi Sun, Chunjun Chen, Andrew H Kemp, and Peter Brooks. An on-board detection framework for polygon wear of railway wheel based on vibration acceleration of axle-box. *Mechanical Systems and Signal Processing*, 153:107540, 2021. doi:10.1016/j.ymssp.2020.107540.

NA Thakkar, JA Steel, and RL Reuben. Rail–wheel interaction monitoring using acoustic emission: A laboratory study of normal rolling signals with natural rail defects. *Mechanical Systems and Signal Processing*, 24(1):256–266, 2010. doi:10.1016/j.ymssp.2009.06.007.

David Thompson. *Railway noise and vibration: mechanisms, modelling and means of control*. Elsevier, 2008.

Luisa F Villa, Aníbal Reñones, Jose R Perán, and Luis J De Miguel. Angular resampling for vibration analysis in wind turbines under non-linear speed fluctuation. *Mechanical Systems and Signal Processing*, 25(6):2157–2168, 2011. doi:10.1016/j.ymssp.2011.01.022.

J Ville. *Theory and applications of the notion of complex signal*. Rand, 1958.

Andrew T Walden and A Contreras Cristan. The phase–corrected undecimated discrete wavelet packet transform and its application to interpreting the timing of events. *Proceedings of the Royal Society of London. Series A: Mathematical, Physical and Engineering Sciences*, 454(1976):2243–2266, 1998. doi:10.1098/rspa.1998.0257.

Ting Hei Wan, Chi Wai Tsang, King Hui, and Edward Chung. Anomaly detection of train wheels utilizing short-time fourier transform and unsupervised learn-

ing algorithms. *Engineering Applications of Artificial Intelligence*, 122:106037, 2023. doi:10.1016/j.engappai.2023.106037.

Jianlin Wang, Qingxuan Wei, Liqiang Zhao, Tao Yu, and Rui Han. An improved empirical mode decomposition method using second generation wavelets interpolation. *Digital Signal Processing*, 79:164–174, 2018. doi:10.1016/j.dsp.2018.05.009.

Zhiwei Wang, Paul Allen, Guiming Mei, Ruichen Wang, Zhonghui Yin, and Weihua Zhang. Influence of wheel-polygonal wear on the dynamic forces within the axlebox bearing of a high-speed train. *Vehicle System Dynamics*, 58(9):1385–1406, 2020. doi:10.1080/00423114.2019.1626013.

Jacek Wodecki. Time-varying spectral kurtosis: Generalization of spectral kurtosis for local damage detection in rotating machines under time-varying operating conditions. *Sensors*, 21(11):3590, 2021. doi:10.3390/s21113590.

Jingmang Xu, Ping Wang, Li Wang, and Rong Chen. Effects of profile wear on wheel–rail contact conditions and dynamic interaction of vehicle and turnout. *Advances in mechanical Engineering*, 8(1):1687814015623696, 2016. doi:10.1177/1687814015623696.

Wentian Xu, Maoru Chi, Wubin Cai, Gongquan Tao, Jianfeng Sun, Yabo Zhou, and Shulin Liang. An anti-disturbance method for on-board detection of early wheel polygonal wear by weighted angle-synchronous moving average. *Measurement*, 216:112999, 2023. doi:10.1016/j.measurement.2023.112999.

Ruqiang Yan, Robert X. Gao, and Xuefeng Chen. Wavelets for fault diagnosis of rotary machines: A review with applications. *Signal Processing*, 96:1–15, 2014. doi:10.1016/j.sigpro.2013.04.015. Time-frequency methods for condition based maintenance and modal analysis.

D-M Yang. The detection of motor bearing fault with maximal overlap discrete wavelet packet transform and teager energy adaptive spectral kurtosis. *Sensors*, 21(20):6895, 2021. doi:10.3390/s21206895.

Yunfan Yang, Liang Ling, Pengfei Liu, Kaiyun Wang, and Wanming Zhai. Experimental investigation of essential feature of polygonal wear of locomotive wheels. *Measurement*, 166:108199, 2020. doi:10.1016/j.measurement.2020.108199.

Xiao-Jun Yao, Ting-Hua Yi, and Chun-Xu Qu. Autoregressive spectrum-guided variational mode decomposition for time-varying modal identification under nonstationary conditions. *Engineering Structures*, 251:113543, 2022. doi:10.1016/j.engstruct.2021.113543.

Yunguang Ye, Dachuan Shi, Philipp Krause, and Markus Hecht. A data-driven method for estimating wheel flat length. *Vehicle System Dynamics*, 2019. doi:10.1080/00423114.2019.1620956.

Chen Yuejian, Xing Zongyi, Li Jianwei, and Qin Yong. The analysis of wheel-rail vibration signal based on frequency slice wavelet transform. In *17th International IEEE Conference on Intelligent Transportation Systems (ITSC)*, pages 1312–1316. IEEE, 2014. doi:10.1109/ITSC.2014.6957868.

Jian Zhang, Cai Lun Huang, and Shao Wu Zhou. An approach to the characteristic spectrum analysis for train wheelset fault diagnosis. *Key Engineering Materials*, 460: 153–158, 2011a. doi:10.4028/www.scientific.net/KEM.460-461.153.

Jie Zhang, Hongli Gao, Qiyue Liu, F Farzadpour, C Grebe, and Ying Tian. Adaptive parameter blind source separation technique for wheel condition monitoring. *Mechanical Systems and Signal Processing*, 90:208–221, 2017. doi:10.1016/j.ymssp.2016.12.021.

Zhifeng Zhang, Zhan Su, Yuling Su, and Zhan Gao. Denoising of sensor signals for the flange thickness measurement based on wavelet analysis. *Optik*, 122(8):681–686, 2011b. doi:10.1016/j.ijleo.2010.05.006.

Xiaomin Zhao, Tejas H. Patel, and Ming J. Zuo. Multivariate emd and full spectrum based condition monitoring for rotating machinery. *Mechanical Systems and Signal Processing*, 27:712–728, 2012. ISSN 0888-3270. doi:10.1016/j.ymssp.2011.08.001.

XN Zhao, GX Chen, ZY Huang, and CG Xia. Study on the different effects of power and trailer wheelsets on wheel polygonal wear. *Shock and Vibration*, 2020, 2020. doi:10.1155/2020/2587152.

Yichang Zhou, Qiuyong Tian, and Markus Hecht. Wheel flat detection on railway vehicles using the angular domain synchronous averaging method: An experimental study. *Structural Health Monitoring*, 23(1):343–359, 2024. doi:10.1177/14759217231166569.

A

MATLAB Scripts

Listing A.1: DW values syntax function

```
% Processing wheel data for determining the DW values function
% between impacts
% ax, ay, az acceleration samples
% fo – sampling rate 1000Hz (original)
% calculation of DW for Daubechies wavelets with 1–10 vanishing moments
% at 7th level of decomposition

clear all

load n01_n04_normal.mat     % wheelnormal raw data (int16)
load f01_f03_flat.mat       % wheel flat raw data (int16)

% list of quiet starts for normal wheels
pn = [429000, 451000, 480000, 503000, 534000, 557000, ...
      585000, 607000, 641000, 667000, 705000];
% list of quiet starts for flat wheels
pf = [298000, 315000, 335000, 350000, 371000, 387000, ...
      412000, 429000, 454000, 472000, 499000];

fs = 1000;                  % sensor sampling rate [1/s]
```

```
% wavelet type  (sym4, coif4 give similar results)
falka = string(["coif1", "coif2", "coif3", "coif4", "coif5"]);
% falka = string(["db3", "coif3", "sym3", "db4", "coif4", "sym4", "db5", "coif5", "sym5"]);
len = 4096;                 % number of samples in data set for WPT
dl = 7;                     % decomposition level
an = zeros(1,len);          % acceleration data vector normal wheels
af = zeros(1,len);          % acceleration data vector flat wheels
DW7 = zeros(length(falka),fs/2);       % wheel detection function
f = 0;                      % start frequency of the slot
lp = 2^dl;                  % number of frequency slots
en = zeros(length(pn),lp);  % energy data vector normal wheels
ef = zeros(length(pn),lp);  % energy data vector flat wheels
men = zeros(length(falka),lp); % energy data vector normal wheels
mef = zeros(length(falka),lp); % energy data vector flat wheels
for j=1:length(falka)
    for i=1:length(pn)
        an = cast(anx(pn(i):pn(i)+len-1), "double"); % normal wheels
        af = cast(afx(pf(i):pf(i)+len-1), "double"); % flat wheels
        an = an - mean(an);         % mean - reduction of bias
        af = af - mean(af);         % mean - reduction of bias
        [~,~,~,energy,~] = modwpt(an, falka(j), dl);
        en(i,:) = energy(:);
        [~,~,~,energy,~] = modwpt(af, falka(j), dl);
        ef(i,:) = energy(:);
    end
    for dk=1:lp         % frequency slot number
        f = floor(dk*fs/lp/2);
        if f == 0 f = 1; end
        mef(j,f) = min(ef(:,dk));
        men(j,f) = max(en(:,dk));
        DW7(j,f) = (mef(j,f) - men(j,f))/men(j,f)*100;
    end
    f = 0; f1 = 0; f2 = 0;
    for i=1:fs/2
        if DW7(j,i) ~= 0  f = DW7(j,i); end
        DW7(j,i) = f;
        if mef(j,i) ~= 0 f1 = mef(j,i); end
        mef(j,i) = f1;
        if men(j,i) ~= 0 f2 = men(j,i); end
        men(j,i) = f2;
    end
    falka(j)
    DW7 = (DW7 > 0).*DW7;  % present only positive values
end

% save('DW7c.mat', 'DW7');
% DW at 420 [Hz]
DW_db(:) = DW7(:,420);
DW_db(6) = NaN;
figure('Color',[1 1 1]);
t = tiledlayout(1,2);
```

```
t.TileSpacing = 'compact';
nexttile;
stem(DW_db,':o');
grid on
% title('Daubechies wavelets');
xlabel('Number of vanishing moments');
ylabel('DW [%]');
% figure
% vibration energy
nexttile;
evf(:) = mef(:,420);
evn(:) = men(:,420);
evn(6) = NaN;
evf(6) = NaN;
stem(evf, ':ro'); hold on
evt = (evf/2 + evn/2);
stem(evt, ':k_','LineStyle','none');
stem(evn, ':bo');
grid on
xlabel('Number of vanishing moments');
ylabel('Vibration energy');
legend('Ef','TH','En','Location','northwest');
legend('boxoff');
%%
```

Listing A.2: Energy variation of the rolling data calculated using the MODWPT coefficients

```
% processing wheel data for energy variation, calculated using the MODWPT coefficients
% between impacts
% ax, ay, az acceleration samples
% fo — sampling rate 1000Hz (original)

clear all

load n01_n04_normal.mat     % wheel normal raw data (int16)
load f01_f03_flat.mat       % wheel flat raw data (int16)
% % list of quiet starts for normal wheels
pn = [432000, 482500, 537500, 588000, 644500, 707500, ...
      453000, 505000, 558500, 609500, 668000];
% % list of quiet starts for flat wheels
pf = [301500, 338000, 374500, 415500, 458500, 502500, ...
      317500, 352500, 389000, 431500, 474000];
fo = 1000;                  % sensor sampling rate [1/s]
dr = 1;                     % decimation rate of raw data
dl = 6;                     % decomposition level
falka = ['coif4'];            % wavelet type  (sym4, db4 give similar results)
len = 4096;                 % number of samples in data set for WPT
fs = (fo/dr);               % sample rate  [1/s]
n = len/dr;                 % vector length after decimation
ax = zeros(1,n);            % acceleration data vector normal wheels
```

```
ay = ax;                    % acceleration data vector flat wheels
dk = 0;                     % number of combined frequency slots
lp = 2^dl;                  % number of freqency slots

figure;
for k=1:lp-dk
for i=1:length(pn)
    ax = decimate(cast(any(pn(i):pn(i)+len-1), "double"),dr); % normal wheels
    ay = decimate(cast(afy(pf(i):pf(i)+len-1), "double"),dr); % flat wheels
    ax = (ax - mean(ax));        % mean - reduction of bias
    ay = (ay - mean(ay));        % mean - reduction of bias
    [nwpt,~,n_cfreq,energy,relenergy] = modwpt(ax, falka, dl);
    n_cfreq = fs*n_cfreq;
    en(k,i) = sum(energy(k:k+dk));

    subplot(3,1,1);
    hold on; plot(n_cfreq, relenergy, 'r'); hold off;
    relN = relenergy(k);

    [fwpt,~,f_cfreq,fenergy,frelenergy] = modwpt(ay, falka, dl);
    f_cfreq = fs*f_cfreq;
    ef(k,i) = sum(fenergy(k:k+dk));
    relF = frelenergy(k);
    hold on; plot(f_cfreq,frelenergy, 'b'); title(['N + F  ', falka, ' dl=', int2str(dl), ' dr=', int2str(dr)
        ]); xlabel('[Hz]'); hold off;

    subplot(3,1,2);
    hold on; plot(f_cfreq, frelenergy, 'b'); title('F'); xlabel('[Hz]'); hold off;

    subplot(3,1,3);
    [nwpt,~,n_cfreq,energy,relenergy] = modwpt(ax, falka, dl);
    n_cfreq = fs*n_cfreq;
    hold on; plot(n_cfreq,relenergy, 'r'); title('N'); xlabel('[Hz]'); hold off;
end
end
df = fs/lp/2;        % size of frequency step
figure;
tiledlayout(2,3);
for k=20:25             %17:lp-dk
    nexttile;
    plot(en(k,:), 'r'); hold on; plot(ef(k,:), 'b');  hold off;
    mef = min(ef(k,:)); men = max(en(k,:));
    k
    roz = (men - mef)/men*100
    title([falka, ' k=',int2str(k), ' dk=', int2str(dk), ' f:', int2str((k-dk-1)*df), '...', int2str(k*df), '
        Hz']);

end
%%
```

Listing A.3: DW values variation relative to sample size and level of decomposition based on MODWPT

```
% processing wheel data for DW values variation relative to sample size and level of decomposition
% between impacts
% ax, ay, az acceleration samples
% fs – sampling rate 1000Hz (original)

clear all

load n01_n04_normal.mat     % wheelnormal raw data (int16)
load f01_f03_flat.mat       % wheel flat raw data (int16)

% list of quiet starts for normal wheels(number of test band)
pn = [432000, 482500, 537500, 588000, 644500, 707500, ...
      453000, 505000, 558500, 609500, 668000];
% list of quiet starts for flat wheels (number of test band)
pf = [301500, 338000, 374500, 415500, 458500, 502500, ...
      317500, 352500, 389000, 431500, 474000];
fs = 1000;                  % sensor sampling rate [1/s]
falka = ['coif4'];            % wavelet type  (sym4, db4 give similar results)
dl = 5;                     % decomposition level
d = length(pn);             % number of test bands

figure;
title([falka, '  dl = ', int2str(dl)]);
xlabel('length of sensor data'); ylabel('difference [%]');

for dl=4:11
    lp = 2^dl;                  % number of freqency slots
    roz = zeros(lp);            % differences
    for j=1:24
        len = j*500 + 2000;     % number of samples in data set for WPT
        llen(j) = len;
        an = zeros(1,len);      % acceleration data vector normal wheels
        af = zeros(1,len);      % acceleration data vector flat wheels
        clear enn enf
        for i=1:d
            an = cast(anx(pn(i):pn(i)+len-1), "double");
            af = cast(afx(pf(i):pf(i)+len-1), "double");
            an = an - mean(an);         % mean - reduction of bias
            af = af - mean(af);         % mean - reduction of bias
            [~,~,~,enn(i,:),~] = modwpt(an, falka, dl);
            [~,~,~,enf(i,:),~] = modwpt(af, falka, dl);
        end

        for dk=0:lp-1
            for k=1:lp-dk
                for i=1:d
                    en(i) = sum(enn(i,k:k+dk));
                    ef(i) = sum(enf(i,k:k+dk));
```

```
                end
                mef = min(ef); men = max(en);
                roz(dk+1,k) = (mef - men)/men*100;  % dl,roz, object function
            end
        end

        [m,k] = max(max(roz));      % frequency slot start number
        [m,dk] = max(max(roz'));    % number of combined neighbouring slots
        dk = dk-1;

        for i=1:d
            epn(i) = sum(enn(i,k:k+dk));
            epf(i) = sum(enf(i,k:k+dk));
        end
        j
        mef = min(epf); men = max(epn);
        blad(j) = (mef - men)/men*100;
    end

hold on; plot(llen, blad); title([falka, '  dl max = ', int2str(dl)]); hold off;
end
%
```

Listing A.4: Railroad drive test threshold values for differentiating fault wheel energy

```
% Processing wheel data for test drives threshold values for differentiating flat wheel energy
% between impacts
% ax, ay, az acceleration samples
% fo - sampling rate 1000Hz (original)
% calculation of DW for wavelets with 3-5 vanishing moments

clear all

load n01_n04_normal.mat     % wheelnormal raw data (int16)
load f01_f03_flat.mat       % wheel flat raw data (int16)

% list of quiet starts for normal wheels
pn = [429000, 451000, 480000, 503000, 534000, 557000, ...
      585000, 607000, 641000, 667000, 705000];
% list of quiet starts for flat wheels
pf = [298000, 315000, 335000, 350000, 371000, 387000, ...
      412000, 429000, 454000, 472000, 499000];
fs = 1000;                  % sensor sampling rate [1/s]
% wavelet type  (sym4, coif4 give similar results)
falka = string(["db3", "coif3", "sym3", "db4", "coif4", "sym4", "db5", "coif5", "sym5"]);
% falka = string(["db4", "coif4", "sym4", "db5", "coif5", "sym5"]);
% falka = string(["db5", "coif5", "sym5"]);
len = 4096;                 % number of samples in data set for WPT
%falka = 'coif5';
dl = 7;                     % decomposition level
an = zeros(1,len);          % acceleration data vector normal wheels
```

```
af = zeros(1,len);          % acceleration data vector flat wheels
lp = 2^dl;                  % number of frequency slots
dk = 107;                   % frequency slot number
DW5 = zeros(1,length(pn));  % wheel detection function
f = 0;                      % start frequency of the slot
blad = 0.02;
en = zeros(1,length(pn));   % energy data vector normal wheels
ef = zeros(1,length(pn));   % energy data vector flat wheels
for i=1:length(pn)
    an = cast(anx(pn(i):pn(i)+len-1), "double"); % normal wheels
    af = cast(afx(pf(i):pf(i)+len-1), "double"); % flat wheels
    an1 = an*(1 + blad);    % normal wheels + sensor error
    af1 = af*(1 + blad);    % flat wheels + sensor error
    an2 = an*(1-blad);      % normal wheels - sensor error
    af2 = af*(1-blad);      % flat wheels - sensor error
    [~,~,~,energy,~] = modwpt(an, falka, dl);
    en(i) = energy(dk);
    [~,~,~,energy1,~] = modwpt(af, falka, dl);
    ef(i) = energy1(dk);
    [~,~,~,energy,~] = modwpt(an1, falka, dl);
    en1(i) = energy(dk);
    [~,~,~,energy1,~] = modwpt(af1, falka, dl);
    ef1(i) = energy1(dk);
    [~,~,~,energy,~] = modwpt(an2, falka, dl);
    en2(i) = energy(dk);
    [~,~,~,energy1,~] = modwpt(af2, falka, dl);
    ef2(i) = energy1(dk);

    DW5(i) = (ef(i) - en(i))/en(i)*100;
end
figure('Color',[1 1 1]);
t = tiledlayout(1,2);
t.TileSpacing = 'compact';
nexttile;
stem(DW5,':o');  hold on
xlabel('test drive number');
ylabel('DW[%]');
grid on
nexttile;
en(12) = NaN; ef(12) = NaN;
en1(12) = NaN; ef1(12) = NaN;
en2(12) = NaN; ef2(12) = NaN;
stem(en, ':o', MarkerSize=4); hold on
stem(ef, ':o');
plot((ef*0 + 2800), 'k--');
stem(en1, ':k_', MarkerSize=12); stem(ef1, ':k_', MarkerSize=12); stem(en2, ':k_', MarkerSize=12);
stem(ef2, ':k_', MarkerSize=12);
xlabel('test drive number'); ylabel('energy');
legend('En','Ef','TH','Location','northwest');
legend('boxoff');
%%
```